Advanced Loudspeaker Modelling and Automatic Crossover Network Optimization

Master Thesis in Acoustics

Lars Enggaard
Lars Juul Mikkelsen

Section of Acoustics
Department of Electronic Systems
Aalborg University
2007

Section of Acoustics
Department of Electronic Systems
Aalborg University

Title:

Advanced Loudspeaker Modelling and Automatic Crossover Network Optimization

Project Period:
10th semester
5. february -
7. june 2007

Project Group:
1060

Group Members:
Lars Enggaard
Lars Juul Mikkelsen

Supervisor:
Søren Krarup Olesen

Number of copies: 4

Report – number of pages: 107

Appendix – number of pages: 25

Abstract:

This thesis documents the use of optimization on loudspeakers in order to improve its magnitude response and dispersion. The thesis bases its results and methods on the hypothesis that a loudspeaker can be improved by optimizing only the crossover network.
A loudspeaker model is created from theories describing a loudspeaker. This model is used as basis for optimization of a loudspeakers magnitude response and dispersion. The optimization method is steepest descent. A reference loudspeaker is constructed from basic methods in order to evaluate the results of optimizing the crossover network. Both the model and optimization algorithm are verified by measurements. The implementations are carried out in Matlab.
Simulations and measurements show, that the loudspeaker model and optimization algorithm work satisfying, and the theory verifications show that the theories are valid. When comparing the reference loudspeaker using the standard crossover network and the optimized crossover network it can be concluded, that the magnitude response and the dispersion can be improved by optimizing the crossover network. The optimized loudspeaker has a more flat magnitude response both on-axis and 30° horizontally off-axis.
It is concluded that the loudspeaker modelling and optimization are successful.

PREFACE

This report documents the master thesis written by the 10th semester group 1060, Section of Acoustics at the Department of Electronic Systems, Aalborg University, 2007. The report is meant to provide the documentation supporting the project work done with the theme of "Master thesis in acoustics".

This thesis investigates loudspeaker modelling, and how optimization automatically can optimize a crossover network to give the loudspeaker a desired target response. The report is intended for the supervisor, censor, 10th semester students and people who have a general interest in loudspeakers and optimization.

The report is divided into a main part and appendices. The appendices include calculations and measurement reports. The report structure is shown in the list below:

- **Introduction:** This chapter presents the background of the project together with the problem statement. This is followed up by the project goal and scope.
- **Theory:** This chapter presents the theory, which is used as basis for the loudspeaker modelling.
- **Project Delimitations:** Here are the project delimitations presented.
- **Optimization:** This chapter presents the optimization algorithm used in this thesis and the theory behind it.
- **Reference Loudspeaker Design:** This chapter describes how the loudspeaker drivers are chosen. These are then measured and the driver parameters are estimated. Finally the reference speaker is designed and constructed.
- **Verification of Theory:** This chapter verifies the theories by measurements made according to each theory.
- **Advanced Loudspeaker Model Design:** In this chapter is presented how the different theories are put together to form the complete model. The model is verified with measurements.
- **Automatic Crossover Network Optimization:** This chapter presents how optimization can be used on the designed loudspeaker model. It is furthermore explained how the model can be reorganized in order to increases the execution time when doing optimization.
- **Evaluation of Reference and Optimized Loudspeaker:** This chapter presents simulations and measurements of both the reference and optimized loudspeaker and a comparison of these.
- **Conclusion:** The final chapter gives the conclusion of the project and results. In addition, suggestions for further investigations are presented.

A CD-ROM is enclosed containing Matlab files, measurement data files, datasheets and this thesis in PDF-format.

Aalborg University, June 7, 2007

Lars Enggaard Lars Juul Mikkelsen

CONTENTS

CHAPTER 1

INTRODUCTION

This chapter presents the background for this project. Afterwards, the problem statement describes different factors that influence the response of a loudspeaker. Finally the project goal and project scope are presented.

1.1 Background

When designing a loudspeaker, the engineer has to do many considerations. Some of the major considerations are which drivers to use, and how to make the crossover network.

To cover the entire audible frequency range, loudspeakers often make use of multiple drivers. These types of constructions introduce practical design issues, since all drivers have to be carefully integrated to cover the full frequency range in a smooth way. Imagine a 2-way speaker consisting of an 8" woofer and 1" tweeter with a crossover frequency at 4 kHz. At this frequency the woofer beams and its dispersion is very narrow. This is due to the fact, that soundwaves from the center and sides of the membrane have different delays. At high frequencies, these distances are large compared to the wavelength, and at certain frequencies it results in destructive interference. The tweeter, which has a smaller membrane, does normally not have these problems at 4 kHz and is therefore close to omnidirectional at this frequency. The outcome is a loudspeaker that has a markable change in dispersion when moving from low to high frequencies. In order to make a natural sounding loudspeaker, it is therefore important to investigate the sound dispersion.
There are several factors that influence the response and dispersion of a loudspeaker: sound pressure decrease because of driver roll off at low frequencies, driver beaming at high frequencies, interference between drivers in crossover regions, the influence of the cabinet diffractions and finally the chosen crossover filters.

The target response of a loudspeaker can be chosen in many different ways. For example, the response can be optimized according to phase response, magnitude response or dispersion. To solve the above mentioned problem about dispersion, it may be interesting to investigate not only the on-axis response, but also off-axis responses when designing the loudspeaker.

This thesis look into how the response and dispersion of a loudspeaker can be improved by optimization. The goal is to optimize for a flat magnitude response at both on-axis and off-axis positions, which will make the speaker less dependent on the listening position. The implemented optimization will output optimized crossover component values according to a desired loudspeaker target response. The optimization will be based on measurements of the drivers electrical impedances and acoustical impulse responses.

1.2 Problem Statement

As mentioned in the background, the dispersion of a loudspeaker can be influenced by multiple factors. To make these factors more clear a description of each is presented.

1.2.1 Driver Roll Off in Infinite Baffle

At low frequencies most speakers are omnidirectional, but the sound pressure level decreases when moving downwards in frequency. This is due to the fact, that the volume velocity of the membrane is lower at low frequencies, and that the radiation impedance is almost pure reactive. The function of an infinite baffle is to prevent the driver back pressure to cancel out the front pressure. When using a closed box it is possible to control the roll off or Q-value to some extent, but it will maintain a second order roll off at 12dB/octave like the infinite baffle. Figure 1.1 illustrates a typical infinite baffle roll off.

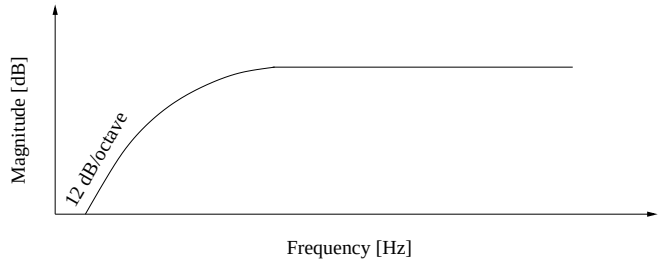

Figure 1.1: *Typical infinite baffle roll off.*

1.2.2 Cabinet Diffractions and Baffle Step

When using a cabinet and not an infinite baffle, diffractions are introduced from the cabinet edges by peaks and dips in the frequency response. This makes it interesting to investigate the edge diffraction behaviour. A baffle step will be present because of the change in radiation space over frequency. At low frequencies, where the wavelength is assumed much larger than the baffle dimensions, the radiation will be into a 4π space. When the wavelength get smaller and within the width of the front baffle the radiation becomes into a 2π space. This change will introduce a theoretically 6 dB sound pressure level increase. In practice it will be less, since the box dimensions will not be invisible to even a 20 Hz tone. The baffle step can be corrected for in the crossover network. Figure 1.2 illustrates the two phenomena.

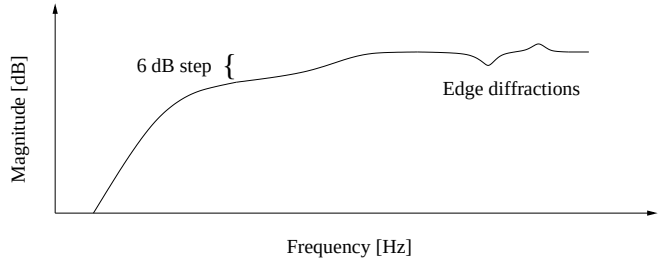

Figure 1.2: *Illustration of 6 dB baffle step and effects due to edge diffractions.*

1.2.3 Driver Beaming

Due to the nature of a driver or piston the beam pattern will change from omnidirectional to very directional when moving up in frequency. Figure 1.3 shows a typical beam pattern from a circular plane piston radiating sound with a wavelength that is a fraction of the diaphragm diameter. The figure is made over 180° in the vertical direction.

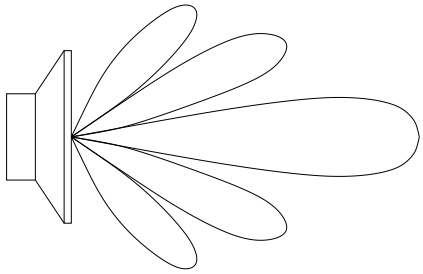

Figure 1.3: *Beam pattern from circular piston radiating sound with a wavelength that is a fraction of the diaphragm diameter.*

To get a flat magnitude response from all listening positions it is important only to use the drivers in the frequency range where the driver has not started to beam. This is often an issue in loudspeaker designs, since the tweeter beams at high frequencies, and it has to be used in that region.

1.2.4 Interference Between two Drivers

A loudspeaker has often two or more drivers to cover the entire audible frequency range. Interference occurs where two drivers overlap each other in frequency in the crossover region. This interference leads to an unequal dispersion of the speaker, and it has to be investigated together with the crossover filters. The interference pattern is 3-dimensional, and figure 1.4 shows the interference in two dimensions at the crossover frequency. The figure is made over 180° in the vertical direction.

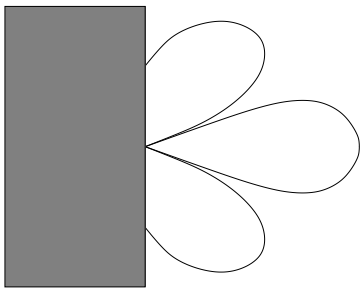

Figure 1.4: *Interference pattern between two drivers. Typical pattern when the crossover wavelength is similar to the distance between the two drivers.*

1.2.5 Acoustic Center Offset

When using a woofer and a tweeter in a 2-way speaker there will typical be a horizontal offset in the drivers acoustic centers, as shown in figure 1.5 on the following page. This is due to the drivers physical constructions, and the woofers acoustic center will be behind the one of the tweeter.

This offset tilts the mainlobe downwards. The offset will be taken into account in the modelling.

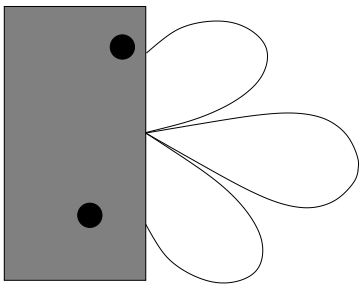

Figure 1.5: *Downward tilt because of driver offset.*

1.2.6 Crossover Network

Loudspeakers make use of filters to make sure that the woofer gets the lower frequencies and the tweeter the higher frequencies. A good design is then to make a smooth transition between this lowpass and highpass filter, see figure 1.6.

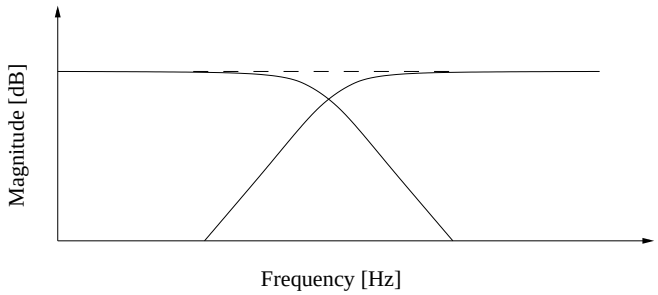

Figure 1.6: *Illustration of low and highpass filters and their summation.*

A lot of things can be manipulated in the filter design. The earlier mentioned baffle step can be avoided by damping the baffle amplified frequencies. The interference between drivers can be modified by choosing different filter slopes, and the chosen crossover frequency should be dependent on the drivers beaming patterns and resonances. Finally it is possible to match the sensitivities of the drivers.

Loudspeakers are often used in rooms, which contribute with reflections, which affect the final sound pattern. The critical room contributions like standing waves and reflections at low frequencies will not be taken into account in the modelling.

1.3 Project Goal

The goal of this project is to assess the hypothesis that it is possible to improve a loudspeakers dispersion, i.e. making it more flat for more listening angles. The loudspeaker modelling will include the following factors:

- Low frequency roll off in a closed cabinet
- Cabinet edge diffractions and baffle step
- Driver beaming

- Interference between two drivers
- Acoustics center offset
- Crossover filters

The optimized loudspeaker will be compared to a reference speaker, that has the same box construction, but with a standard crossover filter. The following question forms the initiating problem:

- **Is it possible to improve a loudspeakers magnitude response and dispersion by optimizing the crossover network?**

1.4 Project Scope

In order to answer the initiating problem, the scope of this project includes

1. An analysis of the problem and a description of the necessary theory to be able to optimize on relevant factors. This includes study of speaker acoustics, speaker construction and filter theory.
2. A design phase which includes choice of drivers and measurements of these. Afterwards a construction of a reference speaker, which includes cabinet and filter calculations.
3. Development of an optimization algorithm, which will be introduced by general optimization theory. Finally a model of the system that is going to be optimized will be made.
4. An implementation of the model and optimization algorithm.
5. Tests of the optimized loudspeaker and comparison to the reference speaker.

CHAPTER 2

THEORY

This chapter presents the theory used in this project. The theories are used when designing the loudspeaker model. Additionally, loudspeaker placement in rooms is discussed.

2.1 Loudspeaker Driver Parameters and Equivalent Diagrams

This section presents the parameters used to describe a loudspeaker driver. These parameters will be used to make a model of the loudspeaker, that will be used through out the project.

2.1.1 Loudspeaker Driver Construction

The idea of a loudspeaker driver is to move air by sending alternating electrical current through a coil positioned in a magnetic field and connected to a membrane. A loudspeaker driver consists of various parts, as it can be seen on figure 2.1.

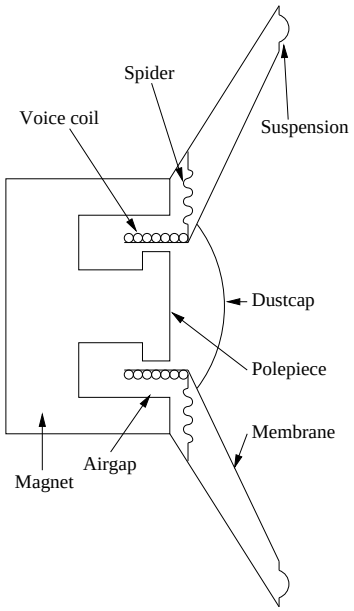

Figure 2.1: *Cross section of an electrodynamic cone loudspeaker driver [8, page 5].*

The magnet and the polepiece are used to create a magnetic field in the airgap. When an alternating current is sent through the voice coil it will make the voice coil and the membrane attached to it move according to the frequency. The spider is used to keep the voice coil centered in the air gap, and keeping it from touching the magnet and the polepiece. The spider and the suspension is responsible

for introducing mechanical resistance and compliance to pull the membrane back to its resting position. The compliance together with the mass create a resonance frequency. The membrane, the dustcap and part of the suspension are the parts of the loudspeaker that moves the air. It is responsible for giving a better coupling to the air, to more efficiently convert movements of the voice coil to movement of air. Furthermore the dustcap and the spider has to protect the airgap against dust.

2.1.2 Loudspeaker Parameteres

This section describes the parameters of loudspeaker.

Voice Coil Resistance, R_e

The voice coil resistance is the part of the voice coil impedance that is resistive. It is measured in Ω.

Voice Coil Inductance, L_e

The voice coil inductance is the part of the voice coil impedance that is reactive. It is measured in Henry.

Voice Coil Inductance Correction Factor n

The voice coil correction factor n is included to have a better model of how a lossy inductor behaves [11, page 102]. The correction factor is used as shown in equation 2.1.

$$j\omega L_e \rightarrow (j\omega)^n L_e \tag{2.1}$$

where n is a value between 0 and 1. When using the correction factor, the size of the inductance has to be adjusted.

Moving Mass, M_m

The moving mass is the weight of the membrane assembly. This includes the membrane, the dust cap, the voice coil and partly the suspension and the spider. This mass does not include the air that moves along with the driver. The moving mass is measured in kg.

Mechanical Resistance, R_m

The mechanical resistance is formed by the suspension and the spider of the driver. It is the part of the drivers mechanical impedance that is resistive. The mechanical resistance is measured in $^{\mathrm{N\cdot s}}/_{\mathrm{m}}$.

Mechanical Compliance, C_m

Mechanical compliance is formed by the suspension and the spider. It is the part of the mechanical impedance that is reactive. It is responsible for pulling the membrane back to its resting position after exitation. The mechanical compliance is measured in $^{\mathrm{m}}/_{\mathrm{N}}$.

Force Factor, *Bl*

The magnetic force is the product of the magnetic flux in the air gap, and the length of the wire in the voice coil. This describes the strength of the loudspeaker motor. The magnetic force factor is measured in $^{N}/_{A}$.

2.1.3 General Equivalent Diagram

The parameters can be used to make a model of how a loudspeaker works. The model consists of three parts describing the electrical, mechanical and acoustical part of the driver. The description of the equivalent diagrams is based on [8].

Electrical Components

The electrical part can be directly derived from knowledge of the construction of a driver. It consist of a coil and a resistor in series connection. It can be seen in figure 2.2.

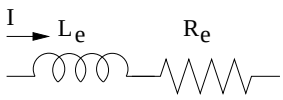

Figure 2.2: *Equivalent diagram of the electrical part of a loudspeaker.*

Mechanical Components

The mechanical part of the model includes the moving parts of the system. That is the membrane assembly, the spider and the suspension. The weight of the moving parts M_m multiplied with the acceleration of the membrane $^{dv}/_{dt}$ describes the force acting on the membrane. v is the velocity of the membrane.
The spider and suspension act as a spring with a total compliance C_m. When the membrane is moved out of its resting position, this spring will pull the membrane to the resting position with a force of $(^{1}/_{C_m}) \int v dt$, where $\int v dt$ is the displacement of the membrane.
Finally there is mechanical loss, R_m. This arises when movement is converted into heat in the suspension and spider of the driver. All the mechanical parts act as forces on the membrane, and they can be added together:

$$v \cdot Z_{mech} = \sum external\ \ forces = M_m \frac{dv}{dt} + r_m v + \frac{1}{C_m} \int v dt \tag{2.2}$$

Laplace transformed:

$$\sum external\ \ forces = sM_m V + r_m V + \frac{1}{sC_m} V \tag{2.3}$$

The external forces is the magnet motor force, $Bl \cdot I$. From the Laplace transformed equation it can directly be seen, that an electrical analogy should consist of a series connection of an inductor, a resistor and a capacitor. This can be seen in figure 2.3 on the next page.

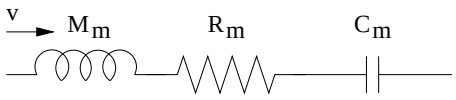

Figure 2.3: *Equivalent diagram of the mechanical part of a loudspeaker.*

Acoustical Components

The acoustical part of the model consists of two forces acting on the membrane. One on the front of the membrane and one on the back. It is only the variance of these forces that should be included in the diagram, since the stationary pressure is the same on both sides of the membrane. The force acting on the membrane is defined as:

$$F = A(p_{back} - p_{front}) \tag{2.4}$$

where A is the area of the membrane. The acoustical equivalent diagram can be seen in figure 2.4. q is volume velocity, which is defined as:

$$q = v \cdot A \tag{2.5}$$

This is used to relate pressure to acoustic radiation impedance:

$$\frac{p_{front}}{q} = \frac{-p_{back}}{q} = Z_r \tag{2.6}$$

where Z_r is the acoustic radiation impedance.

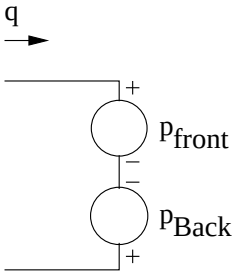

Figure 2.4: *Equivalent diagram of the acoustical part of a loudspeaker.*

The three individual equivalent diagrams can be combined to a complete equivalent diagram for the loudspeaker. The connection between the parts of the diagram is determined by the magnetic force factor Bl and the membrane area A.
The connection from the electrical to the mechanical part is made by a gyrator, with a ratio of Bl:1. The connection between the mechanical and the acoustical part is made by a transformator with a ratio of A:1. The complete equivalent diagram is presented in figure 2.5 on the next page.

2.1.4 Derived Parameters, f_s, Q_t and Vas

The parameters in the previous section gives a description of the loudspeaker driver, but they are not easy to interpret. Therefore the datasheet of a loudspeaker usually contains some derived parameters,

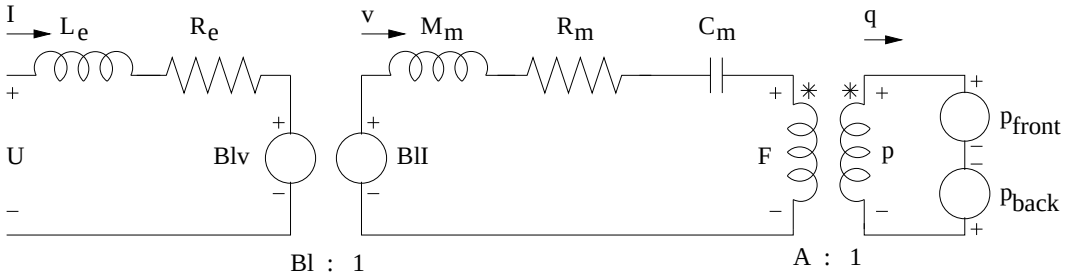

Figure 2.5: *Complete equivalent diagram of a loudspeaker driver.*

namely f_s, Q_t and Vas.
f_s is the free air resonance frequency of the driver. It describes at which frequency the transition between stiffness control and mass control occurs, or in other words at which frequency C_m and M_m cancels each other. This tells how capable a loudspeaker is to produce bass, as it below this frequency rolls of with 12 $^{dB}/_{octave}$, when mounted in an infinite baffle. f_s is calculated as [8, page 19]:

$$f_s = \frac{1}{2\pi \cdot \sqrt{M_m \cdot C_m}} \tag{2.7}$$

f_s is measured in Hz.

Q_t is called the quality of the highpass filter that describes the roll off at low frequencies of a driver in an infinite baffle. It describes the amplitude at the resonance frequency and how steep the first part of the roll off is. Figure 2.6 on the following page shows magnitude and phase responses for second order highpass filters with Q-values from 0.4 to 2.0, all with the same resonance frequency. Q_t is calculated as [8, page 18]:

$$Q_t = \frac{R_e}{R_e \cdot R_m + (Bl)^2} \sqrt{\frac{M_m}{C_m}} \tag{2.8}$$

Q_t is unitless.

Vas is the equivalent volume of the driver. This parameter describes the volume that is needed to achieve the same amount of compliance as the driver has itself. If a driver is mounted in a box with volume *Vas*, it can be derived from equation 2.7 and 2.8, that the resonance frequency and Q_t is increased by a factor of $\sqrt{2}$ compared to infinite baffle. Therefore *Vas* can be used to get an idea of the size of the enclosure needed for a driver. *Vas* is calculated as [11, page 92]:

$$Vas = C_m \cdot A^2 \rho_0 c^2 \tag{2.9}$$

where A is the area of the driver, ρ_0 is density of air and c is the speed of sound in air.
Vas is measured in m^3.

2.1.5 Electrical Impedance

To determine the electrical impedance of a loudspeaker driver, it is most convenient to move everything to the electrical side of the equivalent diagram. This is done by first moving the acoustical parts to the mechanical side, and then moving the mechanical parts to the electrical side.

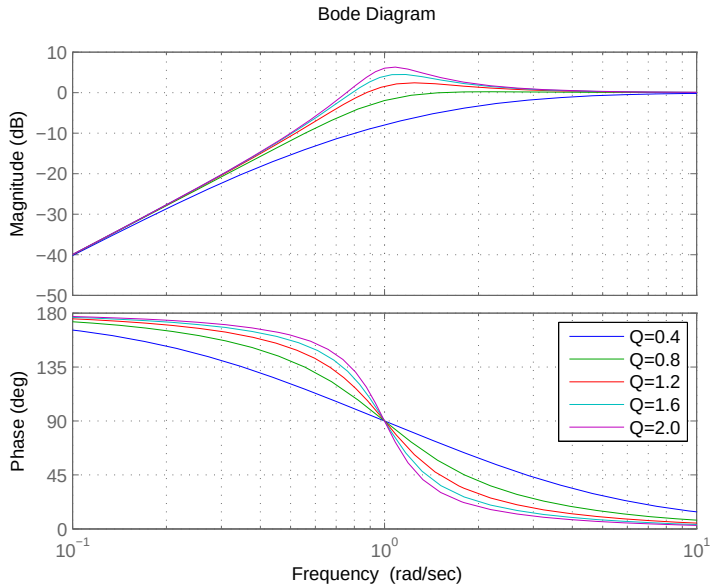

Figure 2.6: *Magnitude and phase response for 2. order highpass filter with Q-values from 0.4 to 2.0.*

When impedances are moved across the transformator between the mechanical and acoustical side, the transformation factor is:

$$Z_{r,mech} = Z_{r,acou} \cdot A^2 \tag{2.10}$$

where $Z_{r,acou}$ is the radiation impedance of the driver and is dependent on how the driver is mounted. The mechanical impedance can be found as:

$$Z_{mech} = j\omega M_m + R_m + \frac{1}{j\omega C_m} + Z_{r,mech} \tag{2.11}$$

To convert everything to electrical impedances all the parts on the mechanical side have to be moved to the electrical side. Since a gyrator is dividing the two sides, the process is:

- Series connections of impedances change to parallel connections of admittances. This means inductors change to capacitors and vice versa.
- Parallel connections change to series connections of admittances. This means inductors change to capacitors and vice versa.
- When moving impedances from the electrical to the mechanical side, first divide by $(Bl)^2$ and then transform to admittance.
- When moving impedances from the mechanical to the electrical side, first transform to admittance and then multiply by $(Bl)^2$.
- Voltage and current are transformed as if it was a normal transformator

By moving all mechanical and acoustical components to the electrical according to the principles mentioned above, the total electrical impedance Z_{tot} can be found as:

$$\begin{aligned} Z_{tot} &= j\omega L_e + R_e + (Bl)^2 \cdot \left(\frac{1}{j\omega M_m} || \frac{1}{R_m} || j\omega C_m || \frac{1}{Z_{r,mech}} \right) \\ &= j\omega L_e + R_e + \frac{1}{\frac{1}{\frac{1}{j\omega \frac{M_m}{(Bl)^2}}} + \frac{1}{\frac{(Bl)^2}{R_m}} + \frac{1}{j\omega C_m (Bl)^2} + \frac{1}{\frac{(Bl)^2}{Z_{r,mech}}}} \end{aligned} \tag{2.12}$$

From equation 2.12 it can be seen that the components from the mechanical side has been transformed into a coil with a value of $C_m(Bl)^2$, a resistor with the value ${}^{(Bl)^2}/_{R_m}$ a capacitor with the value ${}^{M_m}/_{(Bl)^2}$ and an impedance with the value ${}^{(Bl)^2}/_{Z_{r,mech}}$. These components are all connected in parallel and then in series with the original electrical components, as it can be seen in figure 2.7.

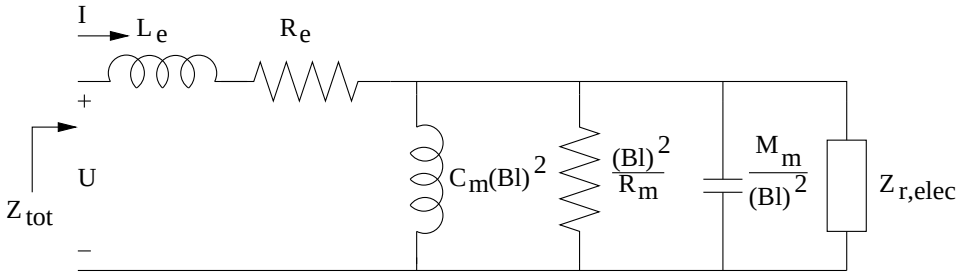

Figure 2.7: *Equivalent diagram of loudspeaker driver, with all components moved to the electrical side.*

The radiation impedance on the electrical side is given as:

$$Z_{r,elec} = \frac{(Bl)^2}{Z_{r,mech}} \tag{2.13}$$

2.1.6 Infinite Baffle

The loudspeaker can be mounted in an infinite baffle to prevent acoustical short circuit between the radiation from the front and the back of the driver. When a driver is mounted in an infinite baffle, the acoustical radiation impedance, $Z_{r,acou}$ is given as [8, page 15]:

$$Z_{r,acou} = \frac{\rho_0 c}{A} \cdot \left(1 - \frac{2J_1\left(\frac{2\omega a}{c}\right)}{\frac{2\omega a}{c}} + j\frac{2H_1\left(\frac{2\omega a}{c}\right)}{\frac{2\omega a}{c}} \right) \tag{2.14}$$

where J_1 is first order Bessel function and H_1 is first order Struve function. This radiation impedance has to be included twice, since there is radiation from both the front and the back of the driver. Figure 2.8 on the following page shows the radiation impedance as a funtion of frequency.

This can be moved to the electrical side using formula 2.10 and 2.13:

$$Z_{r,elec} = 2\,\frac{(Bl)^2}{Z_{r,acou} \cdot A^2} = 2\,\frac{(Bl)^2}{A\rho_0 c \cdot \left(1 - \frac{2J_1\left(\frac{2\omega a}{c}\right)}{\frac{2\omega a}{c}} + j\frac{2H_1\left(\frac{2\omega a}{c}\right)}{\frac{2\omega a}{c}} \right)} \tag{2.15}$$

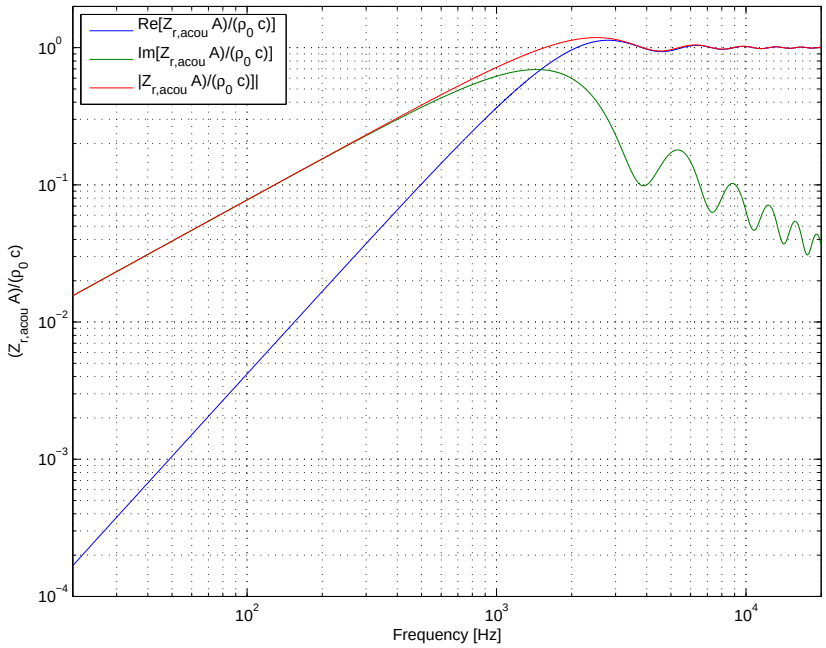

Figure 2.8: *Acoustical radiation impedance, $Z_{r,acou}$. It can be seen that the absolute value of the impedance decreases with 6 $^{dB}/_{octave}$.*

Electrical Impedance

Using the equivalent circuit shown in figure 2.7 on the preceding page and exchanging $Z_{r,elec}$ with the value given in equation 2.15 on the previous page, it is possible to simulate an impedance curve. An example of an impedance curve for a typical 5" driver can be seen in figure 2.9 on the facing page, where the correction of the voice coil inductance, n, has been included as shown in equation 2.1 on page 8. From figure 2.9 on the facing page it can be seen that the peak value of the impedance is at approximately 58 Hz. This is the resonance of the driver. The value of R_e can be found as the minimum value of the impedance curve and where the phase is 0°, at around 500 Hz. Furthermore it can be seen that the impedance rises with increasing frequency. This is caused by the voice coil inductance.

Acoustical Response

To simulate the acoustical response of a loudspeaker, it is most convenient to move all components to the mechanical side. This is shown in figure 2.10 on the next page.

The membrane velocity v can be calculated as the current, electrically seen. When the membrane velocity is known, the volume velocity and the pressure can be found as shown in equation 2.16 and 2.17 [8, page 19].

$$q = v \cdot A \qquad [m^3/s] \tag{2.16}$$

where q is the volume velocity, v is the membrane velocity and A is the effective membrane area. To

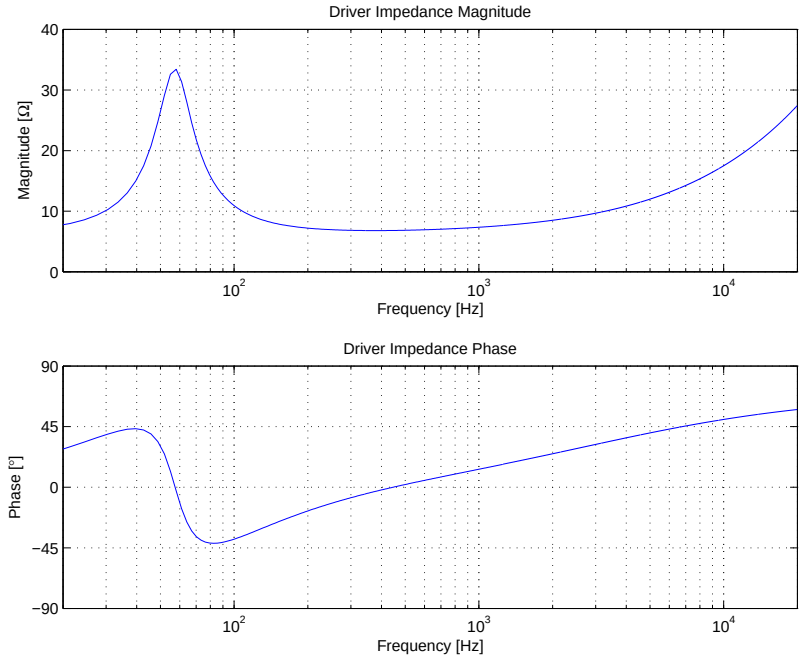

Figure 2.9: *Simulated electrical loudspeaker impedance of an typical 5" driver mounted in an infinite baffle.*

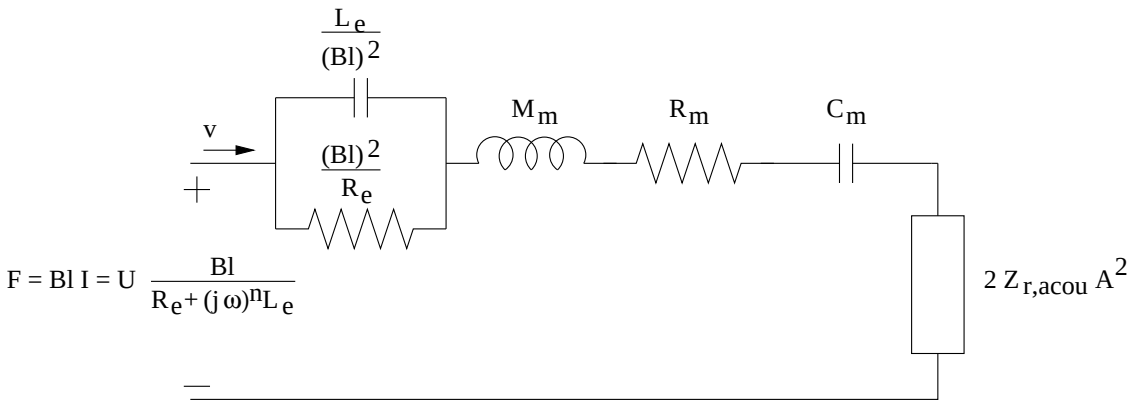

Figure 2.10: *Equivalent diagram of a loudspeaker driver mounted in an infinite baffle, with all components moved to the mechanical side.*

calculate the pressure from the velocity, v, the distance and the area has to be used [8, page 28]:

$$p = \frac{\rho_0 A \cdot v}{2\pi x} j\omega \qquad [Pa] \tag{2.17}$$

where x is the distance to the source from the measurement position. The 2π is used because of the infinite baffle, which causes the loudspeaker to radiate into a hemisphere. Other values could be 4π, describing radiation into free field or $\frac{\pi}{2}$ describing a speaker positioned in a corner.

Figure 2.11 shows the simulated frequency response of a loudspeaker driver mounted in an infinite baffle.

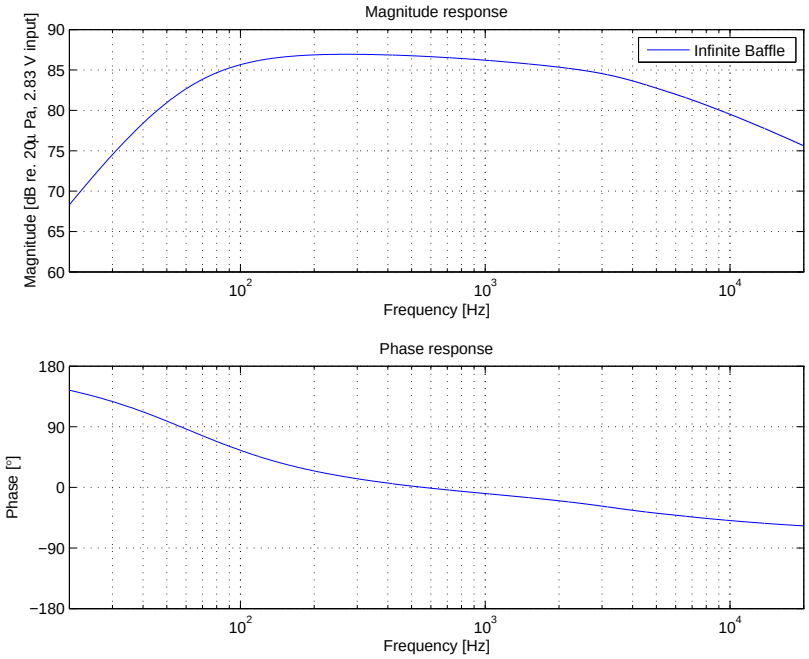

Figure 2.11: *Simulated loudspeaker frequency response from a driver mounted in an infinite baffle, at 1 m. distance.*

From the figure can be seen, that the magnitude decreases below the resonance frequency, at approximately 60 Hz, with a slope of 12 $^{dB}/_{octave}$. This is due to stiffness of the suspension and a decreasing value of radiation impedance, which each contribute with a 6 $^{dB}/_{octave}$ slope. At high frequencies the magnitude decreases with 6 $^{dB}/_{octave}$. This is caused by the voice coil inductance.

2.2 Closed Box Equivalent diagram

A more practical approach to the infinite baffle is the closed box. This is a sealed box with the loudspeaker driver mounted in one of the walls, hence isolating the front and the rear of the loudspeaker. When the loudspeaker driver is mounted in a closed box as shown in figure 2.12, the air in the box will act as a spring, and increase the stiffness of the complete system. A closed box is typically damped with absorbent material, to prevent internal reflections from the box to be radiated out through the driver membrane and to achieve a free field situation at higher frequencies. The radiation impedance into a well damped closed box can be considered the same as if it was radiating into free field, when the absorbtion coefficient of the damping material is above 0.8. [1, Page 219].

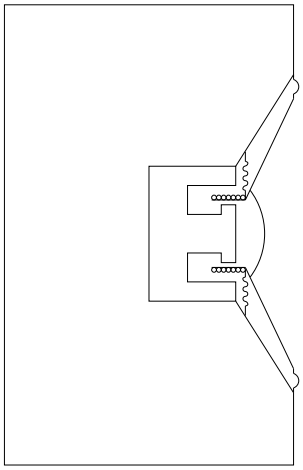

Figure 2.12: *Loudspeaker driver mounted in a closed box.*

The compliance from the cabinet can be represented as a capacitor with a value of C_{box} in series with the other components in the mechanical equivalent diagram, as it can be seen in figure 2.13

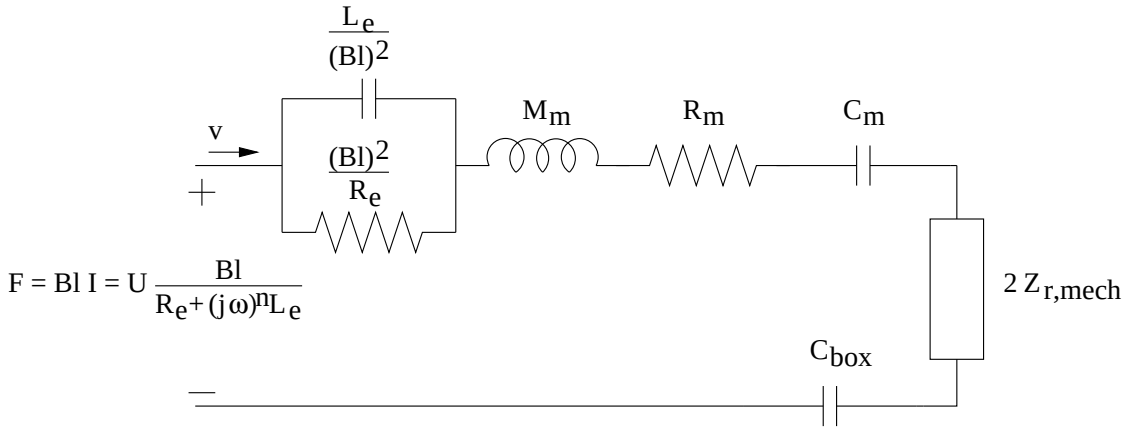

Figure 2.13: *Mechanical equivalent diagram for loudspeaker driver mounted in a closed box.*

The value of C_{box} is given as [11, page 92]:

$$C_{box} = \frac{Volume}{\rho_0 c^2 A^2} \tag{2.18}$$

When the driver is mounted in a box, both the system resonance frequency and the system Q-value is higher compared to the driver mounted in an infinite baffle. The resonance frequency can be calculated as:

$$f_b = \frac{1}{2\pi\sqrt{(M_m + 2 \cdot Im[Z_{r,mech}]) \cdot \left(\frac{1}{C_m^{-1}+C_{box}^{-1}}\right)}} \tag{2.19}$$

The Q-value can be calculated as:

$$Q_b = \frac{R_e}{R_e \cdot (R_m + 2 \cdot Re[Z_{r,mech}]) + (Bl)^2} \sqrt{\frac{(M_m + 2 \cdot Im[Z_{r,mech}])}{\left(\frac{1}{C_m^{-1}+C_{box}^{-1}}\right)}} \tag{2.20}$$

Using equation 2.17 on page 15 and the diagram shown in figure 2.13 on the preceding page it is possible to plot a frequency response of a loudspeaker mounted in a closed box. Figure 2.14 shows a frequency response of a typical 5” driver in a small box along with a frequency response for the same driver in an infinite baffle.

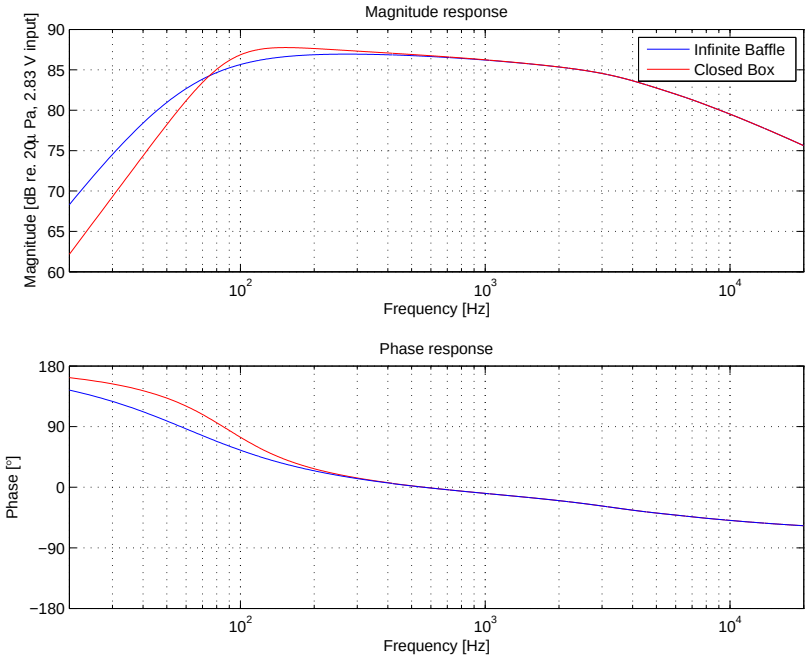

Figure 2.14: *Frequency response of a loudspeaker driver mounted in an infinite baffle and a closed box with an infinite baffle.*

It can be seen, that the box gives an increase in the output near 100 Hz - 200 Hz, and that the roll off begins at a lower frequency but the slope is more steep. At high frequencies the box theoretically does not have any influence.

Figure 2.15 on the facing page shows a simulated electrical impedance of a loudspeaker driver in a closed box. From the figure it can clearly be seen that the resonance frequency moves up in frequency compared to when mounted in an infinite baffle.

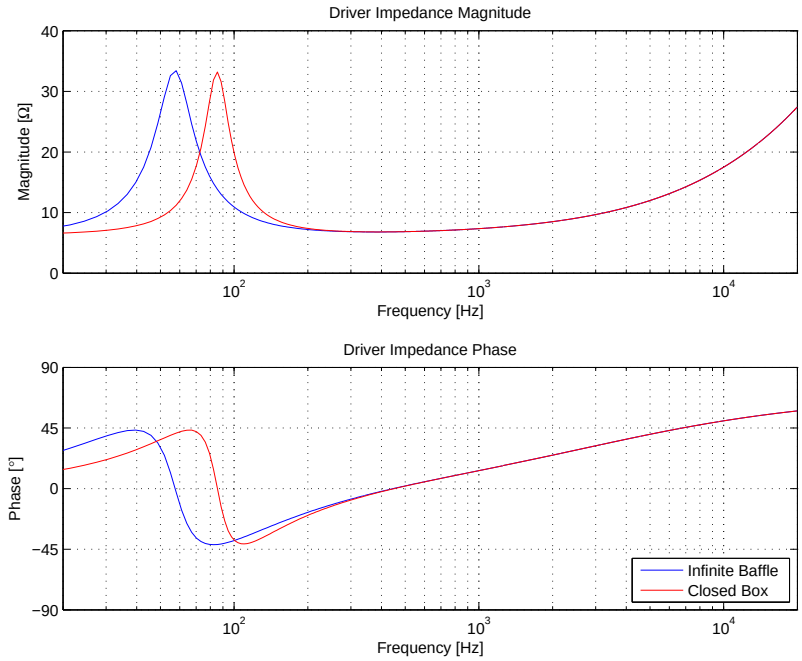

Figure 2.15: *Simulated impedance of a loudspeaker driver mounted in an infinite baffle and a closed box with an infinite baffle.*

2.3 Beaming of Plane Circular Piston

A moving piston starts to beam at wavelengths that are comparable to the piston diameter. It happens because sound waves emitted from different places on the piston do not add up in phase anylonger. Despite that a real loudspeaker diaphragm is not plane, it can be modelled as a circular plane piston. Figure 2.16 shows the geometry of such a piston placed in an infinite baffle.

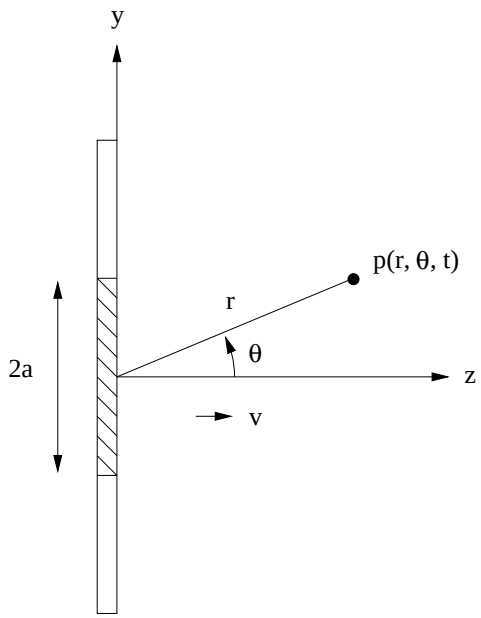

Figure 2.16: *Plane circular piston in infinite baffle.*

p is the pressure at distance r and θ is the listening angle with respect to the normal incidence. a is the radius, and the piston moves uniformly with velocity $v_0 e^{j\omega t}$ in the z-direction. The sound pressure p can be rotated around the z-axis. Assuming that $r \gg a,\ p$ can be calculated as: [6, page 182]

$$p(r,\theta,t) = \frac{j}{2}\rho_0 c v_0 \frac{a}{r} ka \left[\frac{2J_1(ka\ sin\ \theta)}{ka\ sin\ \theta}\right] e^{j(\omega t - kr)} \tag{2.21}$$

where J_1 is the first order Bessel function, and $k = \omega/c$ is the wavenumber. The velocity can be calculated from the equivalent diagram of a loudspeaker. This is done by transffering both the electrical and acoustical parts into the mechanical domain as shown in figure 2.10 on page 15. The velocity can now be calculated as:

$$v = \frac{F}{Z_{mech}} = \frac{U\frac{Bl}{R_e+(j\omega)^n L_e}}{Z_{mech}} \tag{2.22}$$

To demonstrate the outcome of equation 2.21, figure 2.17 on the next page shows the radiation pattern of a piston with radius a = 5 cm. The magnitude is SPL re. 20 μPa at 1m, 2.83V input.

As seen, the dispersion gets more narrow when the frequency goes up. Sidelobes are introduced when ka is close to four. Figure 2.18 on the facing page illustrates the dispersion over the audible frequency range at four specific angles.

As seen, also the on-axis response rolls off at high frequencies. This is due to the voice coil inductance.

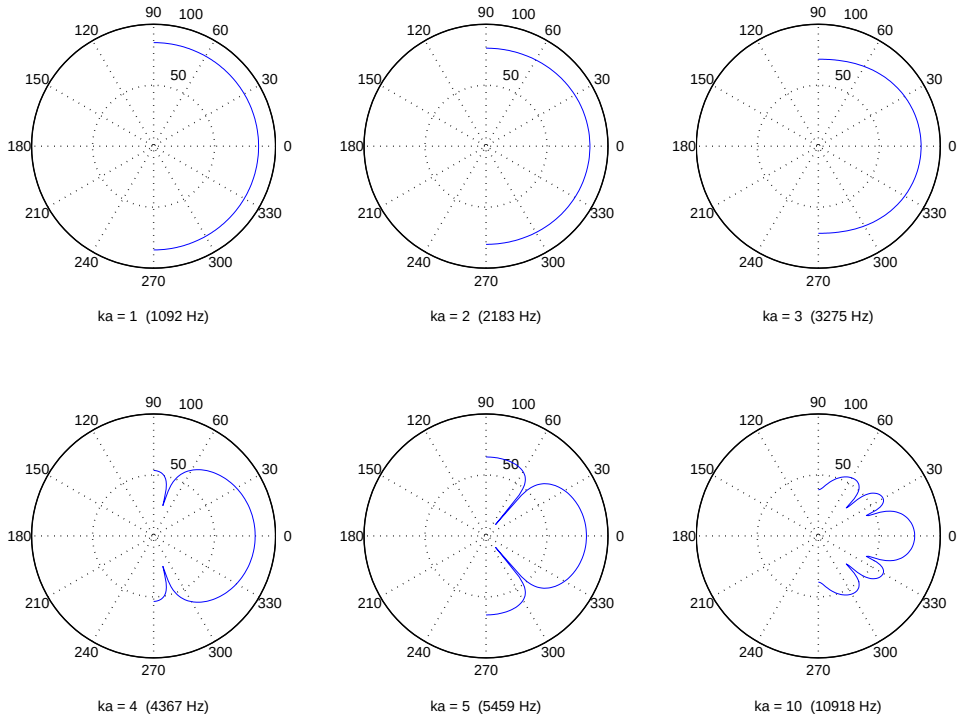

Figure 2.17: *Radiation patterns for a piston with radius a = 5 cm.*

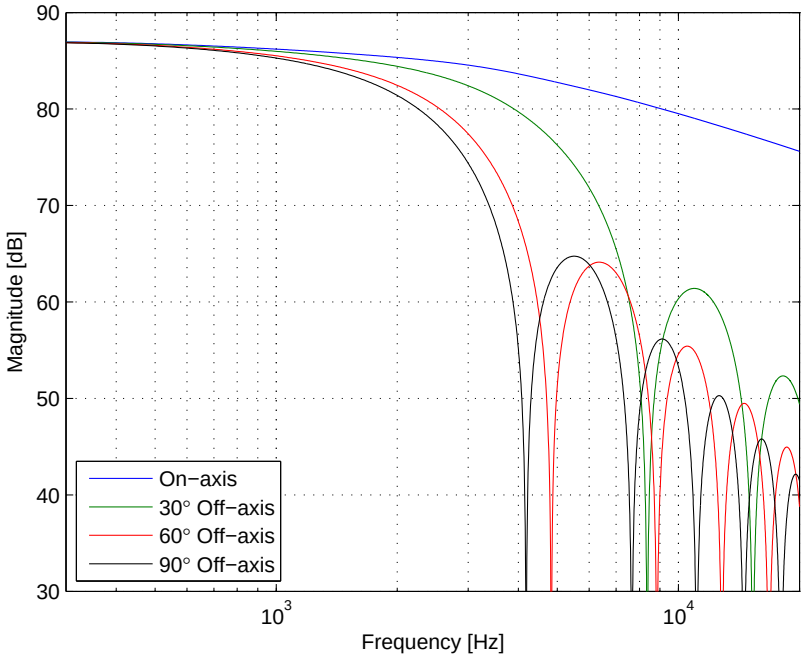

Figure 2.18: *Dispersion for piston with radius a = 5 cm. at 0°,30°,60° and 90° incidence.*

2.4 Crossover Networks and Filter Theory

This section describes general filter theory and the function of the crossover network.

The crossover networks function is to separate the frequencies and send them to the right drivers. For example it has to send the low frequencies to the woofer and the high frequencies to the tweeter. Figure 2.19 illustrates a lowpass, bandpass and highpass filter as it would be in a typical 3-way loudspeaker.

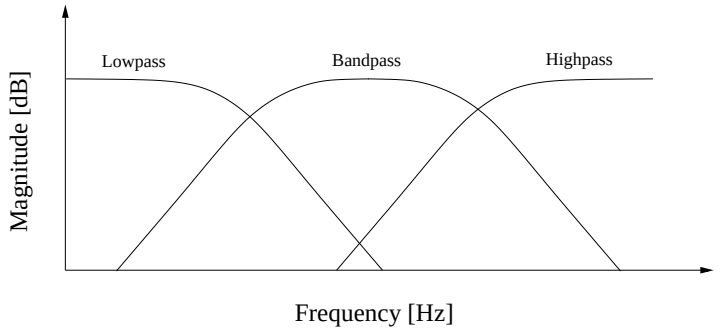

Figure 2.19: *Lowpass, bandpass and highpass in a 3-way loudspeaker.*

A passive filter can be made from coils, capacitors and resistors. Furthermore filters can be made as parallel or series filter, and the number of reactive components determine the filter order. Figure 2.20 shows a second order parallel and series filter [11, page 166].

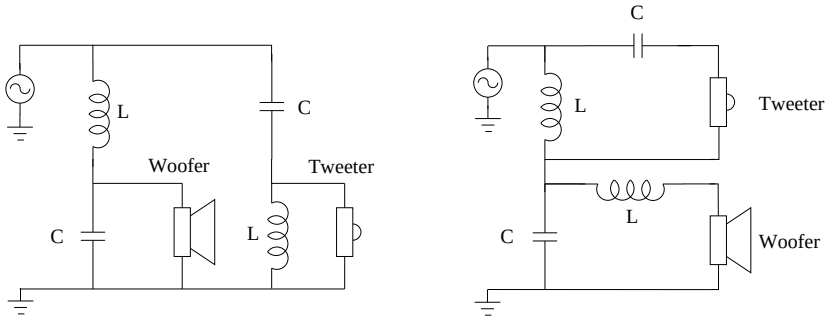

Figure 2.20: *Electrical 2. order parallel and series filter.*

If the driver impedances are assumed resistive, there will be no difference between using the parallel or series connection when focusing on the transfer functions. In real life, driver impedances are complex due to the voice coil and mechanical parts, which introduces differences from a pure resistance. In the series filter, all components influence on all drivers. This means that the woofer impedance will alter the tweeter filter and vice versa. This is not a problem in the parallel filter, which usually makes it the preferred choice [11, page 164].
Furthermore the series filter suffers from problems introduced by back electromotive force (back EMF). The back EMF is a voltage that occurs across the voice coil when it moves in a magnetic field. This means that the tweeter may start moving because of woofer movements.

Filters can generally be described by its roll off steepness, resonance frequency and the Q-value of the filter. The filter slopes can be of different orders, and are typically damping with 6, 12, 18 or 24 dB/octave. The resonance frequency is known as the cut-off frequency, and it describes at which

frequency the filter starts to roll off. The Q-value determines the shape of the filter response at the resonance frequency. Figure 2.21 illustrates Butterworth lowpass filters that roll off with 6, 12 and 18 dB/octave, which correspond to 1., 2. and 3. order electrical filters. The Q-value of a Butterworth filter is $1/\sqrt{2}$, and the cutoff frequency in this example is chosen to 2 kHz.

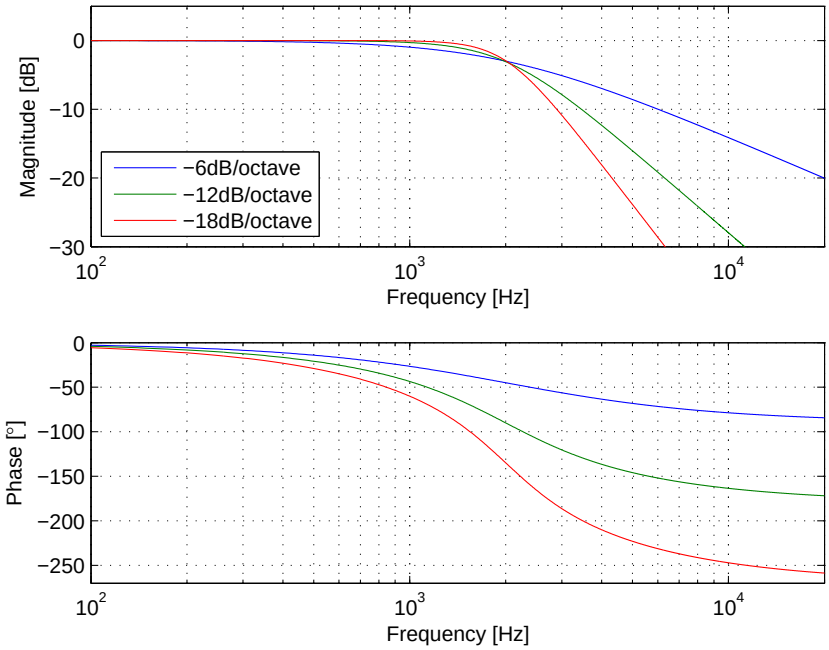

Figure 2.21: *Lowpass filter slopes at -6, -12 and -18dB/octave.*

It can be seen, that the magnitude responses differ near the resonance frequency. This is due to the difference in roll off. The phase is changing more when the filter order increases. On figure 2.6 on page 12 can be seen how different Q-values changes the response at the cut-off frequency.

2.4.1 Filter Summation

When making a complete crossover with a low and highpass filter, it is important that the filters sum in a smooth way. There will always be a certain overlap between the two filter, since practical filters cannot have infinitely sharp slopes. The transition highly depends on the chosen filters. A simple example is the first order Butterworth filter, where the transfer functions are [2, page 234]:

$$T_w(s) = \frac{\omega_w}{s+\omega_w} \quad , \quad T_t(s) = \frac{s}{s+\omega_t} \tag{2.23}$$

When choosing the cut-off frequencies equal for both filters, the summation gives:

$$T_{sum}(s) = T_w(s) + T_t(s) = \frac{\omega_n}{s+\omega_n} + \frac{s}{s+\omega_n} = 1 \tag{2.24}$$

From the result it can be seen, that both the amplitude and phase responses are flat, as shown in figure 2.22 on the next page.

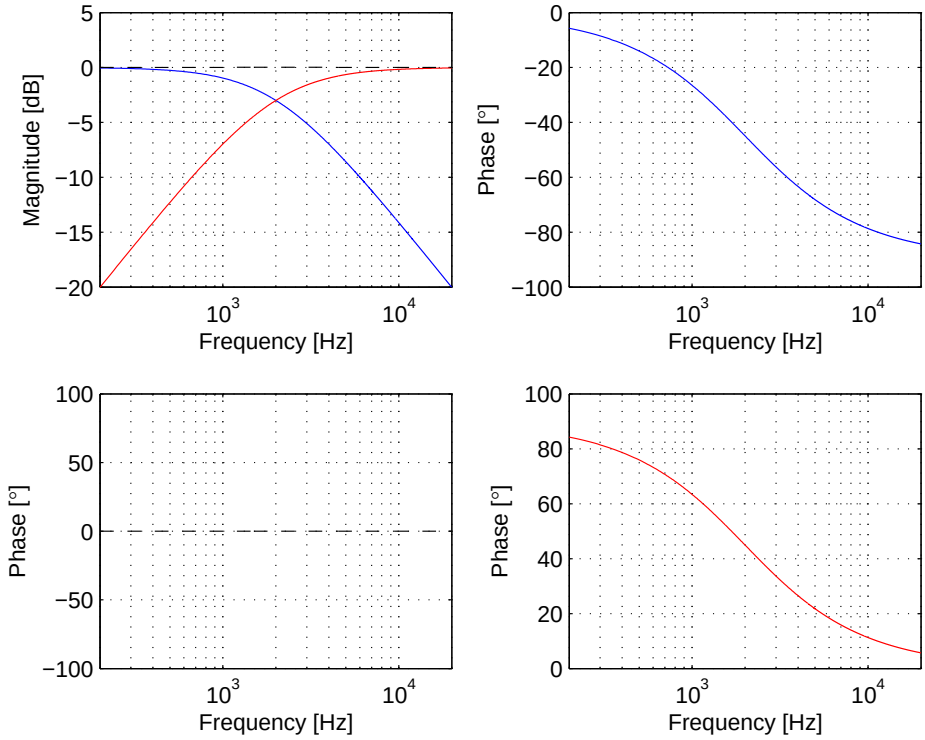

Figure 2.22: *First order Butterworth high and lowpass filters and their summation. The blue curves correspond to the lowpass filter, and the red curves the highpass filter. The black dashed lines are the summed filters.*

As seen, both the magnitude and phase responses of the summation are flat. In the following, the second order Butterworth filter is described. The low and highpass filters can now be calculated as [5, page 567]:

$$T_w(s) = \frac{\omega_w^2}{s^2 + s\frac{\omega_w}{Q_w} + \omega_w^2} \quad , \quad T_t(s) = \frac{s^2}{s^2 + s\frac{\omega_t}{Q_t} + \omega_t^2} \tag{2.25}$$

When using second order filters, the low and highpass filters will be out of phase at the crossover frequency. A way to make the summation better is simply to reverse the polarity of one of the filters. Setting the cut-off frequencies equally, the summed magnitude response is calculated as:

$$T_{sum}(s) = |T_w(s) - T_t(s)| = \left| \frac{\omega_n^2}{s^2 + s\frac{\omega_n}{Q} + \omega_n^2} - \frac{s^2}{s^2 + s\frac{\omega_n}{Q} + \omega_n^2} \right| \tag{2.26}$$

In appendix A on page 109 is shown, that this expression is equal to 1, when the Q-value is set to $1/2$. This implies that the second order Butterworth filter has a non-flat magnitude response since the Q-value is $1/\sqrt{2}$. Figure 2.23 on the next page shows the filters and their summation. The tweeter polarity is reversed.

It is clear, that the summation is not flat anymore. Since the filters are in phase at the -3 dB cut-off frequency, the summation shows a +3 dB bump. The summed phase undergoes a 180° phaseshift.

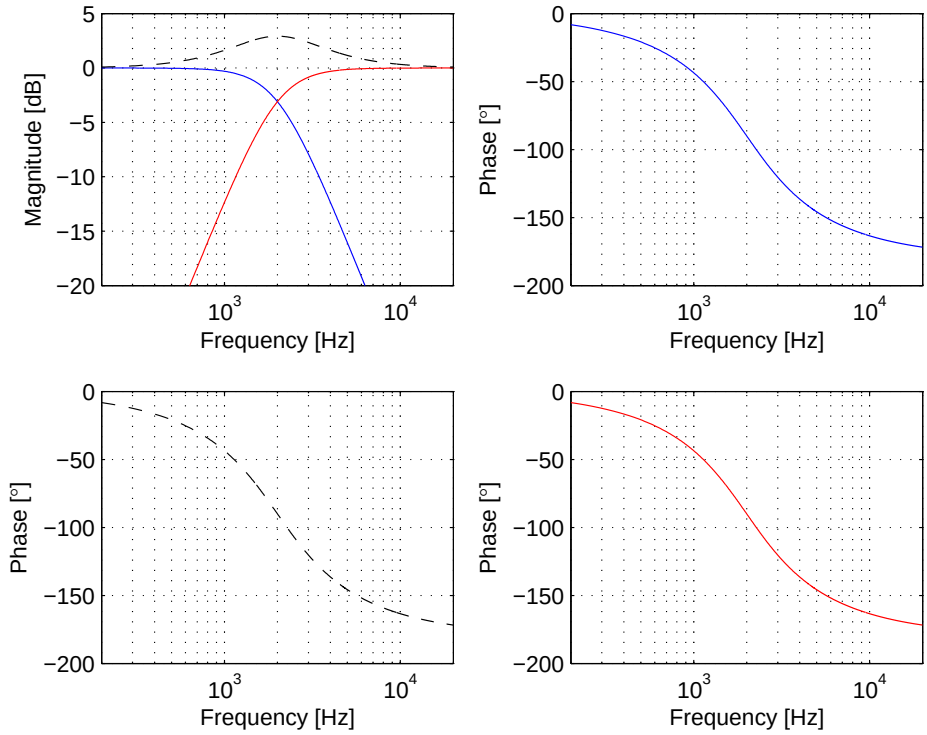

Figure 2.23: *Second order Butterworth high and lowpass filters and their summation. The tweeter polarity is reversed. The blue curves correspond to the lowpass filter, and the red curves the highpass filter. The black dashed lines are the summed filters.*

2.4.2 Driver Attenuation with L-Pad

To match the sensitivities of two drivers, it is possible to attenuate a driver by using a L-Pad circuit, which can be seen on figure 2.24.

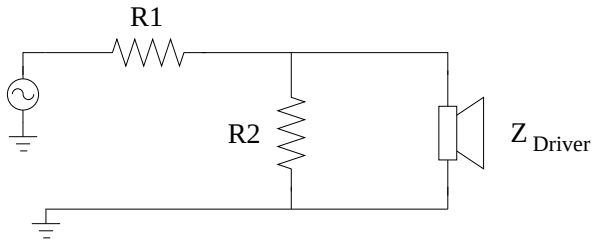

Figure 2.24: *L-Pad attenuation circuit.*

To describe the circuit, two things have to be fulfilled:

$$\text{Attenuation} = \frac{Z_{\text{Driver}} \,||\, R2}{Z_{\text{Driver}} \,||\, R2 + R1} \tag{2.27}$$

$$Z_{\text{Driver}} \,||\, R2 + R1 = Z_{\text{Driver}} \tag{2.28}$$

Equation 2.28 is the impedance seen from the amplifier. The purpose of the circuit is to damp the driver, and to make the amplifier seeing a constant load. R1 and R2 can be calculated from the two expressions when the drivers nominal resistance is known.

2.4.3 Contour Networks

The contour networks can be used to shape the frequency response of a driver. This section describes two different types. Figure 2.25 illustrates a network, which for example can be used to compensate for the baffle step.

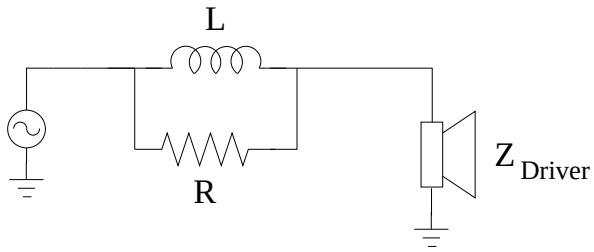

Figure 2.25: *Contour network used for baffle step compensation.*

The voltage transfer function across the driver can be calculated as:

$$H(s) = \frac{Z_{\text{Driver}}}{Z_{\text{Driver}} + R \,||\, sL} = \frac{R + sL}{R + sL + s\frac{RL}{Z_{\text{Driver}}}} \tag{2.29}$$

Figure 2.26 on the facing page shows the response (R=3.3 Ω, L = 2 mH, Z_{Driver} = 8 Ω).

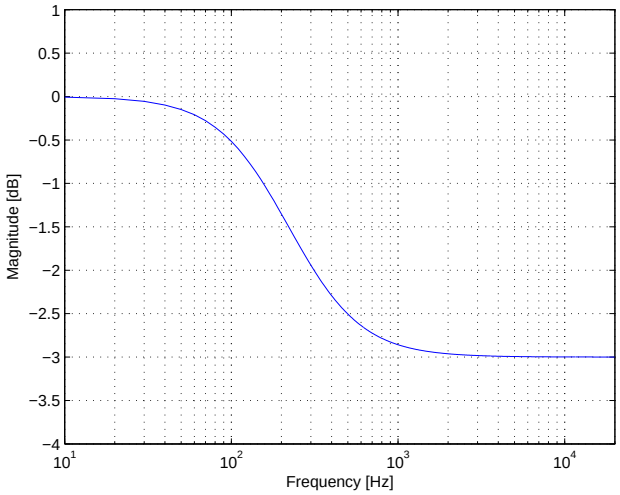

Figure 2.26: *Response of baffle step compensation network.*

Another useful contour network is shown in figure 2.27. It can for example be used to compensate for the tweeter roll off at high frequencies.

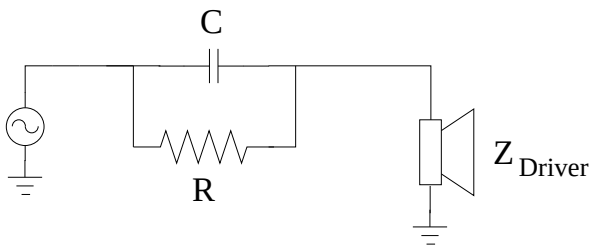

Figure 2.27: *Contour network used for tweeter roll off compensation.*

The voltage transfer function across the driver can be calculated as:

$$H(s) = \frac{Z_{Driver}}{Z_{Driver} + R \,||\, \frac{1}{sC}} = \frac{sRC+1}{sRC+1+\frac{R}{Z_{Driver}}} \tag{2.30}$$

Figure 2.28 on the following page shows the response (R = 3.3 Ω, C = 5 μF, Z_{Driver} = 8 Ω).

2.4.4 Driver Load Compensation

The resonance of a driver introduces a peak in the impedance response, which will influence the filter response. To compensate for that, a series notch filter can be used [3, page 139]. Figure 2.29 on the next page illustrates the series notch filter in parallel with a loudspeaker driver.

The series notch filter is typically used on tweeters, since these may have resonance frequencies near the cutoff frequency of the applied tweeter highpass filter. The notch filter can also be used to reduce or remove a impedance peak on a woofer, but will not be include in the model in this project. To see the function of the series notch filter, Z_{in} is calculated as:

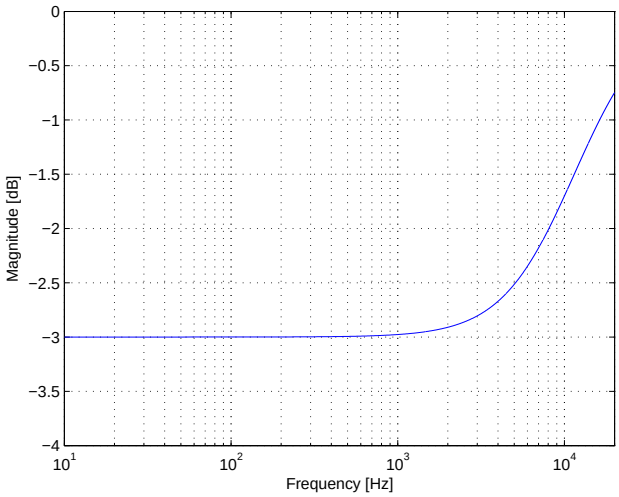

Figure 2.28: *Response of tweeter roll off compensation network.*

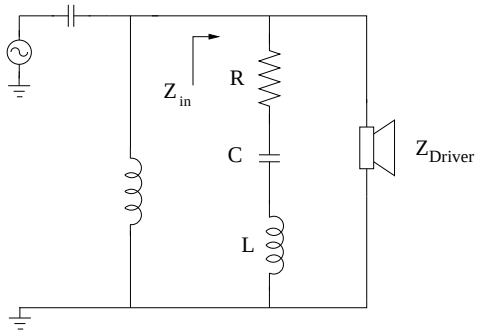

Figure 2.29: *Series notch filter to compensate for driver impedance peak.*

$$Z_{in}(s) = \left(R + \frac{1}{sC} + sL\right) \;||\; \mathrm{Z_{Driver}} \tag{2.31}$$

Figure 2.30 shows Z_{in} when $\mathrm{Z_{Driver}}$ = 8 Ω, R = 8 Ω, C = 25.33 μF and L = 1 mH. This gives a resonance at 1 kHz, where C and L cancel each other. The resistance becomes 4 Ω since two 8 Ω resistors now are parallel connected.

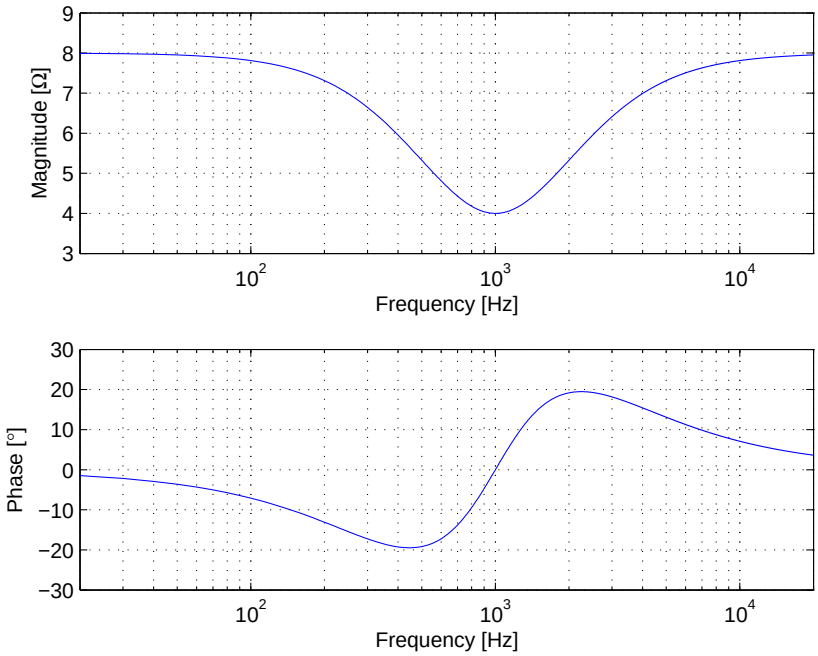

Figure 2.30: *Plot of Z_{in} for a driver load compensation circuit.*

This example would be able to reduce or eliminate an impedance peak of a driver at 1 kHz.

2.4.5 Driver Impedance Influence on Filter Response

The impedance of a real driver is not a constant 8 Ω resistor. It has a peak at the driver resonance, and the voice coil introduces a rice in the impedance at higher frequencies. Figure 2.31 on the next page illustrates the response of a 2. order Butterworth lowpass filter with a cutoff frequency at 2 kHz. The figure shows a curve calculated with an 8 Ω resistor and a curve calculated on a simulated impedance.

It can be seen, that the measured impedance changes the response of the filter. This is expected and it is important to take this into account in the modelling.

2.4.6 Filter Design

- The filter cut-off frequency should be chosen proporly according to the driver dispersion. Also the driver resonance frequency should lay within the filter stopband, except for bass drivers.
- The acoustical center offset should be taken into account when designing the crossover. Avoid wave cancellations in the listening position.

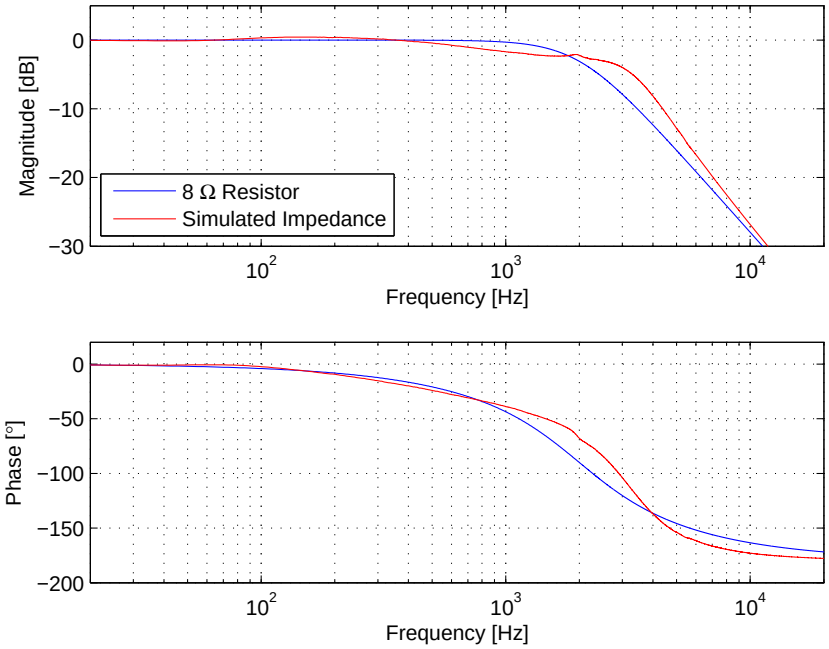

Figure 2.31: *Response of lowpass filter when calculated on 8 Ω resistor or simulated impedance.*

- All filters can be realized by active filters. These will not be described in this project.

2.5 Acoustical Driver Interference

This section describes the radiation interference pattern, that occurs when two sound sources radiate close to each other.

2.5.1 Interference

Interference is known as situations where two waves either add up in a constructive or deconstructive way. This happens when for example two sound sources produce the same signal. At some points in space there will be constructive interference, and in other points deconstructive interference. To describe the behavior of the pattern, it will be presented by summation of two simple sources. Equation 2.32 shows how the pressure p depends on distance r for a pulsating sphere [6, page 171]:

$$p(r,t) = \frac{A}{r} e^{j(\omega t - kr)} \tag{2.32}$$

where A is the amplitude and k is the wavenumber. To simplify the derivations, lets assume that two pulsating spheres are placed on the same vertical line. This is illustrated in figure 2.32.

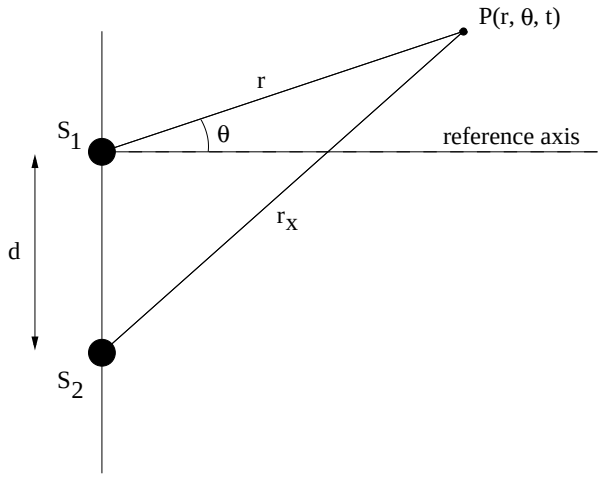

Figure 2.32: *Illustration of interference scenario.*

The reference axis is chosen to be in front of S_1. Therefore the distance to S_1 from the point P will always be r when moving P on a circle or spherical surface centered at S_1. The two sources can be described as:

$$p_1(r,t) = \frac{A}{r} e^{j(\omega t - kr)} \quad , \quad p_2(r_x,t) = \frac{A}{r_x} e^{j(\omega t - kr_x)} \tag{2.33}$$

To calculate the pressure in point $P(r,\theta,t) = p_1(r,t) + p_2(r_x,t)$, the distances r and r_x have to be known. The distance r is a chosen distance, and r_x can be calculated as:

$$r_x = \sqrt{d^2 + r^2 - 2dr \cdot cos\left(\frac{\pi}{2} + \theta\right)} \tag{2.34}$$

which can be derived by use of the cosine relation. In a 2-way loudspeaker, the interference pattern is most pronounced at the crossover frequency. At this frequency, the two drivers produces sound at the

same level. If the lowpass and highpass filter were infinitely sharp, and had no overlap, no interference would excist. This is not practical possible, so the interference has to be taken into account. In the following simulations, the sound sources have the same amplitude, as was it simulated at the crossover frequency. Figure 2.33 illustrates the interference pattern at two different frequencies (a and b) and three different separation distances *d* (a, c and d). The sources are radiating in-phase.

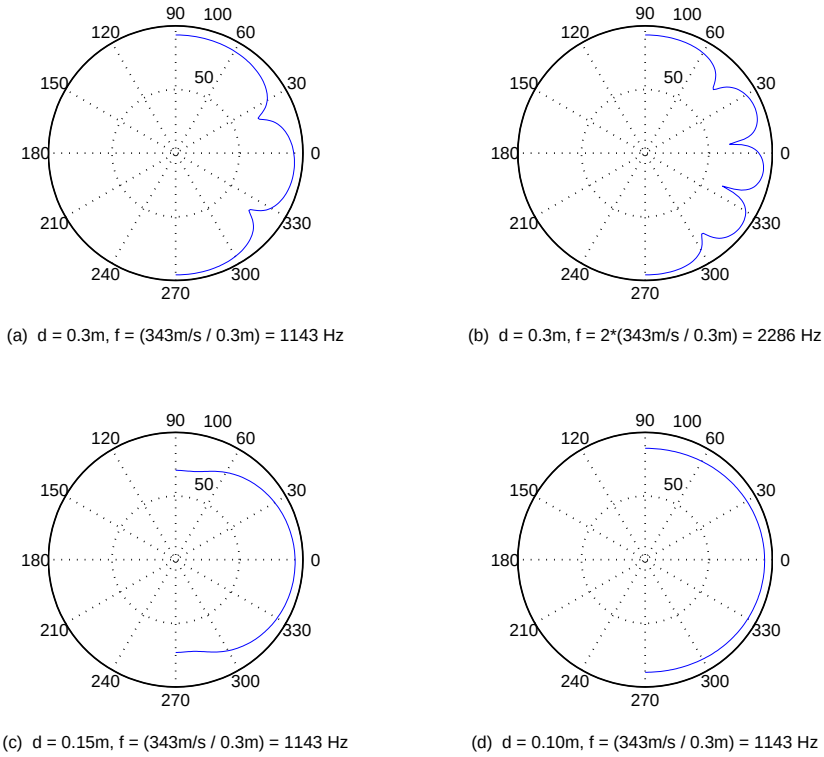

Figure 2.33: *Illustration of interference pattern for different frequencies and source distances d. The levels are in SPL re. 20 μPa.*

The simulations are at r = 1m, and the amplitudes A are equal to 0.5 pascal. As seen on figure 2.33(a), the wave cancellations occur with a spread of approximately 60° when the wavelength is equal to d. The main lobe is pointing a little downwards, since the reference axis is in front of S_1 and not centered between the two sources. This is chosen, since the final measurements will be carried out with reference to the tweeter height. The cancellation level is not infinitely small, which means that the two source levels are not the same at out-of-phase positions. By looking at figure 2.33(b) it can be seen, that when moving up in frequency the interference pattern has more peaks and dips. In figure 2.33(c) the frequency is equal to situation (a), but d is now smaller. As can be seen, this makes the mainlobe wider. Figure 2.33(d) illustrates the situation at d = 0.1 m. The radiation pattern is now close to omni-directional. From this can be concluded, that to minimize interference, a low crossover frequency is needed together with a short source separation distance d. These two factors are always limited by practical reasons. To get a better idea of how the interference pattern behaves, figure 2.34 on the facing page illustrates the interference pattern as function of both frequency and angle. The separation distance d is equal to 0.3 m.

As expected, the amount of peaks and dips gets larger when increasing the frequency and listening

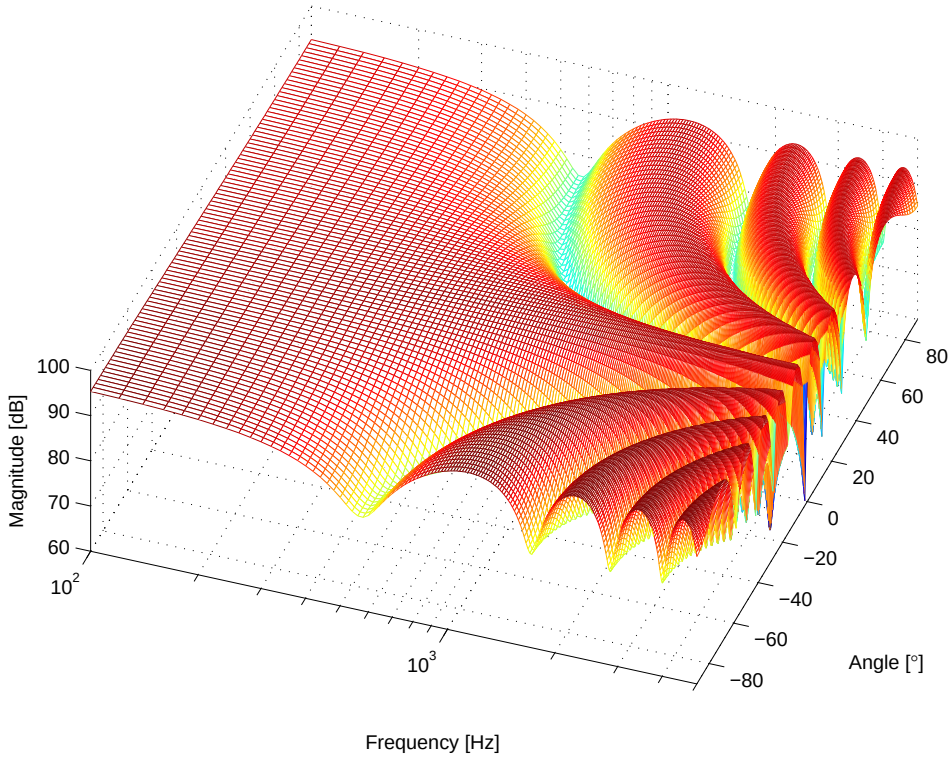

Figure 2.34: *Illustration of interference pattern as function of frequency and angle. $d = 0.3$ m.*

angle.
In the final model, the interference pattern will be described in three dimensions. This will add the interference pattern at horizontal off-axis positions.

2.5.2 Interference and Acoustic Center Offset

In a 2-way loudspeaker consisting of a woofer and tweeter, there will often be an acoustic center offset between the two drivers if they are mounted on a plane baffle. This is the scenario illustrated on figure 2.35.

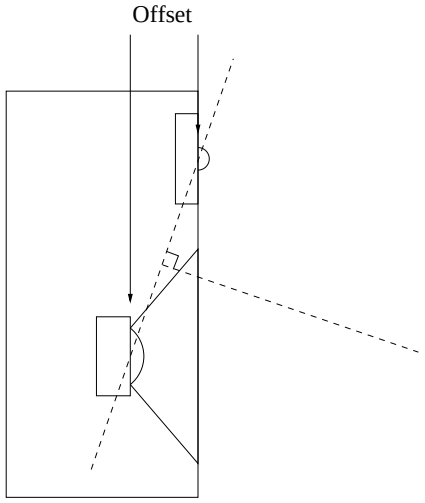

Figure 2.35: *Illustration of acoustic center offset. The woofer acoustic center is behind the one of the tweeter because of the physical construction.*

The offset is caused by differences in the physical constructions. The woofers acoustic center is behind the one of the tweeter. According to [3, page 113], the acoustic center of a driver is dependent on frequency. This is the case since the group delay of a loudspeaker driver is larger near the resonance frequency, since the group delay is derived from the drivers phase response. An approximation is to assume that the acoustic center is in the center of the voice coil [3, page 114]. In figure 2.35 can be seen, that the consequence is an interference mainlobe that points downwards. Figure 2.36 on the next page shows how an acoustic center offset of 3 cm. influences the interference pattern. In the simulation, the acoustic center S_2 is moved 3 cm. behind the tweeter acoustic center.

As expected, the mainlobe is moved downwards. The upper cancellation angle is moving closer to the reference axis because of the offset. The sound pressure at 0° is attenuated 2 dB compared to the situation without any offset. In the simulation of the acoustic center offset, the sound source S_2 is added a simple delay, implemented as $e^{-j\omega T}$. Since the acoustic center offset influences the radiation pattern of a loudspeaker, it will be included in the modelling. The acoustics center offset should be determined at the crossover frequency, where the interference has strongest influence.

In the final model, the interference pattern will be calculated based on sound sources acting as beaming pistons.

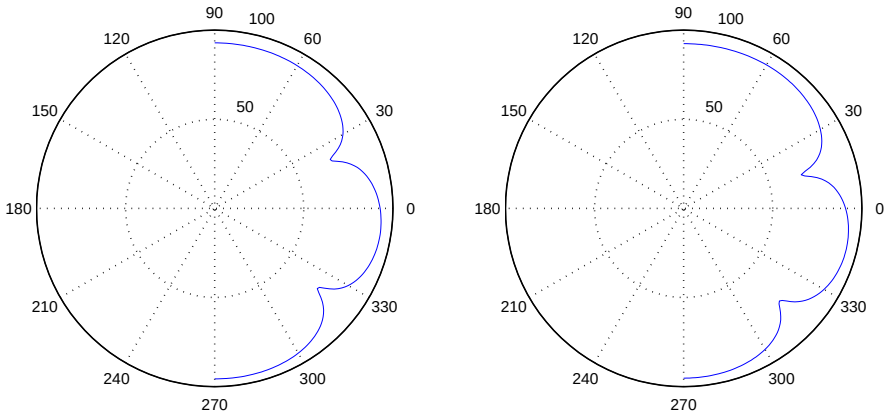

Figure 2.36: *Illustration of interference pattern. Situation (a) is without acoustic center offset. Situation (b) is with an acoustic center offset of 3 cm. The levels are in SPL re. 20 µPa. $r = 1$ m.*

2.6 Cabinet Edge Diffractions

Moving a loudspeaker driver from an infinite baffle to a loudspeaker cabinet makes a significant change in the radiation pattern. The box introduces a baffle step which is a matter of edge diffractions. The baffle step is introduced because the radiation space changes with frequency. At low frequencies, where the wavelength is assumed much larger than the baffle dimensions, the radiation will be into a 4π space. When the wavelength get smaller and within the width of the front baffle the radiation becomes into a 2π space. This change will introduce a theoretically 6 dB sound pressure level increase. In practice it will be less, since the box dimensions will not be invisible to even a 20 Hz tone.
At high frequencies, the cabinet edges introduce peaks and dips in the frequency response. Figure 2.37 illustrates the baffle step and high frequency diffractions.

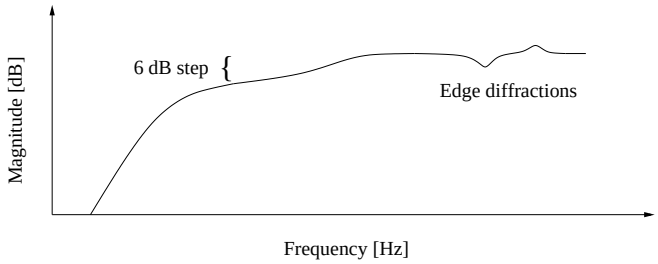

Figure 2.37: *Illustration of 6 dB baffle step and high frequency diffractions.*

2.6.1 Diffraction Theory

The theory is based on [9] and will be presented with focus on cabinets with 90° angled corners. Furthermore it is assumed that the sound source is flush mounted on the front baffle. Figure 2.38(a) and (b) illustrates how the emitted sound travels from the source *S* to the left cabinet edge, and then the diffracted sound to the observation point *P*.

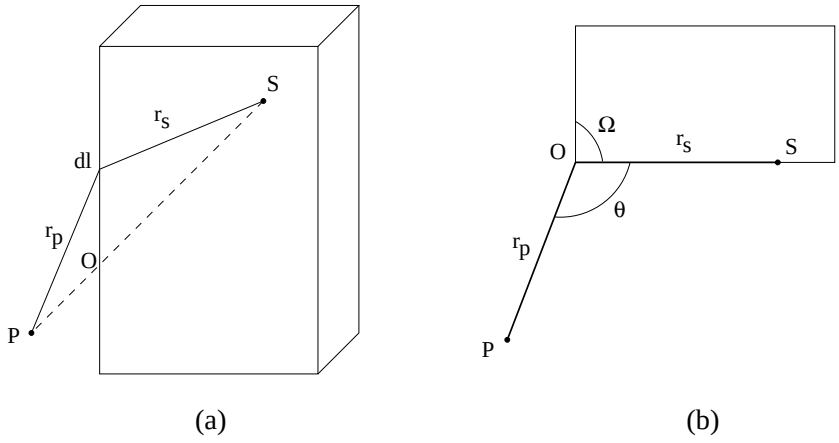

Figure 2.38: *Illustration of cabinet edge diffraction. Figure (a) shows a frontal view, and figure (b) shows a top view.*

The wedge angle Ω is 90°. The angle θ is the observation angle, and it is calculated only from coordinates in the horizontal plane according to the theory. A parameter *v*, which will be used later, and which is related to the open angle of the wedge is defined by

$$v = 2 - \frac{\Omega}{\pi} \tag{2.35}$$

Since the sound source is flush mounted, the sound source pressure is given by

$$p_s = \frac{2}{R}\, e^{-jkR} \tag{2.36}$$

which is the same as a point source with an amplitude of 2. $k = \omega/c$, is the wavenumber. The diffracted field contribution dp_d at P due to the element of length dl a distance l from O can be calculated as

$$dp_d = F(\theta)\, \frac{e^{-jkr_s}}{r_s}\, \frac{e^{-jkr_p}}{r_p}\, \frac{dl}{2\pi} \tag{2.37}$$

where $F(\theta)$ is an angle-dependent factor given by

$$F(\theta) = \frac{\frac{2}{v}\, sin\, \frac{\pi}{v}}{cos\, \frac{\pi}{v} - cos\, \frac{\theta}{v}} \tag{2.38}$$

By combination of equation 2.36 and 2.37 it is possible to simulate the sound from a sound source placed on a loudspeaker baffle.

2.6.2 Shadow Boundary

As mentioned, the diffraction strength depends on the distance, phase, wedge angle and the observation angle θ. In the following, the angle-dependent factor will be described. Figure 2.39 shows the angle factor $F(\theta)$ as a function of observation angle θ. The wedge angle is set to 90°.

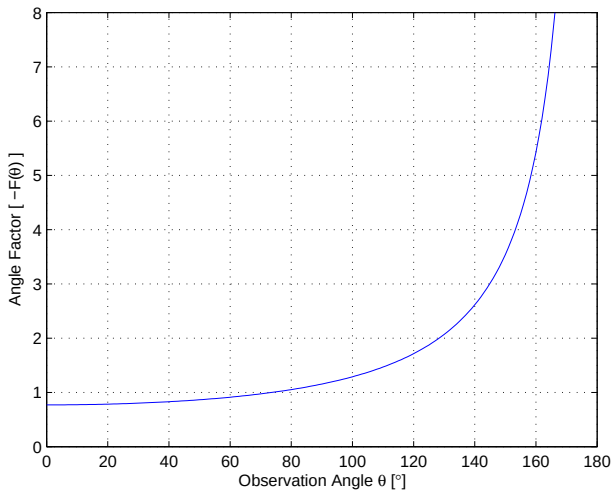

Figure 2.39: *Plot of angle-dependent factor $F(\theta)$ as function of observation angle θ. Notice that it is $-F(\theta)$.*

As can be seen, the diffraction strength is very dependent on the observation angle. The edge diffraction amplitude increases with increasing observation angle. When θ approaches 180°, the amplitude becomes infinite, which can be seen from both equation 2.38 and figure 2.39. This angle represents

what is called the shadow boundary. It is unnatural that the amplitude goes to infinity near the shadow boundary, so the theory does not apply well close to the boundary. According to [9, page 927] the theory is valid when the angle away from the shadow boundary is at least

$$tan^{-1}\left(\sqrt{\frac{\lambda}{d}}\right) \tag{2.39}$$

where d is the distance between the source and the edge. Table 2.1 presents the minimum angles according to five different frequencies. Also the resulting maximum observation angle θ is presented. The distance d is chosen to 10 cm.

Frequency	Minimum Angle	Maximum Observation Angle θ
100 Hz	80°	100°
500 Hz	69°	111°
1 kHz	62°	118°
5 kHz	40°	140°
10 kHz	30°	150°

Table 2.1: *Angles for which the diffraction theory suffices.*

It can be seen, that when simulating the diffractions at 28° off-axis, the simulation will only be valid down to 1 kHz. Generally, the maximum observation angle gets smaller when decreasing the frequency. The theory is made with an high-*kr* approximation. Therefore the theory should not be trusted at low frequencies [9, page 931].

2.6.3 Implementation

The implementation is carried out in the time domian, and is based on equation 2.37 on the previous page. Each edge of the front baffle is subdivided into segments, which have to be smaller than the smallest wavelength of interest. All these edge contributions are then added to the direct sound, given in equation 2.36 on the preceding page. Since the implementation is made in the time-domain, equation 2.36 and equation 2.37 on the previous page both have to be inverse Fourier transformed:

$$p_s(t) = \frac{1}{2\pi}\int_{-\infty}^{\infty}\left(\frac{2}{R}\,e^{-jkR}\right)e^{j\omega t}\,d\omega = \frac{2}{R}\,\delta\left(t-\frac{R}{c}\right) \tag{2.40}$$

$$dp_d(t) = \frac{\frac{2}{\nu}\,sin\,\frac{\pi}{\nu}}{cos\,\frac{\pi}{\nu}-cos\,\frac{\theta}{\nu}}\cdot\frac{\delta[t-(r_s+r_p)/c]}{r_s r_p}\cdot\frac{dl}{2\pi} \tag{2.41}$$

The size of the segments dl, is given by the sampling frequency. The distance-resolution is calculated as:

$$dl_{resolution} = \frac{c}{f_s} \tag{2.42}$$

where f_s is the sampling frequency. The sampling frequency is chosen to 100 kHz, which results in $dl_{resolution} = 3.43$ mm. This resolution is considered acceptable. The diffraction, contributed from

each segment, is then calculated by equation 2.41 on the facing page. Because of the discretized time resolution of $1/f_s$, the calculated continuous time delay has to be converted into an integer sample number. The continuous time delay $t_{con.\ delay}$ is calculated as:

$$t_{con.\ delay} = f_s \cdot \frac{r_s + r_p}{c} \tag{2.43}$$

This delay is then splitted into the previous and next sample by rounding $t_{con.delay}$ down and up. This way, two edge diffraction contributions are added, together describing the diffraction contribution for the continuous time delay $t_{con.delay}$. The diffraction pressure amplitudes at $t_{previous}$ and t_{next} are then assigned values corresponding to the distance from the point $t_{con.delay}$. Figure 2.40 illustrates the scenario.

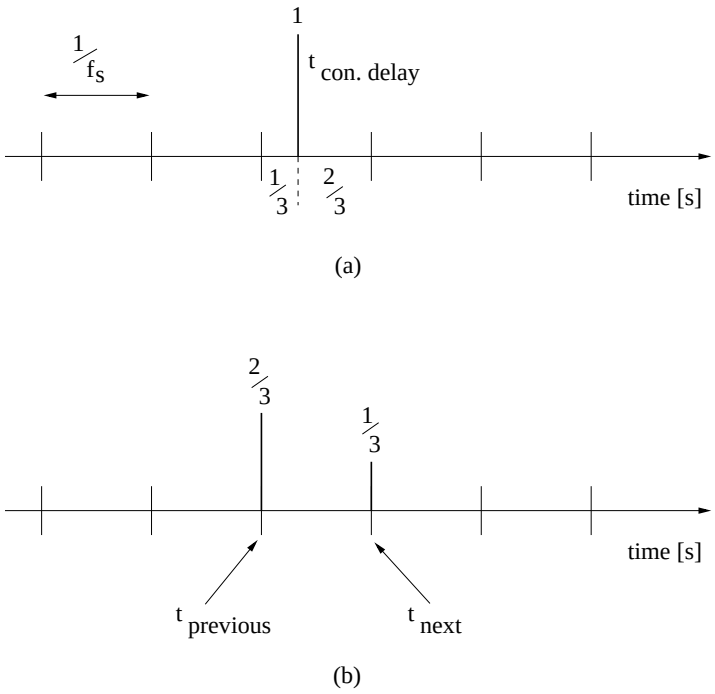

Figure 2.40: *Illustration of how edge segment contribution points are positioned in time. The new positions are based on the calculated continuous time delay* $t_{con.\ delay}$. *Figure (a) shows the situation when* $t_{con.\ delay}$ *has been calculated having an amplitude of 1. Figure (b) shows the situation after the splitting with* $t_{previous}$ *and* t_{next} *sharing the amplitude of* $t_{con.\ delay}$.

All edge contributions are finally positioned in an impulse response at the position corresponding to the time delay in number of samples.

In order to be able to simulate low frequencies, it is necessary to include both 1., 2. and 3. order reflections. This is carried out to be able to simulate the baffle step, which is positioned in the low frequency range. According to [9, page 931], the low frequency simulations still have deviations despite that 3. order reflections have been included. Furthermore it has been shown that 3. order reflections from the back of the cabinet have very little influence on the net response. The simulations are therefore only taking into account the edges at the front baffle.

2.6.4 Simulations

This section presents simulations based on the edge diffraction model. The simulations are made from a front baffle as illustrated in figure 2.41, where the sound source is placed in the center of the baffle. In this situation, the diffractions from the two vertical sides will add up in-phase, and the top and bottom edges the same.

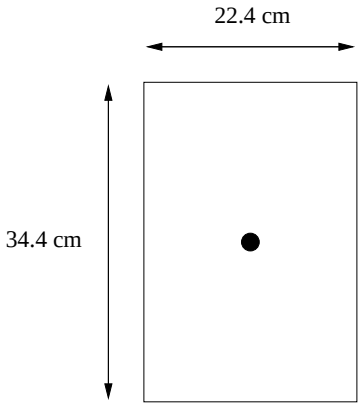

Figure 2.41: *Front baffle used for simulations of edge diffractions.*

The first simulation is made by placing the microphone 1 m away right in front of the sound source, which radiates sound with a pressure of 1 Pa. Figure 2.42 shows the time and frequency plot simulation.

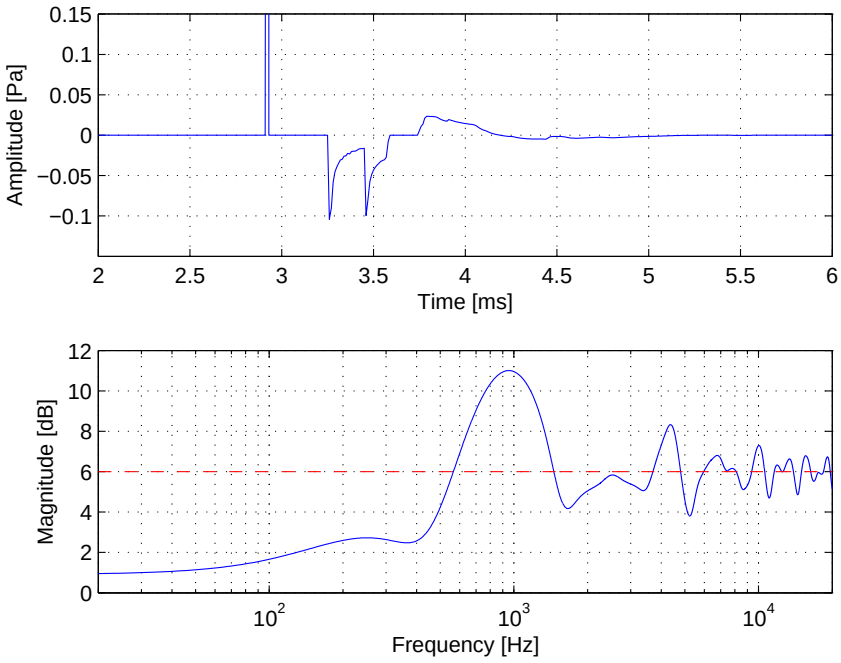

Figure 2.42: *Edge diffraction simulation. Microphone at 1 m distance in front of the sound source.*

As can be seen in the time plot, the direct sound is delayed with 2.9 ms corresponding to the 1 m distance. The amplitude of the direct sound is 2 Pa. The next two peaks are negative, and they come

from the first order reflections, which are reflections that only hit one edge. It can also be seen, that the amplitudes of the first order reflections are much smaller compared to the direct sound amplitude. The following positive amplitudes are caused by 2. order reflections, and the amplitudes are smaller compared to the 1. order reflections. Finally the 3. order reflections gives negative and even smaller amplitudes.
The frequency plot looks like expected. There are peaks and dips at high frequencies, and the baffle step is clearly seen. At low frequencies the magnitude approaches 0 dB and becomes 6 dB when increasing the frequency. The small dip from 300 Hz - 500 Hz is an error introduced by the theory [9, page 931]. Still the results at low frequencies should be considered carefully, since the theory is based on high-*kr* assumptions. At high frequencies the magnitude is dominated by peaks and dips around a level of 6 dB. It is noteworthy that the magnitude change is close to 10 dB from the lowest magnitude at 20 Hz to the highest magnitude at 950 Hz.
The next simulation is made by moving the microphone 30° off-axis in the horizontal plane. Figure 2.43 shows the results.

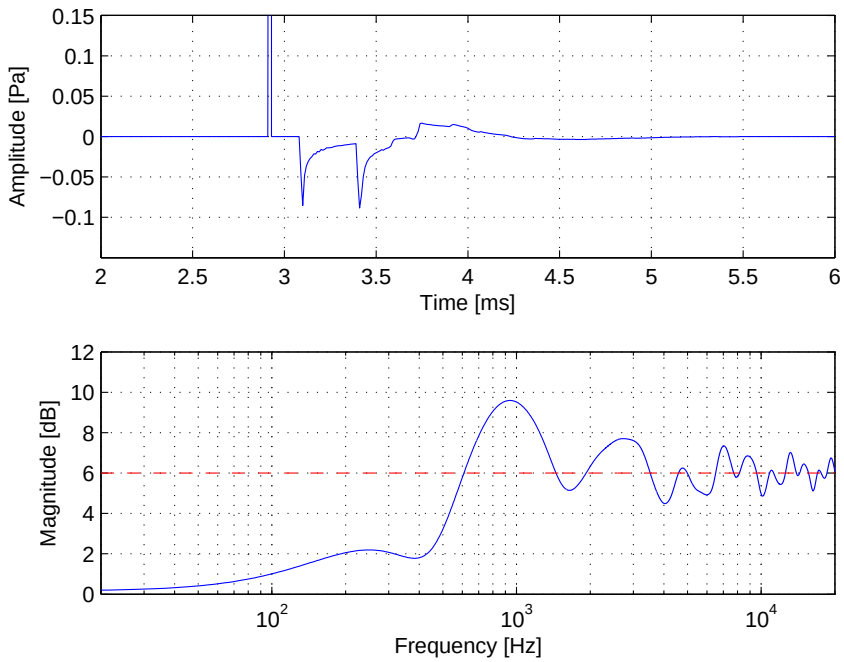

Figure 2.43: *Edge diffraction simulation. Microphone at 1m distance 30° off-axis in the horizontal plane.*

It can be seen, that the tendencies are similar to the on-axis situation. The first order reflections are not as delayed compared to the on-axis situation. At low frequencies there is a small deviation compared to the on-axis situation. According to equation 2.39 on page 38, the theory is not valid below approximately 1 kHz at observation angles above 118°, which correspond to 28° off-axis. Despite that, the result at figure 2.43 still seems to be reliable when compared to the on-axis result. At high frequencies, a peak at 2.9 kHz is now more pronounced compared to the on-axis response, and the peak at 4.2 kHz at the on-axis response is flattened out in the off-axis response.

In practice, the diffraction at high frequencies will not be as pronounced as shown in the simulations. This is due to the fact that sources beam at high frequencies, and therefore less sound will hit the

cabinet edges. The worst case scenario is when placing the source equidistant from all edges. This way all the diffractions sum up in-phase.

2.7 Loudspeaker Placement in Rooms

This section describes briefly how a rigid surfaced room influences the sound of a loudspeaker. The situation changes according to the placement of the speaker in the room. To make this more clear, a description of standing wave patterns and floor reflections are presented.

2.7.1 Standing Waves

To explain how standing waves occur, consider a rectangular room as illustrated in figure 2.44

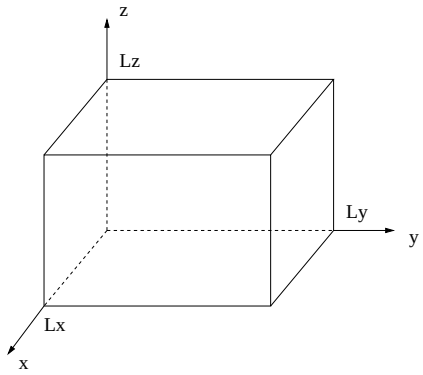

Figure 2.44: *Rectangular room with dimensions Lx, Ly and Lz.*

The standing waves, or room resonances, can be calculated as [6, page 247]:

$$\omega(r,s,t) = c\sqrt{\left(\frac{r\,\pi}{Lx}\right)^2 + \left(\frac{s\,\pi}{Ly}\right)^2 + \left(\frac{t\,\pi}{Lz}\right)^2} \tag{2.44}$$

where r, s and t = 0,1,2,... according to the different modes. To illustrate the standing waves, s and t is set to zero. This means, that the focus is on the one-dimensional standing waves in the x-direction. Equation 2.44 then simplyfies to:

$$\omega(r,0,0) = c\,\frac{r\,\pi}{Lx} \quad \Rightarrow \quad f(r,0,0) = c\,\frac{r}{2\cdot Lx} \tag{2.45}$$

It can be seen, that the first mode occurs when the wavelength is corresponding to two times the distance between two parallel walls. Figure 2.45 on the facing page illustrates f(1,0,0), f(2,0,0) and f(3,0,0). The plot shows the absolute values of the pressure waves, since humans cannot detect the difference between positive and negative pressure.

The places where the curves have a value of 0, are the pressure nodes. The places where the curve have a value of 2, are the pressure antinodes. If a pressure sound source is positioned in a node position, that corresponding standing wave will not be excited. Opposite, the mode will be excited maximally if the source was placed at the antinode position.

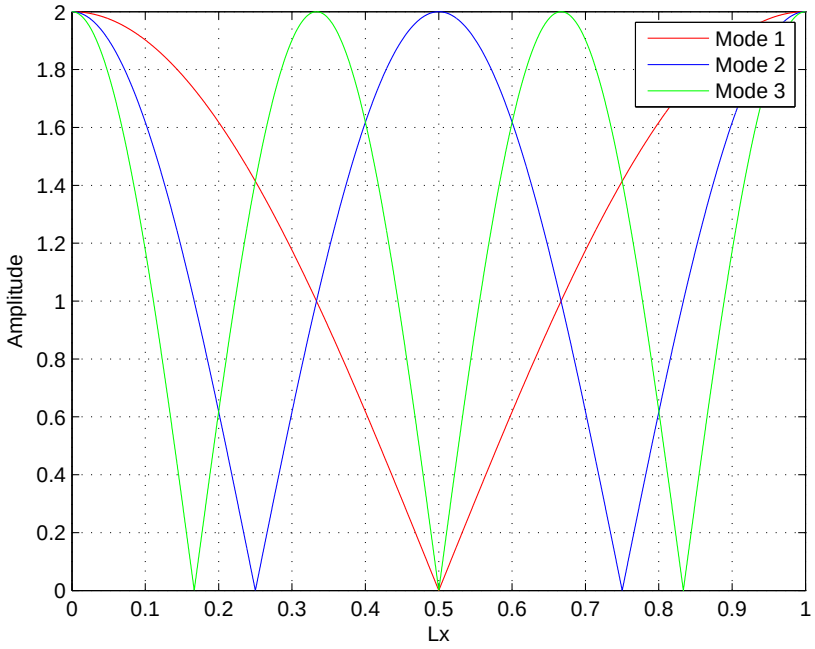

Figure 2.45: *The first three room modes in the dimension Lx in a rectangular room.*

Looking at figure 2.45 it can be seen, that to avoid exciting the first mode, the loudspeaker has to be placed in the middle of the room. By looking at the figure, a distance of 0.2 from one of the walls might be a good solution for placing the loudspeakers. In this location, both the second and third mode will be excited just a little and the first mode is excited almost completely. That might not be that harmfull since the first mode often is at a very low frequency where the loudspeaker itself does not give a high pressure output. For example if the room is 4 m long, the first mode has a frequency of 43 Hz.

2.7.2 Reflections

In a room with rigid surfaces, these will add reflections to the direct sound of the loudspeaker. In figure 2.46 is considered a situation, where a floor reflection is added to the direct sound.

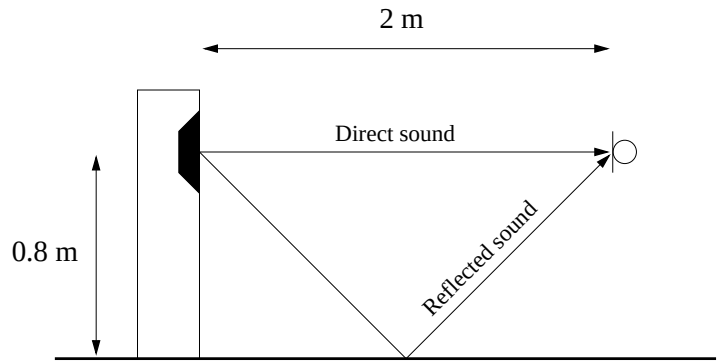

Figure 2.46: *Microphone measuring direct sound and floor reflected sound from a single driver loudspeaker.*

This summation causes a comb filter effect, since the two paths have a distance difference. The distance

difference *DD* can be calculated as:

$$DD = 2 \cdot \sqrt{(0.8\text{ m})^2 + (1\text{ m})^2} - 2\text{ m} \tag{2.46}$$

At some frequencies, *DD* corresponds to half a wave length or a multiple hereof, which results in a wave cancellation. At other frequencies *DD* corresponds to a wavelength or multiple hereof, which results in a positve wave summation. Below the first cancellation in frequency, the two waves will add up more and more in-phase approaching a halfspace situation with a gain of 6 dB. Figure 2.47 shows the spectrum of the situation in figure 2.46 on the previous page.

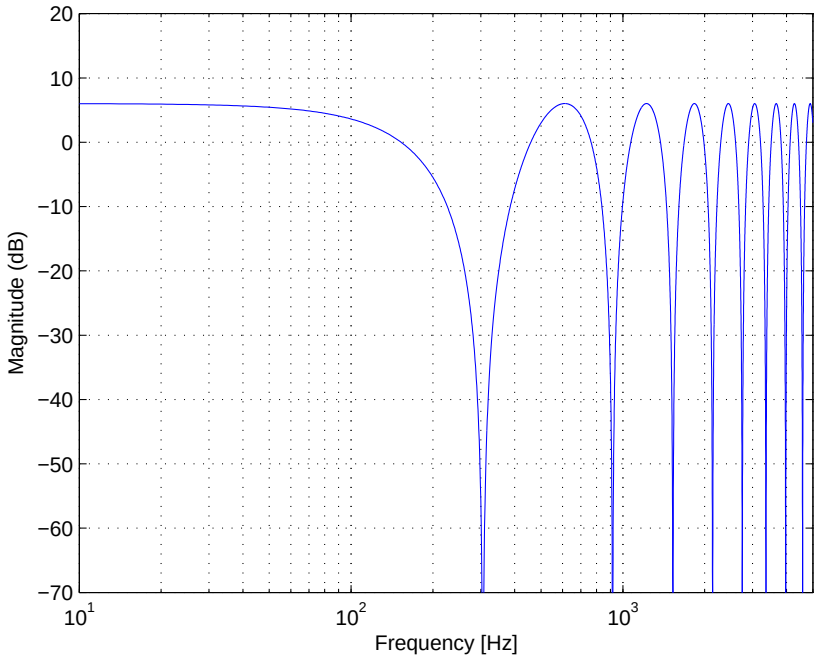

Figure 2.47: *Comb filter result from situation on figure 2.46 on the previous page.*

As seen, the wave summations results in a comb filter effect. The listening room contributes with reflections from any walls, so this comb filter effect is present from side walls, ceiling and the backwall to.

CHAPTER 3

PROJECT DELIMITATIONS

This section describes the delimitations of the project. The following could be included in the model, but is chosen not to because of its minor expected influence on the simulations or its complexity of modelling.

Near Field Axial Pressure

In the near field of a plane circular piston, the pressure amplitude is like illustrated in figure 3.1 [6, page 181]

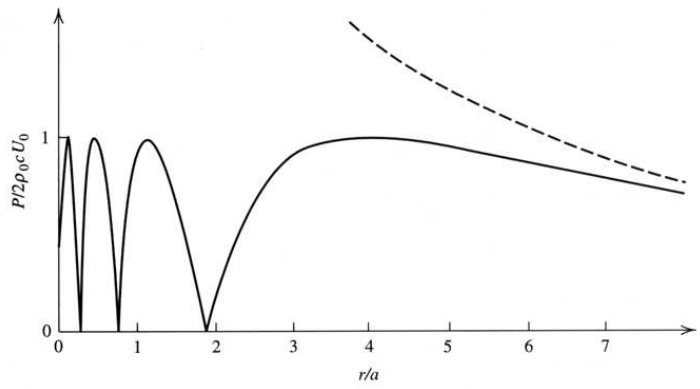

Figure 3.1: *Axial pressure amplitude of a baffled plane circular piston. $ka = 8\pi$*

where the peaks and dips are caused by phase differences between pressure and particle velocity. Moving downwards in frequency cause the dips to move to the left, and the radiation will approach that of a simple source. The dashed line is the far field approximation. It can be seen that when $r/a \gtrsim 7$ the far field approximation is valid. In other words this means, that when the listening position is more than seven times the piston radius away, the far field approximation is valid.

Membrane Break up Patterns

At low frequencies, a membrane moves almost uniformly. This is not the case at higher frequencies. The membrane starts to break up, which means that parts of the membrane move differently. Figure 3.2 on the next page shows normal modes of vibration for a circular membrane fixed at the rim [6, page 97]

These vibrations appear as peaks and dips at higher frequencies in the magnitude response. The calculations of these modes will not be included in the model. They will indirecly become a part of the

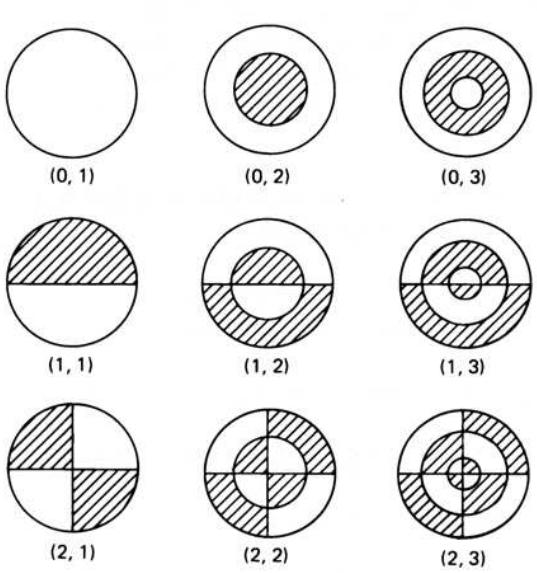

Figure 3.2: *Normal modes of vibration for circular membrane fixed at the rim. The black and white areas vibrate out of phase.*

model, since it will be based on the measurements of the individual drivers.

Membrane Shapes

All modelling in this project is based on plane circular piston theory, even if loudspeaker drivers have cone shaped diaphragms in order to make them rigid [2, page 50]. This different shape might change the radiation pattern at high frequencies.

Box Shapes

A loudspeaker box can be made in several ways. It changes both the internal and extern sound characteristics. Figure 3.3 illustrates how the cabinet edges can alter the magnitude response.

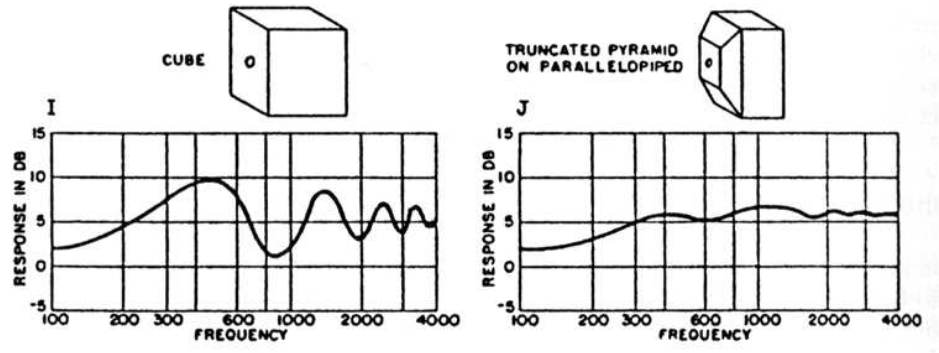

Figure 3.3: *Cabinet edge diffraction influence on magnitude response.*

It can be seen, that the edge shape can change the response. This project focuces on rectangular boxes with 90° angled corners.

- **Other Enclosure Types**
  This project only deals with closed box designs. Later development could include for example a vented box design.

- **Cabinet Wall Vibrations**
  Any sound contributions from cabinet walls are not include in the model.

- **Loudspeaker/Amplifier Interface**
  The model does not take any amplifier interface into account. This means, the final loudspeaker impedance is not going to be fitted to any desired response.

- **Room Influence**
  The model does not take any room contributions into account.

CHAPTER 4

OPTIMIZATION

This chapter presents the optimization method used in this project. The optimization method presented is the steepest descent with updating of stepsize. No further methods are investigated, since the steepest descent algorithm performed well and fulfilled the demands for this project. This chapter is based on [7, Page 37-40].

4.1 Method of Steepest Descent

The idea of the steepest descent method is to minimize a performance function. This is achieved by calculating the gradient of the performance function in each step. The gradient is used to determine in which direction each parameter of the performance function has to be changed to minimize the performance function, as shown in equation 4.1 and figure 4.1, where $\overline{F}(n)$ is a vector containing the parameters to the performance function P. This minimization is repeated until the maximum number of iterations is reached or the performance function has reached a satisfying minimum level.

$$\overline{F}(n) = \overline{F}(n-1) - step \cdot \nabla P(\overline{F}(n-1)) \tag{4.1}$$

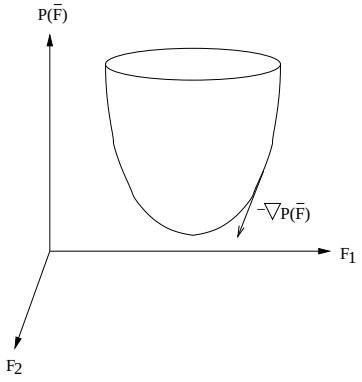

Figure 4.1: *Minimization of performance function P by updating the parameter vector F. The parameters are changed in the opposite direction of the gradient of the performance function ∇P.*

The performance function is used to describe how good an estimation is. The result of the evaluation of the performance function has to give a single number, that should be zero when the estimation is perfect. A typical implementation of a performance function, when the goal is to make a model fit a measurement, is to sum the squared errors over a variable as for example the frequency. An example is shown in figure 4.2 on the next page.

The solid line is the measured values and the dotted line is the simulated values with the current set of parameters. The hatched area is the difference, and the size of the errors are squared and summed over

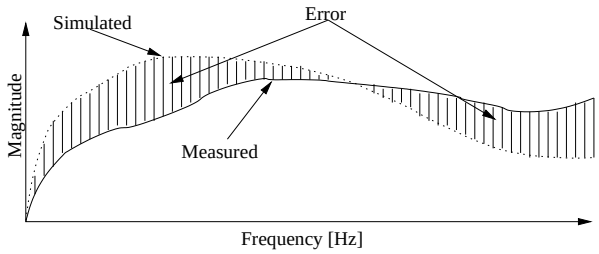

Figure 4.2: *Performance function. The dotted curve is the simulation and the solid is a measurement.*

frequencies. The values are squared to extract the absolute values, and also to give a higher penalty for values that are far from the target curve relative to the values close to the target curve.

4.2 Optimization Structure

The optimization consists of two nested loops as shown in the blockdiagram in figure 4.3. In the figure, $\overline{F}(n)$ is a vector with the variables of the performance function, P. *step* is the stepsize and *stop* is the maximum number of iterations.

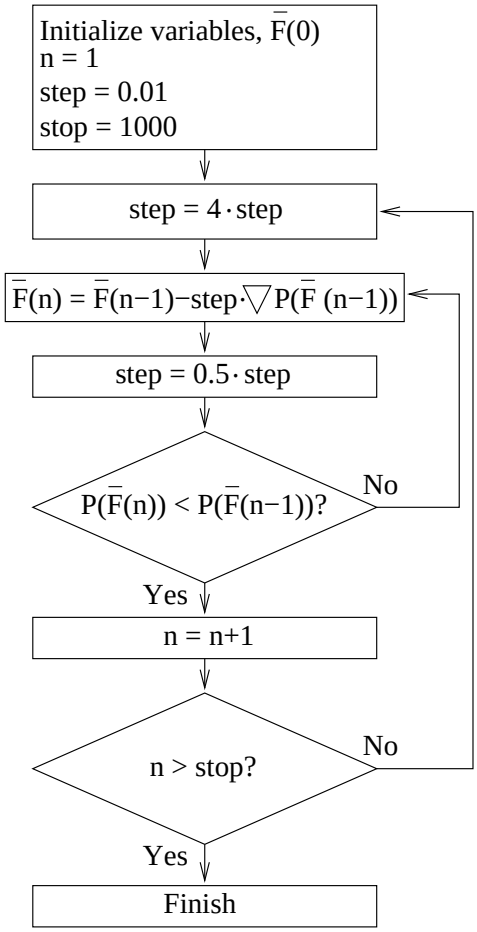

Figure 4.3: *Optimization block diagram for steepest descent algorithm.*

The purpose of the inner loop is to keep the stepsize at an optimum value at any time. This is done by increasing the value of the stepsize before entering the loop, and then decreasing the value until an improvement of the performance function is achieved. By optimizing the stepsize continuously, the optimization algorithm will be fast when it is far from the minimum of the performance function and graduately change to be precise when it approaches the minimum.

The outer loop performs the optimization. The parameters, $\overline{F}(n)$ to the performance function, P, are in each iteration adjusted in the opposite directions of the gradient vector. The size of the adjustment is determined by the optimized stepsize and the size of the gradient. In this way, the parameters to the performance function bring the value of the performance function closer to a minimum for each iteration, until a minimum or the maximum number of iterations are reached.

A problem by this method is the risk of finding a local minimum of the performance function in stead of finding the global minimum. This can be solved by adding noise to the parameters to the performance function.

4.3 Numerical Differentiation

To be able to use the steepest descent algorihm, it is necessary to determine the gradient of the performance function. This can be conducted analytically, but often this is not possible, if for example the performance function contains measured values. In these cases numerical differentiation can be used.

To find the gradient of $f(t)$ in the point t in figure 4.4, the function has to be evaluated at $t-\varepsilon$ and $t+\varepsilon$, where ε is a small number.

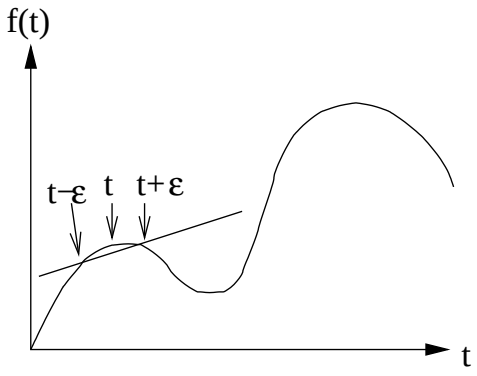

Figure 4.4: *Numerical differentiation.*

The gradient of the function can be calculated as:

$$\nabla f(t) = \frac{f(t+\varepsilon) - f(t-\varepsilon)}{2 \cdot \varepsilon} \tag{4.2}$$

This is an expression of the slope of the line showed in figure 4.4, and for small ε this is equal to the gradient of f in the point t.

CHAPTER 5

REFERENCE LOUDSPEAKER DESIGN

This chapter presents the loudspeaker drivers that are used in the project and construction of a reference loudspeaker, that will be used as comparison to the optimized loudspeaker.

5.1 Presentation of Loudspeaker Drivers

For this project a 5” bass-midrange driver and a 1” dome tweeter are chosen. The drivers are selected with price as an important factor, since it is desired to show what can be done to improve the performance of a cheap loudspeaker by optimizing the crossover network. The chosen drivers are both from Visaton. Some selected datasheet parameters are shown in table 5.1.

	Woofer	**Tweeter**
Model	W 130 S 8 ohm	SC 10 N 8 ohm
Free air resonance frequency	52 Hz	1500 Hz
Sensitivity	87 dB SPL/W/m	90 dB SPL/W/m
Q_t	0.47	n/a
Vas	13 l	n/a
Recommended box volume	7 l	n/a
Price	195 DKK	135 DKK

Table 5.1: *Loudspeaker driver datasheet parameters.*

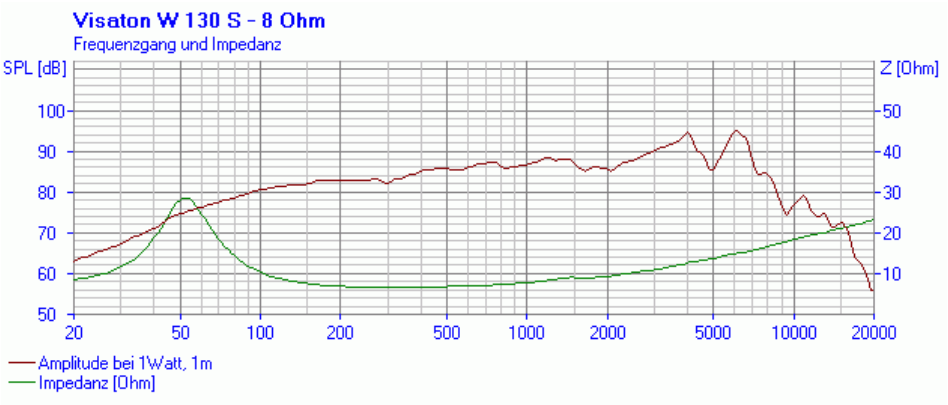

Figure 5.1: *Frequency response and impedance of the woofer from the datasheet.*

The parameters shown in table 5.1, the frequency responses in figure 5.1 and 5.2 on the next page and

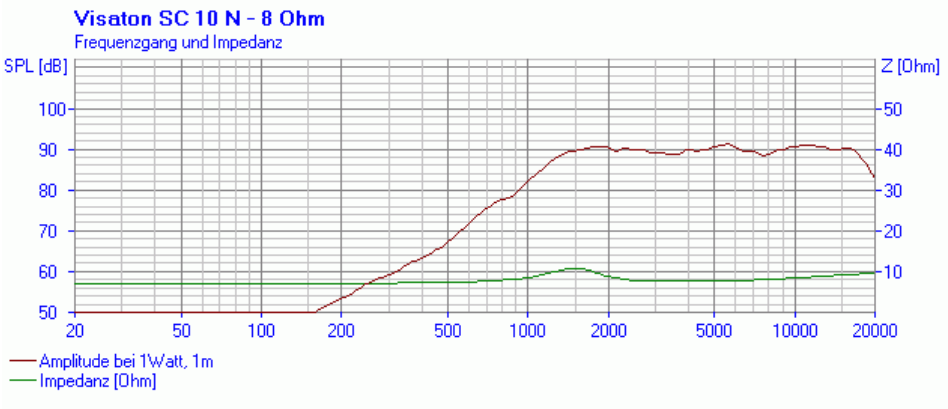

Figure 5.2: *Frequency response and impedance of the tweeter from the datasheet.*

Figure 5.3: *Picture of the woofer.*

Figure 5.3: *Picture of the tweeter.*

the pictures of the drivers in figure 5.3 are from the homepage of the manufactor [10].

These drivers are selected since they fulfill the following demands:

- A 5” woofer is chosen so that the dispersion is not to narrow at a typical crossover frequency compared to the tweeter, as the situation would be for a 12” woofer.
- The frequency responses of both drivers are relatively flat in the area where they are expected to be used. That is from the resonance frequency to approximately 5 kHz for the woofer and from 1500 Hz and upwards for the tweeter. This ensures an overlap of responses to make sure that a reasonable crossover frequency can be selected.
- The sensitivity of the tweeter should not be lower than that of the woofer. This is due to the fact that damping the bass with an attenuation circuit will make the damping factor of the amplifier to the driver significantly lower, whereas damping the tweeter does not introduce any problems.
- The value of *Vas* for the woofer indicates that the box will be of a reasonable size.
- The drivers are relatively cheap.

5.2 Measurements of Loudspeaker Drivers

To verify the parameters from the datasheet, the drivers are measured. The measurements are infinite baffle frequency responses and electrical impedances. The measurements are described in appendix B.3 on page 114.

Figure 5.4 and 5.5 on the next page show the magnitude responses of the drivers measured in an infinite baffle.

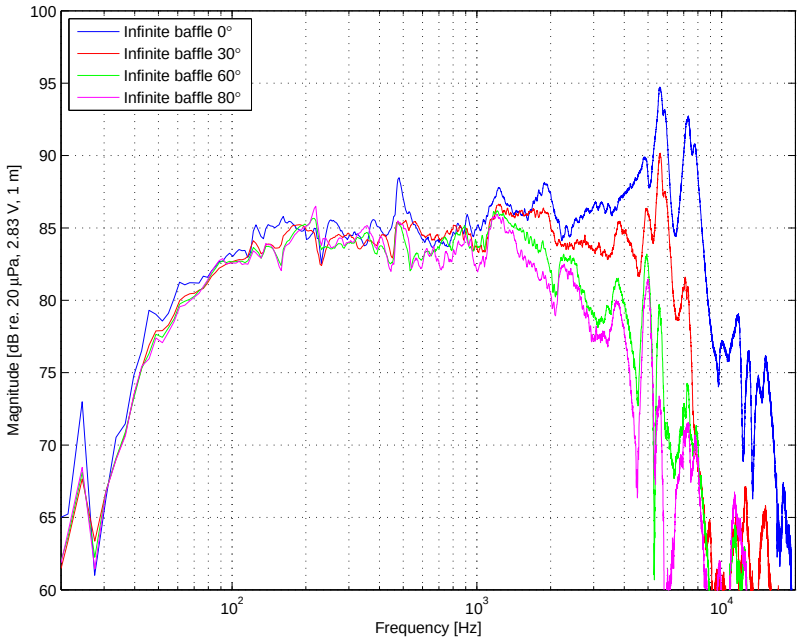

Figure 5.4: *Measured magnitude response of the woofer.*

It can be seen from figure 5.4, that the bass driver has an acceptable dispersion at 30° up to approximately 5 kHz, since the difference relative to the on-axis response is not larger than approximately 5 dB. Furthermore it can be seen, that the sensitivities of both drivers are lower than indicated in the datasheet. The sensitivities are estimated to be 85 dB SPL for the woofer and 87 dB SPL for the tweeter. Finally it can be seen, that the magnitude responses are more or less flat as in the datasheet.

The impedances of the drivers are measured as described in appendix B.3 on page 114, and the results are presented in figure 5.6 and 5.7 on page 57.

In figure 5.6 on the next page the resonance frequency of the woofer is found as the top of the peak at low frequencies of the impedance curve. The resonance frequency is found to be just below 60 Hz, which is significantly higher than the 52 Hz from the datasheet. It is expected that the resonance frequency will get lower as the suspension of the driver gets softened during use of the driver. Apart from the higher resonance frequency, the measured impedances seems to be similar to the impedances presented in the datasheets.

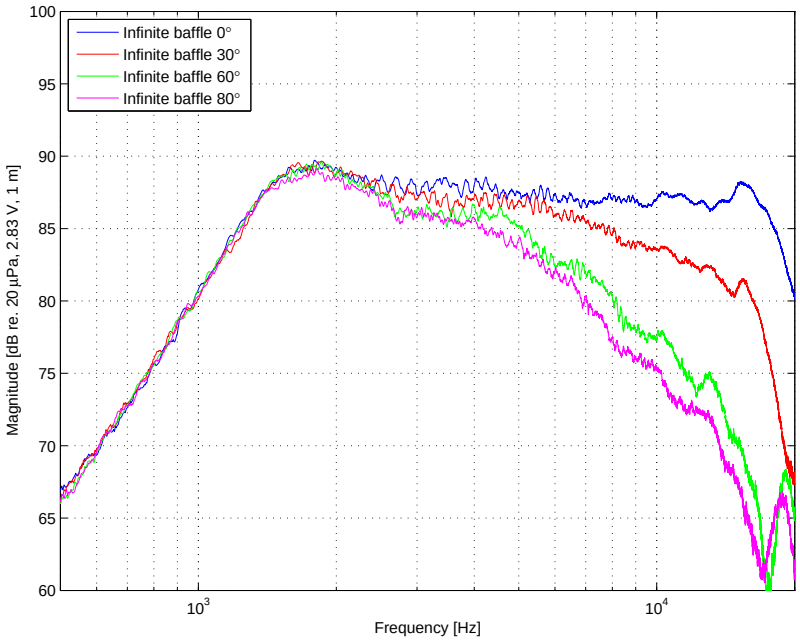

Figure 5.5: *Measured magnitude response of the tweeter.*

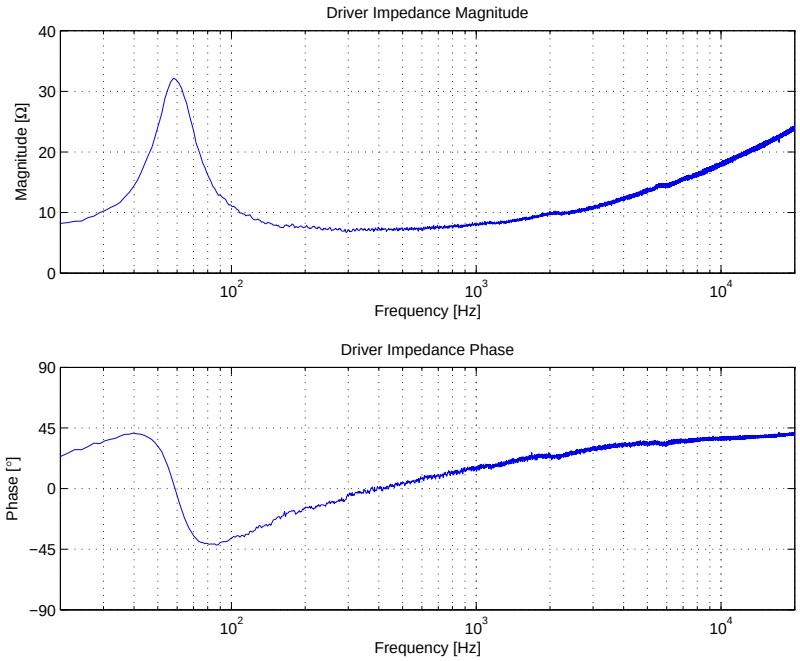

Figure 5.6: *Measured impedance of the woofer.*

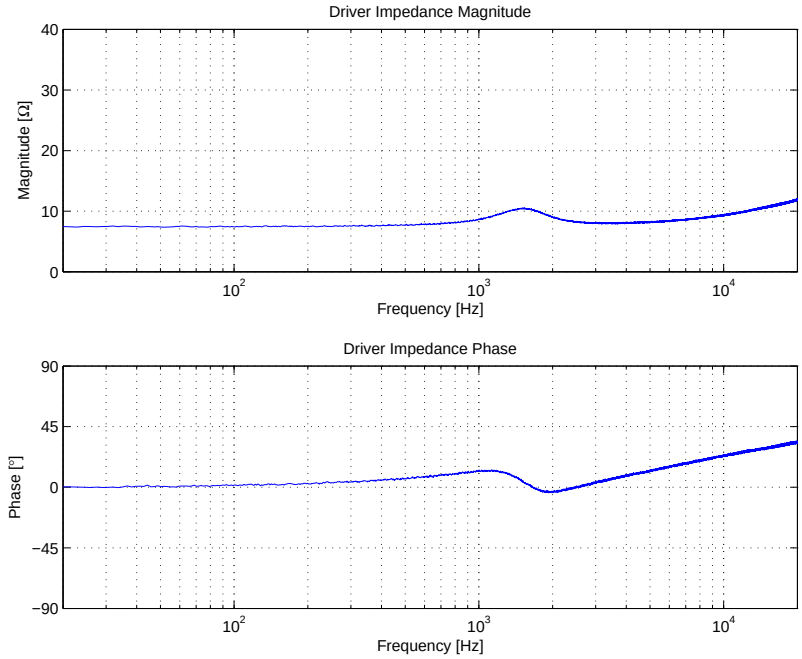

Figure 5.7: *Measured inpedance of the tweeter.*

5.3 Loudspeaker Parameter Estimation

Since the resonance frequency for the woofer and the sensitivities for both drivers differ from the datasheet values, it is decided to develop a program that is able to determine all parameters of the loudspeaker drivers on basis of a measured impedance curve. In this way it is ensured, that the parameters used in the model are the correct parameters for the loudspeaker driver.

The program is made in Matlab, and uses the optimization algorithm introduced in chapter 4. As mentioned in that chapter, this algorithm requires the definition of a performance function. This performance function should describe how far away the current estimation is from the measurement. The performance function should be zero when the fit is perfect.
The performance function includes the measured impedance as a function of frequency, $meas\_imp(f)$, and the simulated impedance as a function of frequency $sim\_imp(f)$. The simulated impedance is defined in equation 2.12 on page 13.
The performance function P uses the complex numbers for the impedances, so that the phase information is also taken into account. To calculate the performance function, the differences between the two curves are found as complex numbers at each frequency. The magnitude of these differences are then squared and summed over frequency:

$$P = \sum_{f=f_0}^{f_{max}} abs\Big(meas\_imp(f) - sim\_imp(f)\Big)^2 \tag{5.1}$$

where $abs()$ is the magnitude of a complex number.

Frequency Vector

The impedance is measured as described in appendix B.3 on page 114. The sampling frequency is 100 kHz. The measured signal is Fourier transformed to move the impedance to the frequency domain using a 32768 point Fourier transformation. The resulting frequency vector is linearly spaced with a resolution of 3.05 Hz. The linearity is not desirable for this purpose, since the optimization will put higher weight on the high frequencies, where there are many points per octave, compared to low frequencies. Therefore a new vector, containing the number of the wanted places in the original frequency vector is created. Using this pointer vector, the frequencies are logarithmically distributed with approximately 6-7 points per octave, resulting an equal weighting of all octaves. This vector also sets the highest and lowest frequency of interest. A benefit of using a logarithmically distributed frequency vector is that the computation speed of the optimization is dramatically increased due to decreased number of frequencies. The number of frequencies changes from 16384 to 67 for a frequency range from 20 Hz to 20 kHz.

Optimization Results

The optimization is performed with the following conditions:

	Woofer	**Tweeter**	**Scaling factor and unit**
Iterations	1000	1000	
Minimum frequency	20 Hz	20 Hz	
Maximum frequency	5 kHz	20 kHz	
Start values:			
Re	6	6.9	$1 \cdot \Omega$
Le	1	0.04	10^{-3} H
C_m	1	0.1	10^{-3} m/N
Bl	4.6	2	$1 \cdot$ N/A
R_m	1	1	$1 \cdot$ Ns/m
M_m	5.5	0.1	10^{-3} kg
n	0.8	0.9	1

Table 5.2: *Driver parameter estimation conditions.*

From the table it should be noted, that there are used scaling factors to make sure that the loudspeaker parameter values all are in the same order of magnitude, since they will share a common step size. In this way a step of 1 will have approximately the same influence on Re and M_m. This would not be the case if M_m was given in Kg.

Test shows that 1000 iterations is a good compromise between speed and accuracy, as a larger number of iterations do not change the results significantly.

The frequency range for the woofer is limited, since estimating parameters with the full frequency range, sacrifies accuracy near the resonance frequency to make a better fit at high frequencies. This error is a lack in the modelling of the lossy inductance in the voice coil at high frequencies. It is chosen that accuracy near the resonance frequency is preferred over accuracy at high frequencies. Therefore the maximum frequency for the woofer is set to 5 kHz.

The result of the optimization is presented in table 5.3 and figure 5.8 and 5.9.

	Woofer	**Tweeter**
Re	7.01 Ω	7.36 Ω
Le	1.43 mH	0.56 mH
C_m	1.18 $^{mm}/_{N}$	0.05 $^{mm}/_{N}$
Bl	4.41 $^{N}/_{A}$	1.82 $^{N}/_{A}$
R_m	0.75 $^{Ns}/_{m}$	1.14 $^{Ns}/_{m}$
M_m	5.64 g	0.22 g
n	0.82	0.81

Table 5.3: *Estimated driver parameters.*

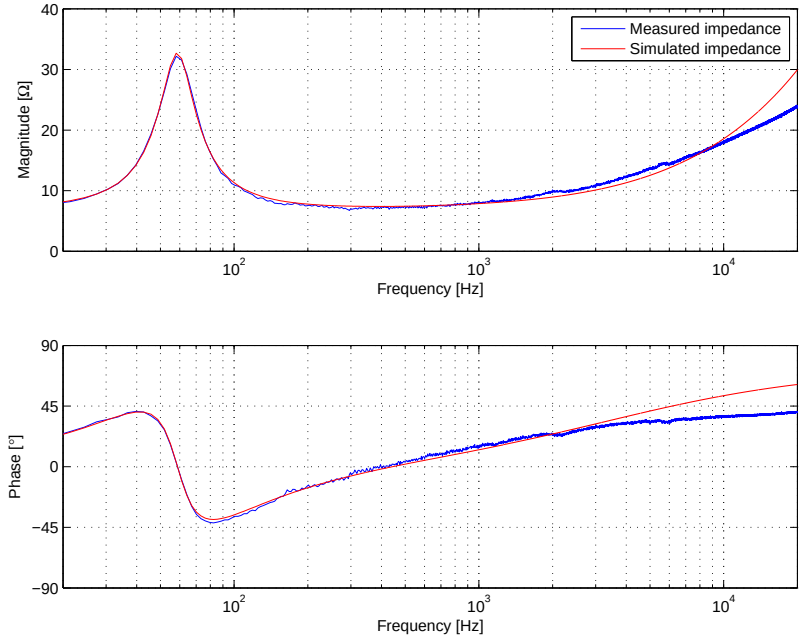

Figure 5.8: *Measured and simulated impedance for the woofer.*

As it can be seen in the figures, the optimization of the impedance is exact for the tweeter whereas there are deviations above 4 kHz for the woofer. This is expected, since the upper frequency limit for the woofer parameter estimation is set to 5 kHz. This is not expected to have any major effect on the transfer function of the crossover network, since the deviations are above the expected working area of the woofer. The estimated parameters found during the optimization are considered to be reliable, since they do not deviate much from the datasheet values, and the simulated curves match the measured well.

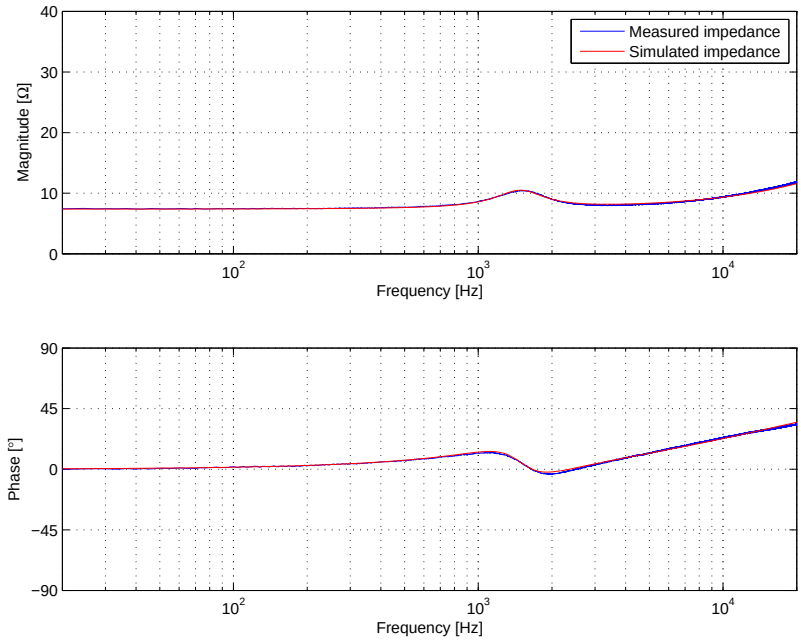

Figure 5.9: *Measured and simulated impedance for the tweeter.*

Driver Membrane Radius

The radius of the drivers is measured, since the radius is used in the model. The radius is found by measuring the diameter of the membrane including $1/3$ of the suspension, and dividing by two. The radius of the woofer is found to be 4.5 cm and the tweeter to 1.26 cm. In section 3 on page 45 it is mentioned that the far field assumption is fulfilled when the observation point is more than seven times the driver radius away. This is 31.5 cm for the woofer and 9 cm for the tweeter. Therefore the model is valid for microphone distances greater than 31.5 cm.

5.4 Reference Loudspeaker

This section describes the design of a two way loudspeaker. The design of the loudspeaker is made with the use of simple knowledge and formulas. The idea of building a loudspeaker with these simple tools is to show what can be obtained by a novice loudspeaker constructor and how this result can be improved with the use of the optimization system presented in this thesis.

5.4.1 Design of Reference Loudspeaker Crossover Network

It is chosen to make a parallel second order passive filter for both the highpass and lowpass sections. The filter order is selected as a compromise between a high damping of the stopband and a desire for a simple and cheap filter.

The Q-values of both filters are selected to be 0.5. This is done to get a flat magnitude response as described in section 2.4.1 on page 23. To obtain the flat response, the polarity of the tweeter is reversed,

as required.

The crossover frequency is selected by comparing the frequency responses from the datasheets for both drivers, that are shown in figure 5.1 and 5.2 on page 54. It can be seen, that the lowpass cut-off frequency for the woofer should be below 4 kHz since the response is relatively flat up to this frequency. For the tweeter the cut-off frequency of the highpass filter should be above 1500 Hz, where the tweeter starts to roll off. Furthermore the cut-off frequency should be well above the resonance frequency to ensure that the tweeter does not get overloaded. As a compromise between these demands, a crossover frequency of 2500 Hz is selected.

With all specifications selected, the complete filter can be designed. The filter is made according to the parallel filter in figure 2.20 on page 22.
The values of the components are calculated as described in [11, page 166]:

$$L_w = \frac{R_w}{2 \cdot \pi \cdot f_{c,w} \cdot Q_w} = \frac{8\ \Omega}{2 \cdot \pi \cdot 2500\ \text{Hz} \cdot 0.5} = 1.02\ \text{mH} \tag{5.2}$$

$$C_w = \frac{Q_w}{2 \cdot \pi \cdot f_{c,w} \cdot R_w} = \frac{0.5}{2 \cdot \pi \cdot 2500\ \text{Hz} \cdot 8\ \Omega} = 3.98\ \mu\text{F} \tag{5.3}$$

$$L_t = \frac{R_t}{2 \cdot \pi \cdot f_{c,t} \cdot Q_t} = \frac{8\ \Omega}{2 \cdot \pi \cdot 2500\ \text{Hz} \cdot 0.5} = 1.02\ \text{mH} \tag{5.4}$$

$$C_t = \frac{Q_t}{2 \cdot \pi \cdot f_{c,t} \cdot R_t} = \frac{0.5}{2 \cdot \pi \cdot 2500\ \text{Hz} \cdot 8\ \Omega} = 3.98\ \mu\text{F} \tag{5.5}$$

The filter is constructed with standard component values. For the coils, 1 mH are selected, and for the capacitors it is chosen to use a parallel connection between two capacitors with values of 3.3 μF and 0.68 μF, yielding the calculated 3.98 μF. The resistance of the coils are 0.5 Ω.

To match the sensitivities between the drivers, where the woofer has a sensitivity of 87 dB and the tweeter has 90 dB according to the datasheet, a L-Pad circuit is designed with a damping of 3 dB. From this dB value the attenuation of the circuit can be calculated:

$$att = 10^{damping/20} = 10^{-3/20} = 0.708 \tag{5.6}$$

From formula 2.27 and 2.28 on page 26 the following component values are calculated:

$$\text{R2} = \frac{R_t \cdot att}{1 - att} = \frac{8\ \Omega \cdot 0.708}{1 - 0.708} = 19.4\ \Omega \tag{5.7}$$

$$\text{R1} = R_t - \frac{R2 \cdot R_t}{R2 + R_t} = 8\ \Omega - \frac{19.4\ \Omega \cdot 8\ \Omega}{19.4\ \Omega + 8\ \Omega} = 2.3\ \Omega \tag{5.8}$$

The calculated resistor values are not available, so the nearest standard values are selected. This changes R1 to 2.2 Ω and R2 to 22 Ω. Calculations show that the change in input resistance and damping is negliable.

The complete filter is constructed as shown in figure 5.10 on the following page and table 5.4 on the next page.

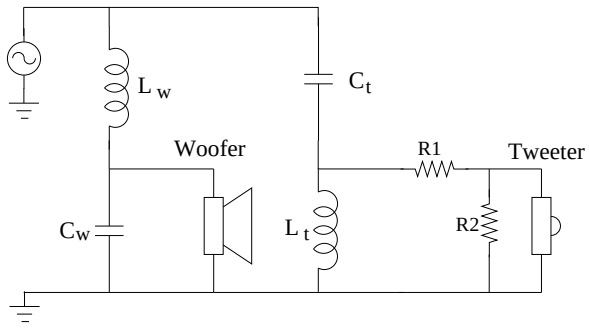

Figure 5.10: *Crossover network for reference loudspeaker.*

Component	Value
L_w	1 mH
C_w	3.98 μF
L_t	1 mH
C_t	3.98 μF
$R1$	2.2 Ω
$R2$	22 Ω

Table 5.4: *Component values for reference loudspeaker crossover network.*

5.4.2 Loudspeaker Enclosure

The enclosure is chosen to be a closed box, and with the 7 l volume suggested in the datasheet, in table 5.1 on page 53 is used. To this volume is added 0.2 l to compensate for the volume occupied by the drivers and the filter. The box is build from 16 mm MDF plates.

The dimensions of the box are chosen, so the ratio between the inner dimensions is 2.6:1.6:1 as this ratio gives the greatest uniformity in the frequency distribution of standing waves [3, page 100]. The smallest inner dimension can be calculated by:

$$X = \sqrt[3]{\frac{0,0072\,l}{2.6 \cdot 1.6}} = 0.12\,m \tag{5.9}$$

When the smallest inner dimension is known, then the remaining can be calculated by multiplying the smallest dimension with 1.6 and 2.6 respectively. To find the outer dimensions, two times the material thickness has to be added, and the box is then calculated to be 34.4 cm high, 22.4 cm wide and 15.2 cm deep. The box is loosely stuffed with Acoustilux to reduce internal reflections [3, page 34]. With the size of the box known, the resonance frequency and the Q-value can be calculated. This is done using formula 2.19 and 2.20 on page 18. The resonance frequency is calculated to 80.5 Hz and the Q-value is calculated to 0.94 using the estimated parameters for the woofer, adding 0.5 Ω to R_e, as this is the series resistance of the coil in the crossover. Furthermore it is asumed that the damping material adds 10 % to the volume of the box [3, page 100]. The Q-value is higher than $1/sqrt2$, which results in an amplification of the frequencies near the resonance frequency.

The drivers are mounted above each other and horizontally centered, so the center of the woofer is 10.5 cm from the bottom of the box and the center of the tweeter is 26 cm above the bottom. These

positions are selected from a visual design perspective. The drivers are counter sunk in the baffle, to decrease reflections from the driver edges. The completed loudspeaker is shown in figure 5.11.

Figure 5.11: *Reference loudspeaker.*

CHAPTER 6

VERIFICATION OF THEORY

This chapter presents results of measurements and simulations in order to verify the theory presented in chapter 2.

The measurements shown in this chapter are all conducted with the loudspeaker drivers chosen in section 5.1 on page 53. All measured responses are not reliable below 60 Hz, since this frequency is the lowest frequency where the anechoic room can be considered anechoic.
The simulations are based on the driver parameters estimated in section 5.3 on page 57. The closed box simulations and measurements are conducted by using the box, designed in section 5.4 on page 60. It is assumed in the simulations, that the internal damping material adds 10% to the cabinet volume [3, page 100].

Most figures shown in this chapter present two plots in a specific way. The upper plot shows two curves, which can be either measured or simulated responses. The lower plot then presents the difference between the two upper curves together with a corresponding simulated response.

6.1 Infinite Baffle Magnitude Response

This section presents the measured and simulated infinite baffle magnitude responses. The simulations are based on section 2.1 on page 7, and the corresponding measurements are described in appendix B.3 on page 114.

The results of the measurement and simulation are shown in figure 6.1 on the following page.

It can be seen, that the measured and simulated responses are similar from 400 Hz and downwards in frequency. This result is acceptable since the infinite baffle simulation is only going to be used when simulating the low-frequency roll off. The lower curve shows the difference from the simulated response to the measured response. It is seen, that the simulation does not take into account the membrane breakup contributions, which are significant above 1 kHz. The simulated response rolls off at high frequencies because of the voice coil inductance.

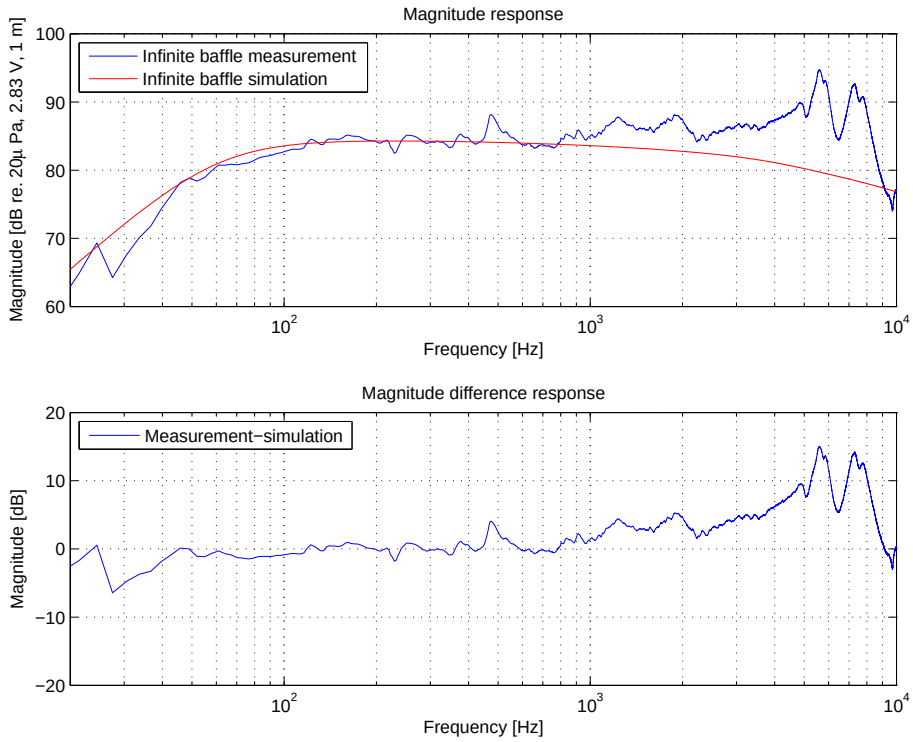

Figure 6.1: *Infinite baffle measurement and simulation. The lower curve shows the difference from the simulated response to the measured response.*

6.2 Closed Box Magnitude Response and Impedance

This section presents the influence in the magnitude and impedance response when placing the woofer in a closed box with an infinite front baffle. The simulations are based on section 2.2 on page 17, and the corresponding measurements are described in appendix B.4 on page 117.

6.2.1 Closed Box Magnitude Response

The results of the measurements and simulations are shown in figure 6.2.

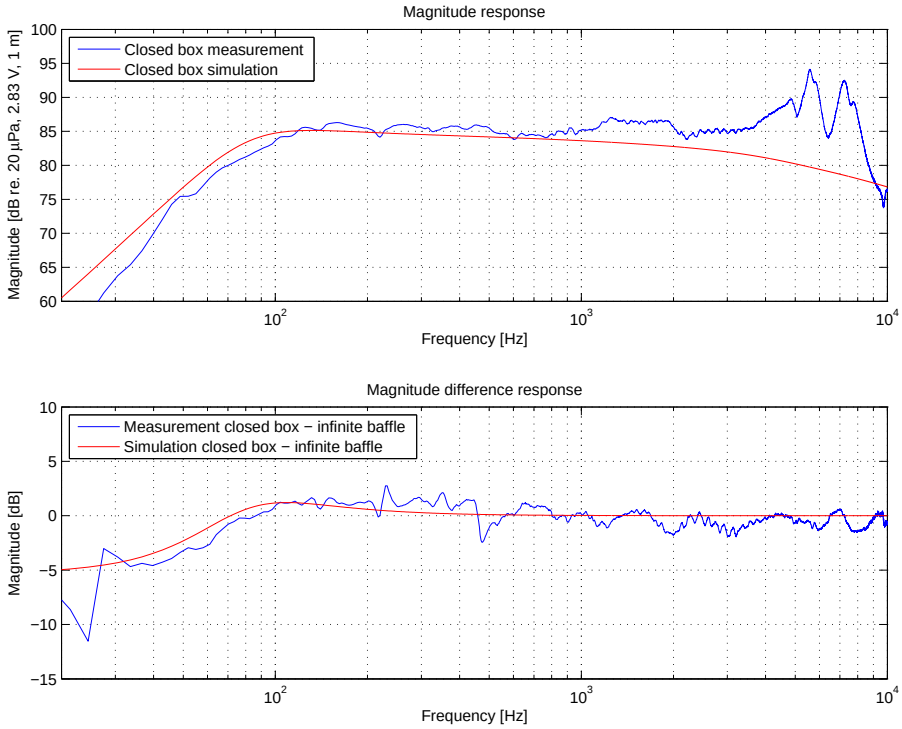

Figure 6.2: *Closed box measurements and simulations. The front baffle is infinite. The lower red curve shows the difference from the simulated infinite baffle response to the simulated closed box response. The same curve is shown for the measurement responses.*

From the lower curves can be seen, that the simulated influence of the closed box is similar to the measured influence. The box attenuates the low frequencies, which in this example is below 75 Hz. From 75 Hz to 300 Hz the box amplifies the response.
At low frequencies from 100 Hz and downwards, there is a general magnitude difference at 1-2 dB. The closed box simulation is made from the assumption, that the acoustilux damping material adds 10% to the cabinet volume. This assumption might be the reason for the difference at low frequencies. To get a more precise simulation, the used damping material should add less than 10% to the volume, which would bring up the system resonance frequency and furthermore result in a more steep roll off. This deviation is not considered as a problem in the modelling, since the simulation is close to the measurements.

Furthermore it can be seen, that the box smoothes the magnitude response. The peak near 500 Hz in

the infinite baffle measurement on figure 6.1 on page 66 is not present in the closed box measurement in figure 6.2 on the previous page. It can be seen in the magnitude difference response, that the peak is removed by the box.
From 1 kHz and upwards, the measured magnitude difference response seems attenuated 1 dB. This might be another influence of the damping material.

6.2.2 Closed Box Impedance

The results of two impedance measurements are presented in figure 6.3. The impedances are measured in the infinite baffle and in the closed box.

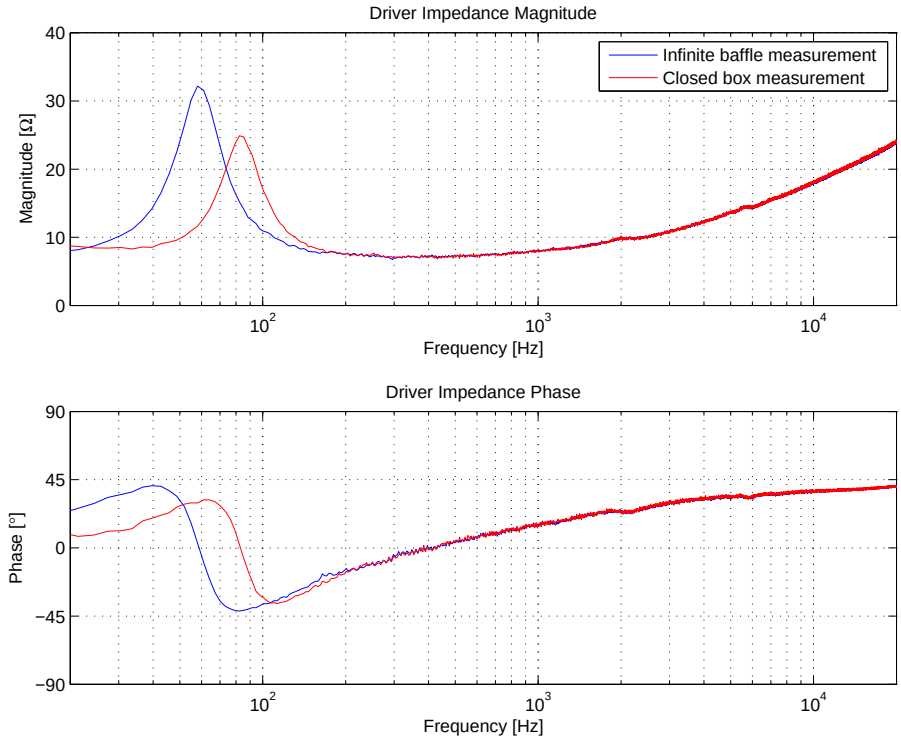

Figure 6.3: *Measurements of electrical driver impedances.*

It is seen, that the resonance frequency moves upwards when the driver is placed in the closed box. This is expected, and the simulation on figure 2.15 on page 19 predicts the two same resonance frequencies at approximately 60 Hz and 80 Hz respectively. The difference between the simulated and measured closed box impedance is the magnitude at the resonance frequency. The measured impedance drops to a level of 24 Ω compared to the simulated 32 Ω on figure 2.15 on page 19. The impedance magnitude at the resonance frequency can be calculated as [8, page 33]:

$$Z_{e,res} = R_e + \frac{(Bl)^2}{r_m} \tag{6.1}$$

It can be seen, that to decrease $Z_{e,res}$ the mechanical resistance r_m has to be increased. When placing the driver in the box, energy is transferred into movements of the cabinet walls, and into heat in the

air inside the box [1, page 4]. Furthermore the damping material contributes with mechanical losses, since the acoustic energy is converted into heat in the damping material [6, page 340]. These ways, the mechanical resistance increases, which brings down the impedance magnitude at the resonance frequency. In addition, the phase change of the closed box response is less when compared to the infinite baffle response.

The used theory does not predict the right impedance magnitude at the resonance frequency for the closed box situation. This is not considered as a problem, since it will not significantly influence the crossover transfer function.

6.3 Driver Beaming

This section presents the measured and simulated beam patterns of the woofer. The simulations are based on section 2.3 on page 20, and the corresponding measurements are described in appendix B.3 on page 114.

6.3.1 Woofer Beaming

The results of the measurement and simulation for the woofer at 30° off-axis are shown in figure 6.4.

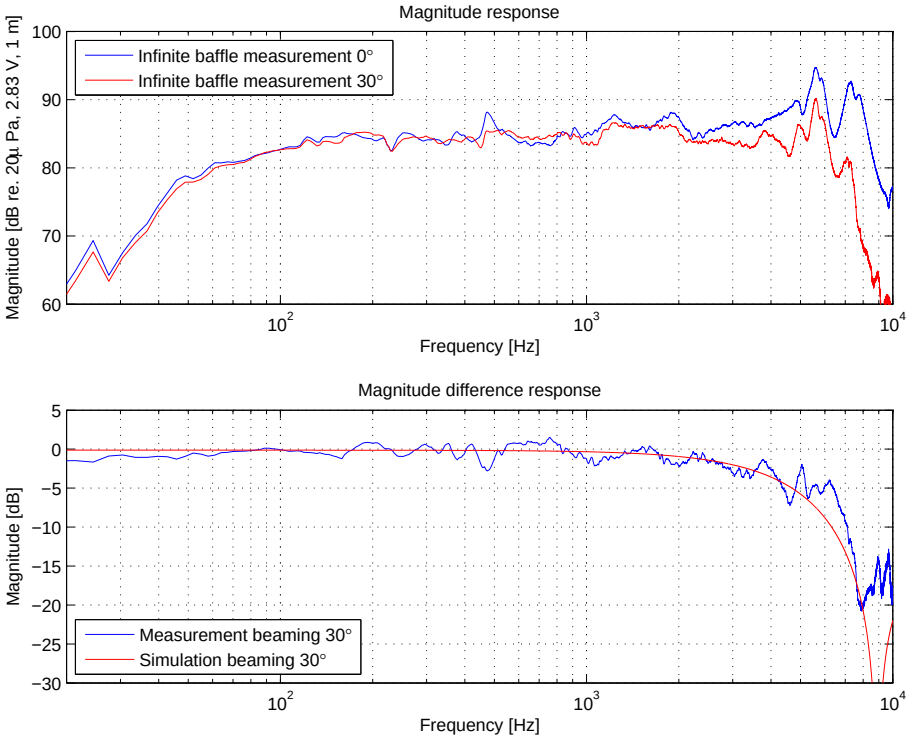

Figure 6.4: *Beaming of woofer at 30° off-axis.*

It can be seen from the lower two curves, that the simulation is similar to the measured response. The deviation at approximately 6 kHz may be caused by different contributions from the membrane

breakup patterns at 0° and 30°. This deviation is not considered as a problem, since the 6 kHz frequency typically lies in the stopband of the woofer lowpass filter.

Figure 6.5 illustrates the measurement and simulation for the woofer at 60° off-axis.

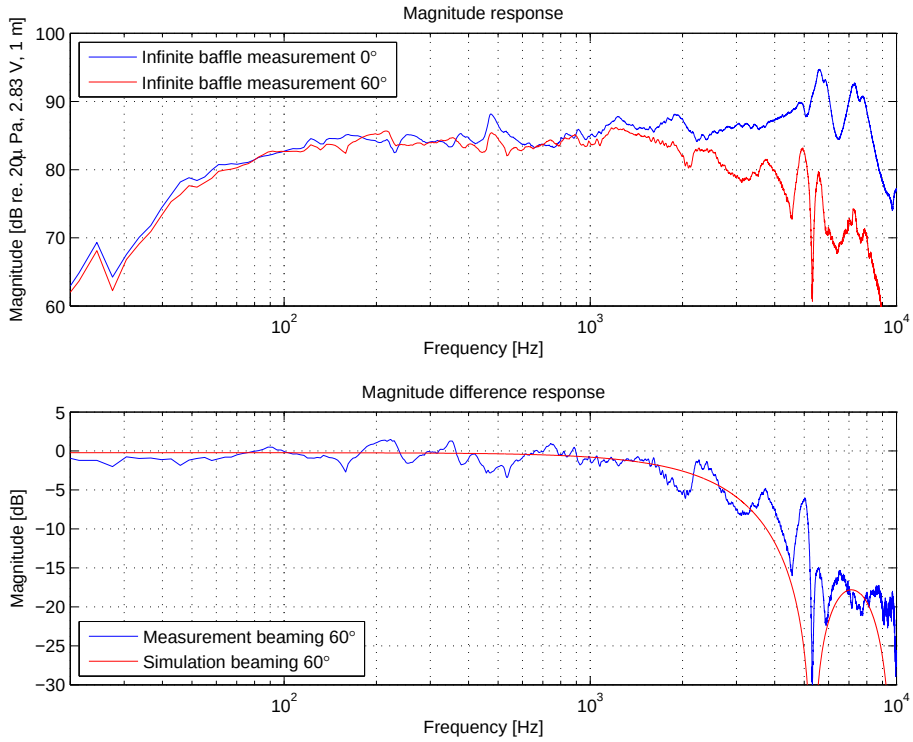

Figure 6.5: *Beaming of woofer at 60° off-axis.*

From figure 6.5 is seen, that the simulation is similar to the measurement. Again the membrane breakup patterns contribute differently at 0° and 60°. The beam theory is concluded to be valid for the woofer.

6.3.2 Tweeter Beaming

The outcome of the measurement and simulation for the tweeter at 30° off-axis is shown in figure 6.6 on the facing page.

The simulation and measurement response is close to each other. From 8 kHz and upwards in frequency, there are deviations up to approximately 4 dB at 20 kHz. The deviation might be caused by the tweeters horn loading, which will make the dispersion smaller [2, page 35]. Otherwise the deviations are close to 2 dB. The difference can be caused by the assumptions made in equation 2.21 on page 20. This equation is based on plane circular pistons, which is not the case for a 1" dome tweeter. The simulation is also sensitive to small changes in the chosen membrane radius a. The deviations at high frequencies are not considered as a problem. The model, which will use the beam theory, will probably not predict the exact beaming of the tweeter, but the result of the simulation is still close to the measurements.

From figure 6.7 on page 72 is seen, that the simulation has the same tendency as in the measurement.

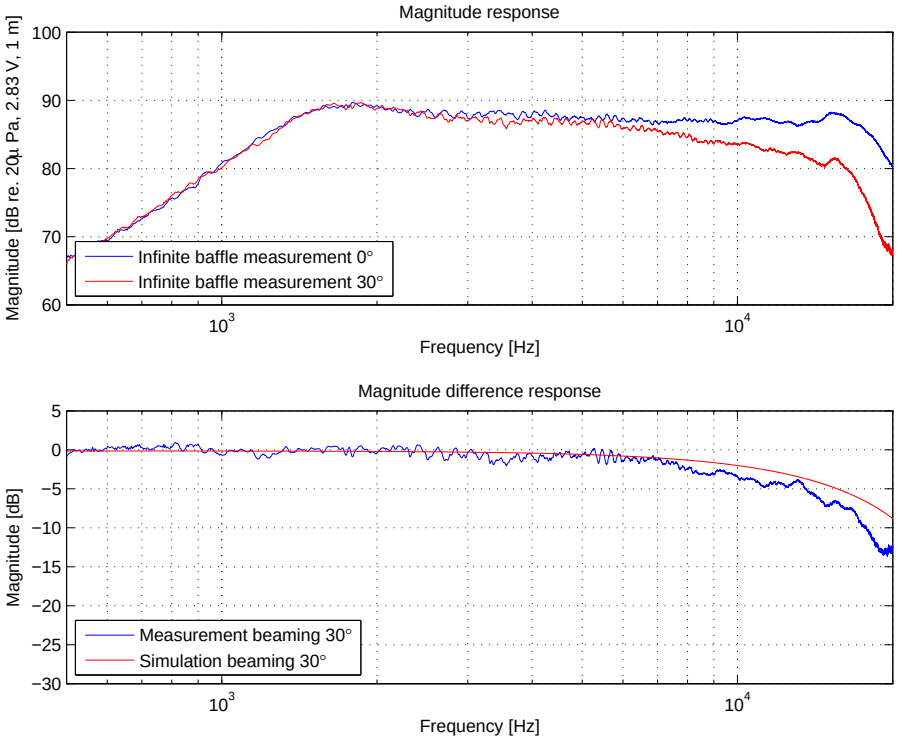

Figure 6.6: *Beaming of tweeter at 30° off-axis.*

From 2.5 kHz and upwards in frequency, deviations starts to be present. Up to approximately 13 kHz the deviations are still not more than approximately 4 dB. The deviations are not considered as a problem since the deviations are relatively small, and a loudspeaker response at 60° is typically not optimized as much as the on-axis response and the 30° off-axis response. Furthermore it can be seen, that the dip at approximately 18 kHz is predicted right by the simulation.

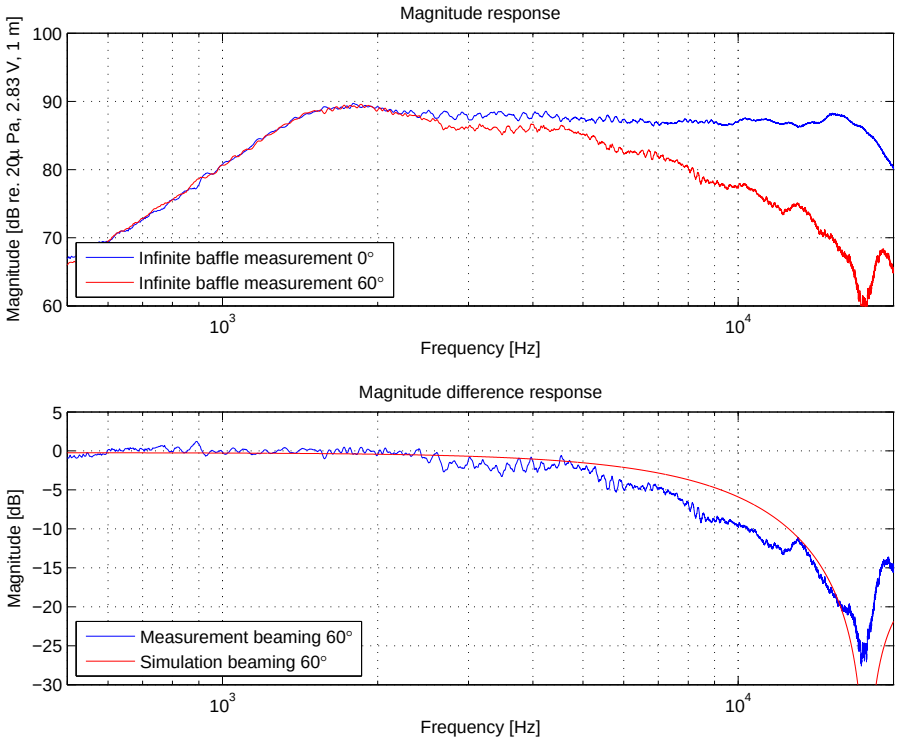

Figure 6.7: *Beaming of tweeter at 60° off-axis.*

6.4 Filter Magnitude Response

This section presents the measured and simulated crossover network transfer functions. The simulations are based on section 2.4 on page 22, and the corresponding measurements are described in appendix B.5 on page 119.

6.4.1 Woofer Transfer Function

Figure 6.8 shows the lowpass filtered woofer magnitude response.

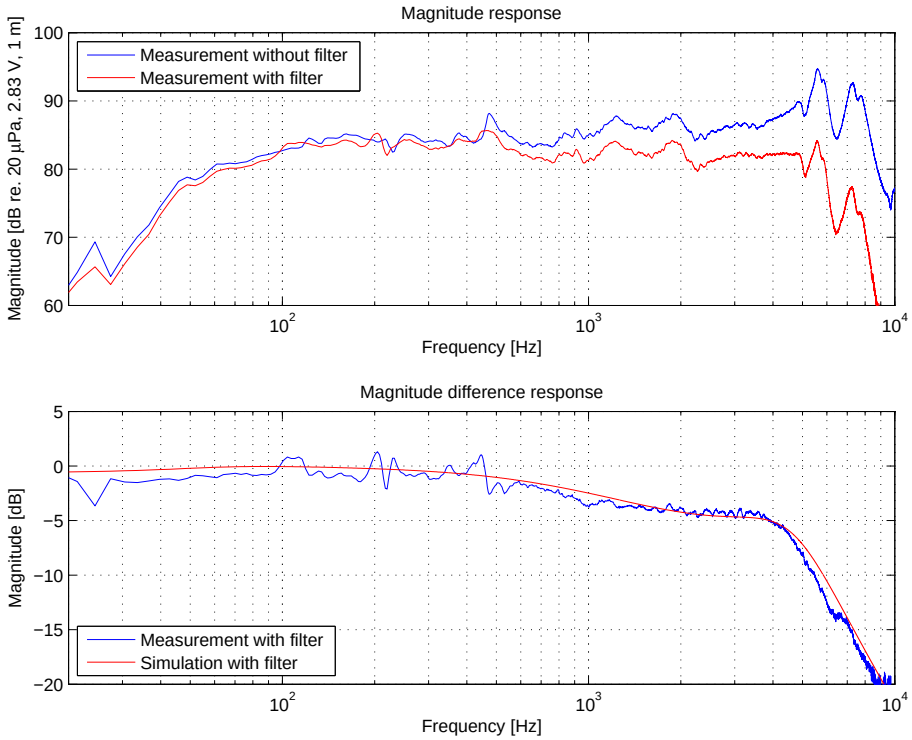

Figure 6.8: *Lowpass filtered woofer magnitude response.*

It can be seen, that the simulated electrical transfer function is similar to the acoustical transfer function. Above 4 kHz the deviations are caused by the used estimated impedance response. In section 5.3 on page 58 can be seen, that the estimated impedance response does not fit the measured impedance above this frequency. This will introduce differences in the filter transfer function. The deviations are small, and will not be considered as a problem in the modelling process, since the deviations lies within the typical stopband of a woofer lowpass filter.

It can further be seen, that the filtered response has an attenuated low-frequency roll off. This might be due to the resistance in the used crossover coils. These have a resistance of 0.5 Ω. From equation 2.8 on page 11 can be seen, that when placing a resistance in series with the voice coil resistance R_e, increases the Q-value. This finally results in a faster and more steep roll off. Also the 0.5 Ω works as a simpel attenuation, because of voltage division with the woofer impedance.

6.4.2 Tweeter Transfer Function

Figure 6.9 shows the highpass filtered tweeter magnitude response.

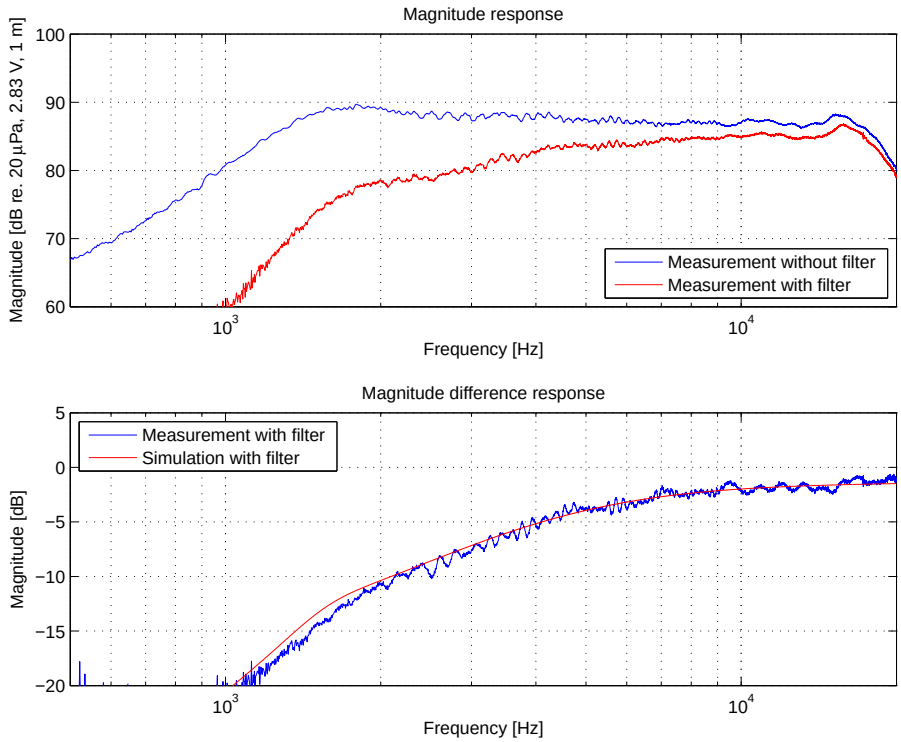

Figure 6.9: *Highpass filtered tweeter magnitude response.*

Again it is seen, that the simulated and measured curves coinside.

6.5 Driver Interference

This section presents the measured and simulated interference pattern, when placing two identical woofers with a center distance of 30 cm. The simulation of the interference pattern is based on section 2.5 on page 31, and the corresponding measurements are described in appendix B.6 on page 121.

Figure 6.10 illustrates the result of the simulation and measurement. The measurement can be compared to the simulation, since the drivers are almost omnidirectional at the chosen frequency, as it can be seen in appendix B.3 on page 114.

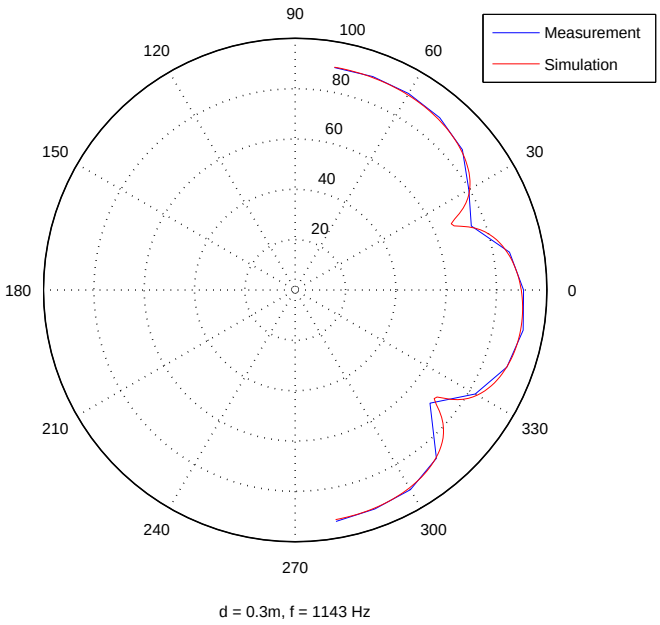

Figure 6.10: *Interference pattern of two woofer placed with a distance of 30 cm. The frequency is 1143 Hz.*

It can be seen, that the simulation is similar to the measurement result. The cancellation angles are equal in both the simulation and measurement. It is concluded, that the interference theory is valid.

Figure 6.11 on the next page shows the interference pattern as function of angle and frequency.

This plot should be compared to figure 2.34 on page 33. It can be seen, that the tendencies are the same. The dips are placed equal in the two plots. Above approximately 2 kHz the used drivers in the measurements start to beam. Therefore figure 6.11 on the next page is not directly comparable to the simulated plot above this frequency.

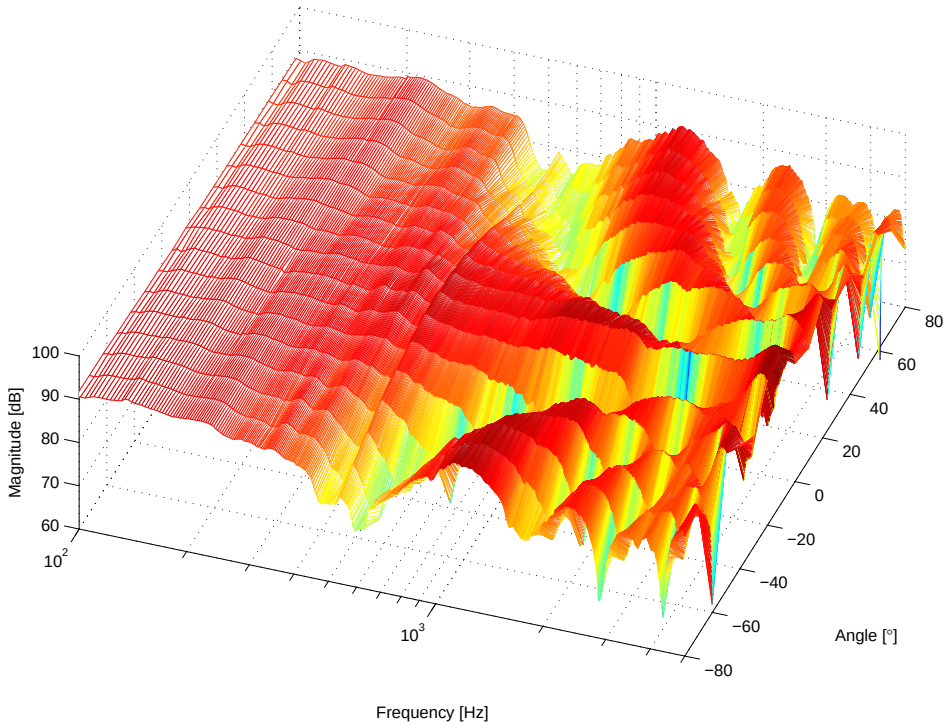

Figure 6.11: *Interference pattern as function of angle and frequency.*

6.6 Edge Diffraction

This section presents the measured and simulated cabinet diffraction contributions. The simulation is based on section 2.6 on page 36, and the corresponding measurements are described in appendix B.7 on page 123.

6.6.1 Woofer Diffractions

Figure 6.12 illustrates the result of the simulation and measurement using the woofer. The microphone is placed in front of the woofer.

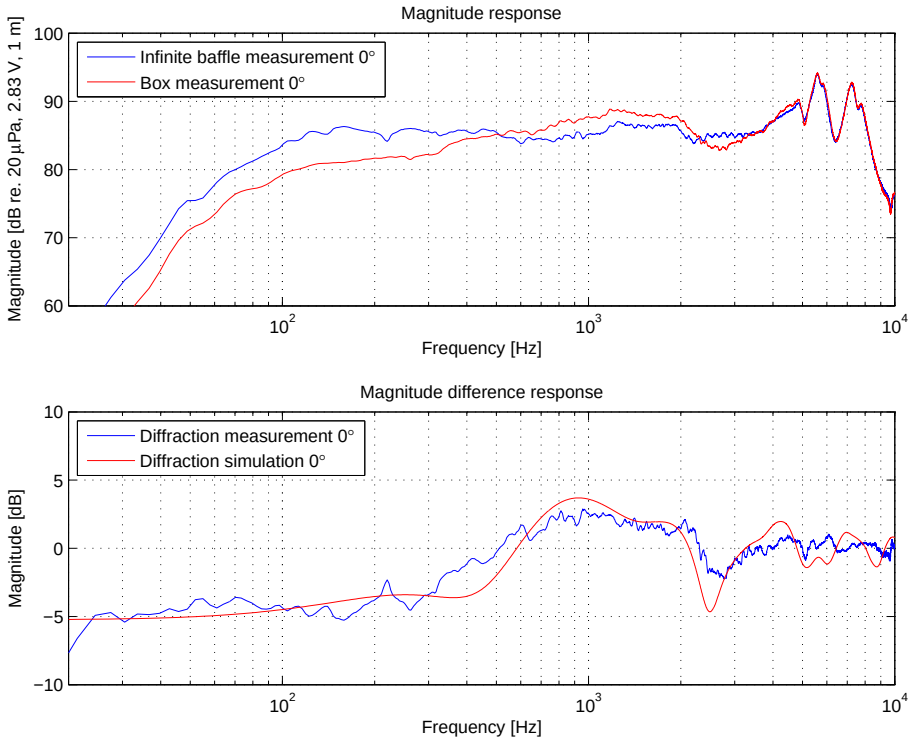

Figure 6.12: *Cabinet edge diffraction simulation and measurement. The microphone is placed in front of the woofer.*

It can be seen, that the simulation and measurement is similar. The deviation from approximately 300 Hz - 600 Hz is due to the diffraction theory [9, page 931]. The dip at approximately 2500 Hz is less pronounced in the measured response. This might be due to the woofers beaming at that frequency. The beaming results in a smaller edge diffraction contribution to the direct sound of the woofer. This effect can also be seen at the high frequencies, where the measured response has less ripples.

Figure 6.13 on the next page illustrates the result of the simulation and measurement using the woofer. The microphone is placed 30° off-axis in the horizontal direction.

As seen, the tendency is the same for the simulated and measured response. At high frequencies there are deviations up to 5 dB. This is not considered as a problem, since these frequencies typically lies in the woofers lowpass filter stopband.

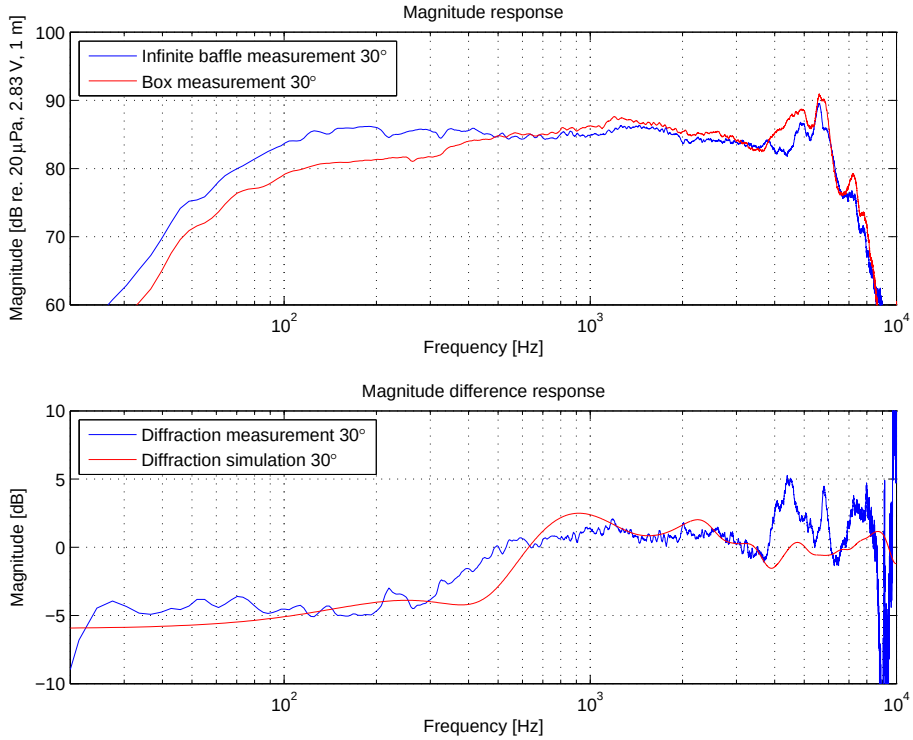

Figure 6.13: *Cabinet edge diffraction simulation and measurement. The microphone is placed 30° off-axis in the horizontal direction.*

6.6.2 Tweeter Diffractions

Figure 6.14 on the facing page illustrates the result of the simulation and measurement using the tweeter. The microphone is placed in front of the tweeter.

From the figure can be seen, that the simulated and measured responses are similar. Again the measured response at high frequencies is more flat because of the beaming tweeter.

Figure 6.15 on the next page illustrates the result of the simulation and measurement using the tweeter. The microphone is placed 30° off-axis in the horizontal direction.

The simulated curve fits the measured curve closely. At frequencies above approximately 14 kHz the simulation does not predict the right response. The deviations might be reflections from the tweeter mounting screws. This is not considered as a problem, since the deviations are relatively small.

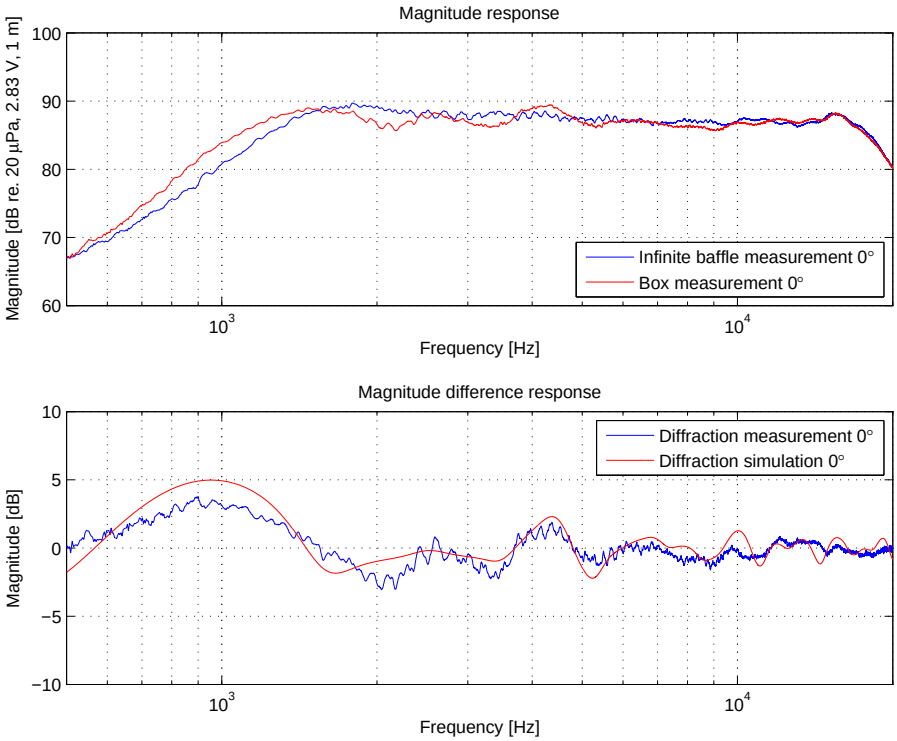

Figure 6.14: *Cabinet edge diffraction simulation and measurement. The microphone is placed in front of the tweeter.*

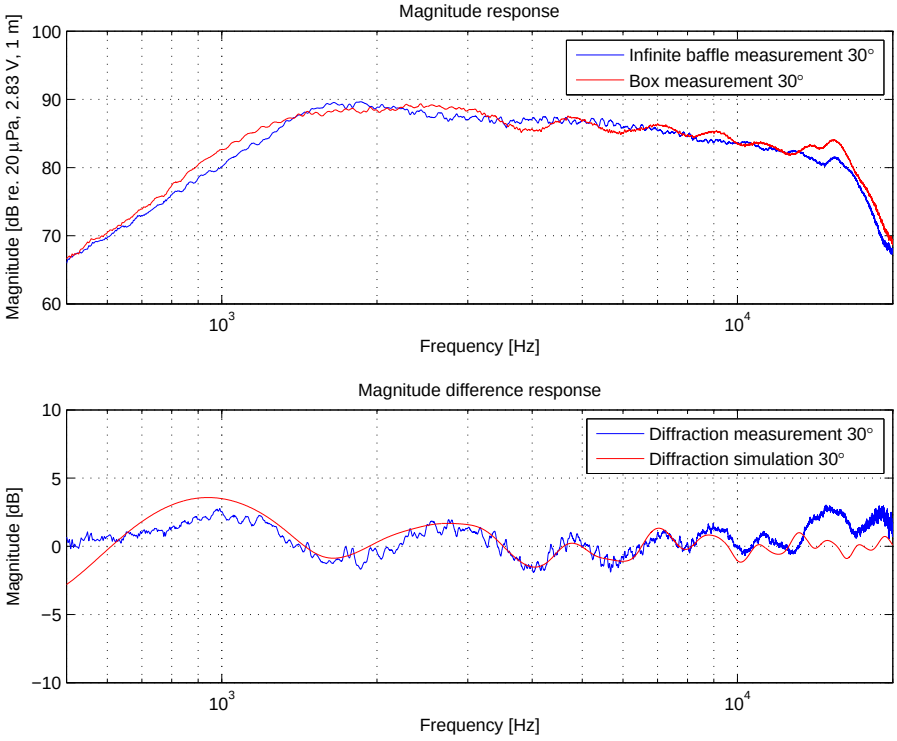

Figure 6.15: *Cabinet edge diffraction simulation and measurement. The microphone is placed 30° off-axis in the horizontal direction.*

6.7 Damping Material

This section presents measurements of a closed box magnitude response. A situation with and without Acoustilux damping material inside the cabinet. The front baffle is the infinite baffle. Finally is shown how the damping material influences on the electrical impedance. The measurements are described in appendix B.8 on page 125.

6.7.1 Magnitude Responses

Figure 6.16 shows the measurement of the box with and without damping material.

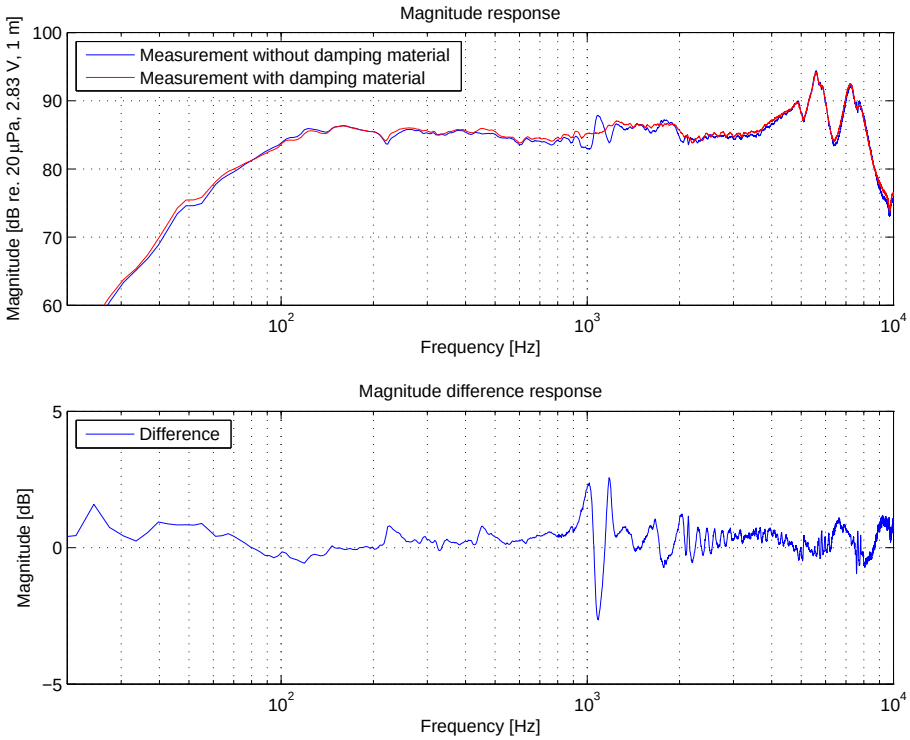

Figure 6.16: *Measured magnitude responses with and without damping material placed inside the loudspeaker cabinet.*

As seen in the upper blue curve, there are reflections inside the cabinet. Calculations show, that the 2. standing wave, in the height dimension inside the cabinet, is approximately 1100 Hz. This could be what is seen in the measured response. This reflection is clearly damped when putting damping material inside the box. From the magnitude difference curve can easily be seen, that the damping material causes an amplification of the frequencies below approximately 80 Hz. This is due to the increased volume when using damping material, which again result in a less steep low-frequency roll off.

6.7.2 Impedance

Figure 6.17 shows the measurements of the electrical impedances of the woofer positioned in the designed closed box. Situations with and without damping material are presented.

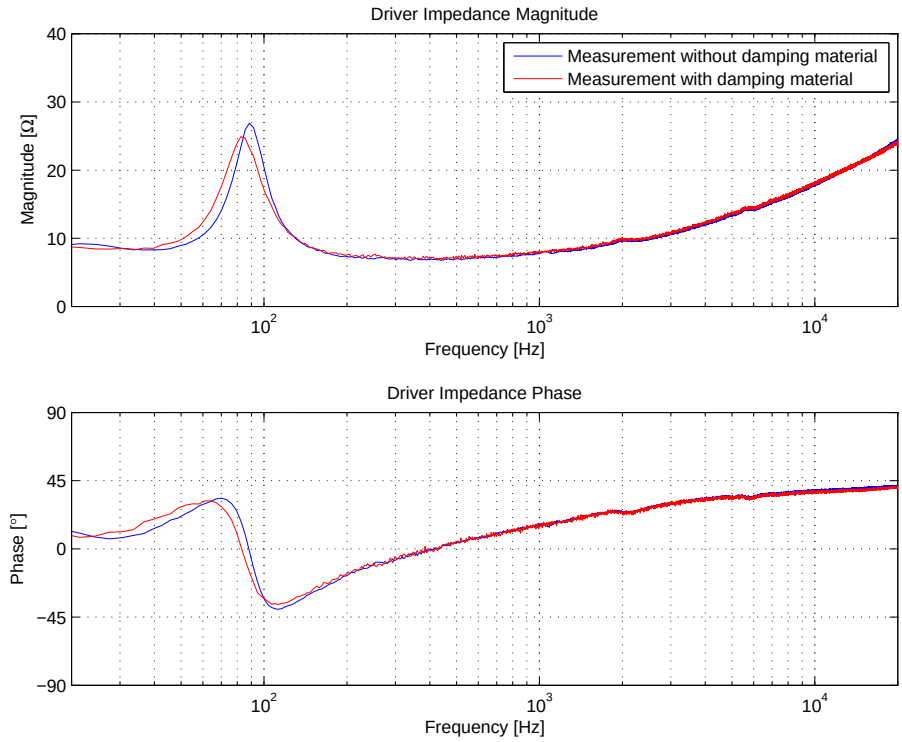

Figure 6.17: *Electrical impedances of the woofer positioned in the designed closed box.*

As seen, the damping material brings down the resonance frequency. This is due to the effect of increased cabinet volume. Also the magnitude at the resonance gets lower, which is a consequence of introduced mechanical losses by the damping material. Some of the acoustical energy is converted into heat in the damping material.

It is concluded, that damping material increases the cabinet volume seen from the drivers point of view. Furthermore the damping material attenuates internal cabinet reflections.

Summary

The simulations based on the theories compared to measurements show, that there are some minor deviations. These deviations are considered to be small, and are not expected to have any major influence on the performance of the complete model. In next chapter, the theories will be put together to make the complete loudspeaker model.

CHAPTER 7

ADVANCED LOUDSPEAKER MODEL DESIGN

This chapter presents the design of the advanced loudspeaker model developed in this thesis. This model is based on the theory presented in chapter 2. Furthermore, the model is verified using measurements and simulations of the reference speaker designed in chapter 5. The model is made in Matlab.

7.1 Definition of Variables

The model requires information about the loudspeaker box, the drivers and the microphone position in order to model the complete response from the loudspeaker at any microphone position. In the implementation all these parameters are gathered in a struct, that is used throughout the model. In this way, changing a parameter has only to be done in one place. This struct consists of 4 substructs with constants and optimization variables, filter component values, woofer parameters and tweeter parameters. In the main struct there are parameters to define the box dimensions and plate thickness, the position of the tweeter and woofer on the front baffle and the microphone position. From these parameters for example the volume of the box, the distance between the drivers or the distance from each driver to the microphone can be calculated.

A frequency vector is constructed using the defined parameters for sampling frequency and FFT-size. As described in section 5.3 on page 58 a new frequency vector containing logarithmically spaced frequencies is calculated, to decrease calculation time.

7.2 Model Design

It is desired to make a model that is easy to modify. To ensure this, the model is made of a number of blocks each containing one of the theories presented in chapter 2. The organization of the model is shown in figure 7.1 on the following page.

The blocks all work in the same way. They are made as seperate functions that take a frequency vector or a pointer to the desired frequencies in the frequency vector defined by the sampling frequency and FFT-size. These functions all return a frequency response calculated from the logarithmically spaced frequency vector. In this way the output from each block is similar and can be handled in the same way. Most of the functions require more parameters as for example the struct containing all settings or the output from another block. In the block diagram in figure 7.2 on page 85 the input parameters of all blocks can be seen. It should be noted that the only blocks, that depend on other blocks, are

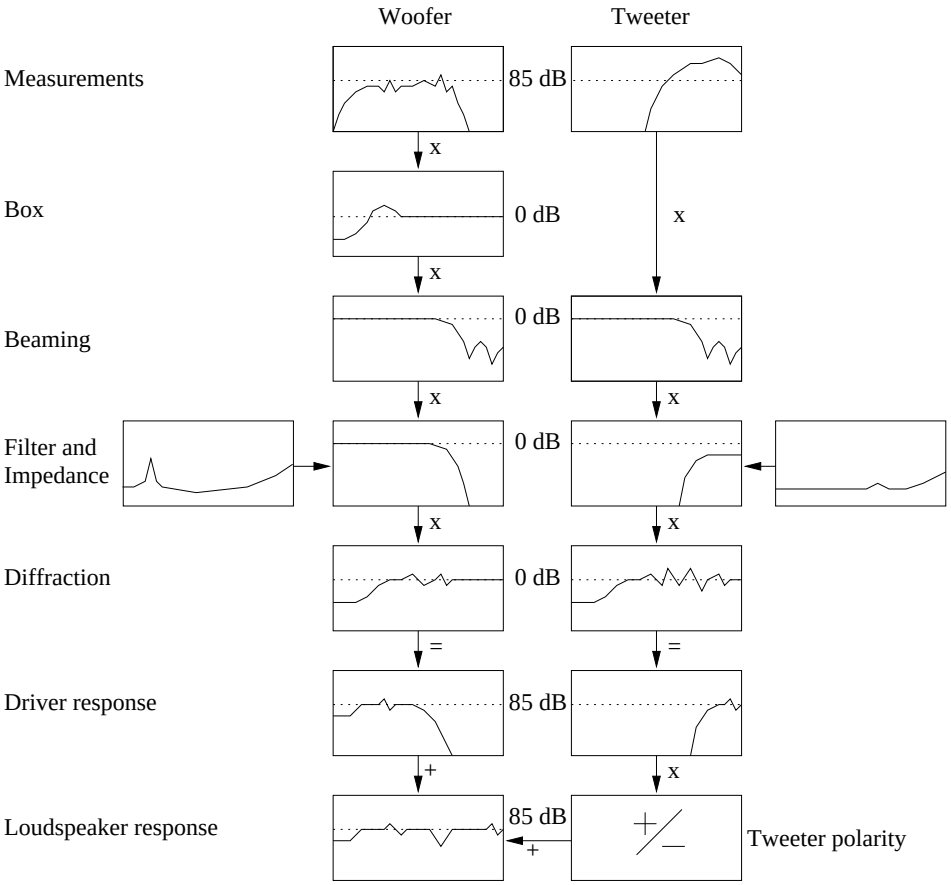

Figure 7.1: *Organization diagram for the loudspeaker model.*

the simulations of the filter responses, which requires the simulated impedances of the corresponding driver. Appart from that, all blocks are independent.

When the model is constructed it is important to ensure, that each phenomena of the loudspeaker is included only once. This could for example be the distance from the driver to the microphone which, under normal conditions is included in several of the theories presented. The following list presents what is included in each block of the model:

- **measb, meast**
  This block loads an infinite baffle on-axis measurement of the woofer or the tweeter respectively. This measurement must be made in one meters distance from the baffle with the drivers mounted as they would be on the loudspeaker baffle. In this way their acoustical center offset relative to the baffle is included for each driver. This block also includes level and phase shift corresponding to 1 meter distance.
  The block works by loading a time signal measured with the MLS-system as described in appendix B.3 on page 114, and moving the signal to the frequency domain using a Fourier transformation. Finally the frequencies, described by the frequency pointer, are selected from the calculated frequency vector.

- **simbox**
  This block represents the change from adding a box to the speaker. It is calculated as the dif-

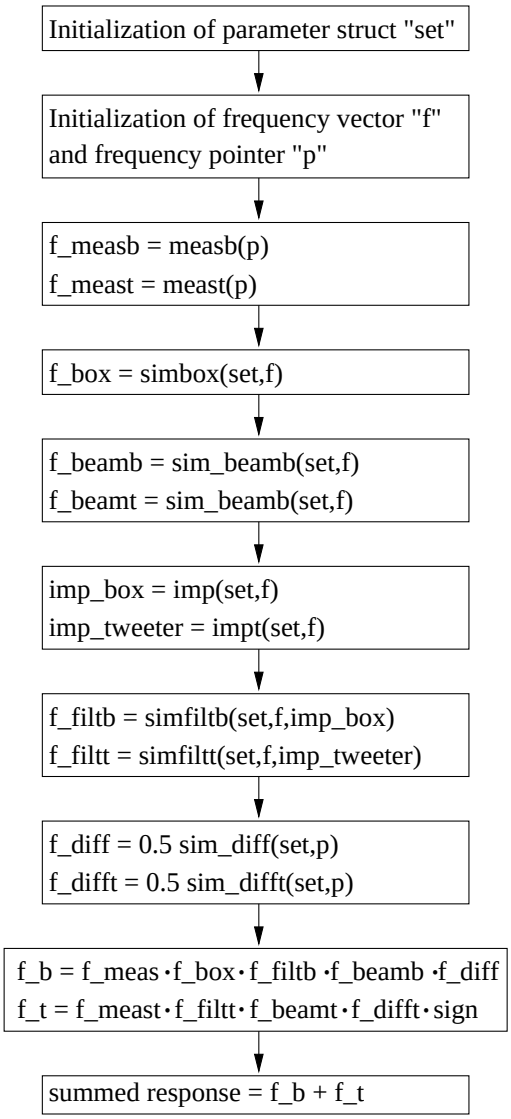

Figure 7.2: *Block diagram for the loudspeaker model.*

ference between simulations of a closed box and an infinite baffle. This includes magnitude and phase changes.

- **sim_beamb, sim_beamt**
  This block contains the simulated frequency responses of the beaming of the drivers. Furthermore the distance from each driver to the microphone is calculated, and the level and phase of the signal is changed according to the distance. The distance of 1 meter that were used in the measurements is subtracted from the calculated distance so the total distance included in the model is correct.
  The calculation of level and phase shift caused by distance, is used when calculating the interference between the drivers, when they are summed.

- **imp, impt**
  This block calculates the electrical impedance of the tweeter and the woofer mounted in a box. This is done with the parameters estimated from the measured impedance curve in section 5.3 on page 57. A simulated impedance, calculated with the parameters derived from the measured impedance is used to be able to calculate the correct impedance for any box, since changes in the box volume, leads to changes in the resonance frequency.

- **simfiltb, simfiltt**
  In this block, the responses of the filters are calculated. To do this correct, it is necessary to know the impedances of the drivers, which are given as input parameters to this block.

- **sim_diff, sim_difft**
  This block calculates the edge diffractions from the box for the woofer and the tweeter respectively. This block calculates a time signal as described in section 2.6 on page 36. This time signal is transformed to a frequency signal in the same way as described for the measured signal above.

- **sign**
  This block sets the polarity of the tweeter and can be 1 or -1.

Every block of the simulation, except the measurements of the drivers, are designed so that the block output is the difference that it contributes to the corresponding driver. To maintain this, it is necessary to decrease the level of the diffraction simulation with 6 dB since the simulation, as shown in figure 2.42 on page 40 has a level of 6 dB as reference. The level correction is made by multiplying the result of the simulation by 0.5.
With each block of the simulation containing the difference that it contributes to the corresponding driver, each block can be considered as a filter to the measured response, and the final response for the woofer and tweeter respectively can be calculated by multiplying all the responses together. The complete loudspeaker response can be found by summing the responses of the two sound sources, with respect to the polarity of the tweeter, as shown in the last block of the block diagram.

7.3 Model Simulation and Verification

To verify the model, the frequency response of the reference speaker is measured on-axis and at 30° horizontally off-axis as described in appendix B.9 on page 128. The same two situations are simulated and the results are shown in figure 7.3 on the next page and 7.4 on page 88.

From the upper plot in figure 7.3 on the next page it can be seen, that there are deviations between the measured and the simulated response. Especially in the range from 3 kHz to 6 kHz, where the simulation generally has a higher level than the measured, and the dip around 5.5 kHz is not situated at the same frequency.
The lower plot shows the individual responses from the drivers for measurements and simulations. This reveals, that the deviations in the edge diffraction model for the woofer around 400 Hz and 1 kHz described in section 6.6 on page 77 remain. From the individual responses no explanation can be found on the raised level from 3 kHz to 6 kHz and why the dip at 5.5 kHz is moved upwards in frequency. It is expected that these errors in the summed simulation response are introduced by phase shift that is not simulated correct.

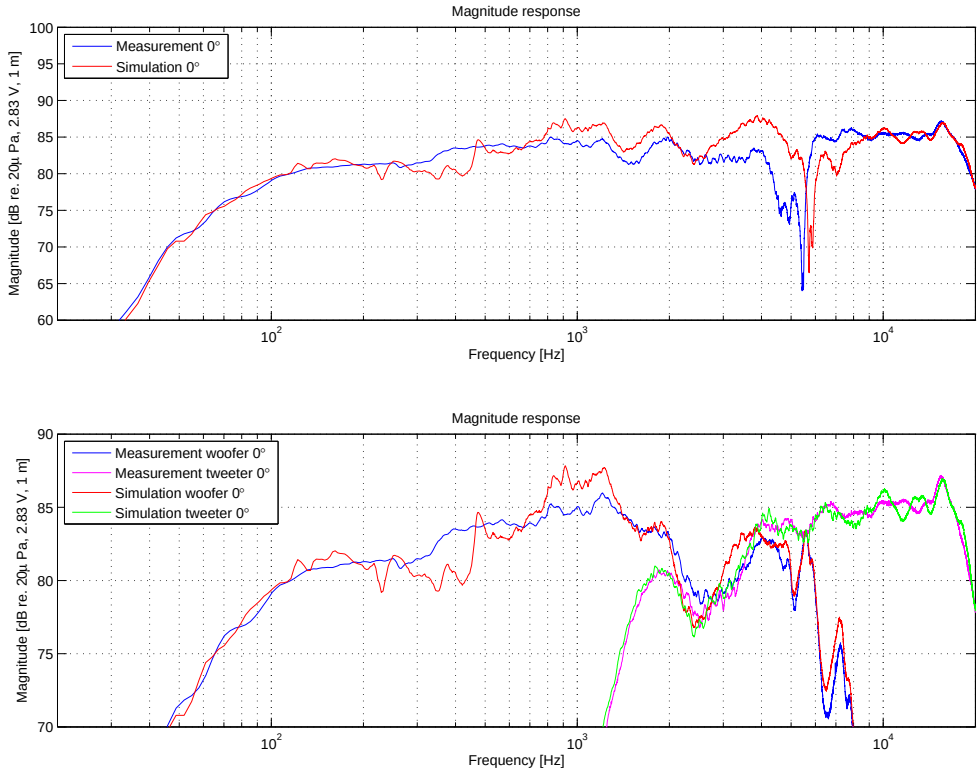

Figure 7.3: *Simulation and measurement of reference loudspeaker on-axis.*

Apart from the mentioned deviations, it can be seen that the simulated and measured responses for both drivers are similar.

In figure 7.4 on the next page the upper plot shows, that the deviations introduced by edge diffraction are still present as discussed above. Furthermore the dip at 5 kHz is not as pronounced in the simulation as it is in the measurement, but the position seems to be correct. By examing the lower curves, the reason for the level difference can be found to be the level difference in the woofer responses, where the simulated response is lower than the measured. This causes the cancellation between the drivers to be less pronounced in the simulation. The deviations between the woofer responses at 4 kHz to 6 kHz, are the same that is found in the verfication of the diffraction theory in section 6.6 on page 77.
For the off-axis measurements and simulations it can also be seen that the results are similar.

The deviations of the loudspeaker model found in this section are not expected to have any major influence on the results of the optimization of the crossover network, so the model is considered to be valid and is used in the rest of this thesis.

The complete model can be found on the attached CD-ROM. A readme.1st file describes the use of the model.

The next chapter uses the designed loudspeaker model, to make an automatic crossover optimization system.

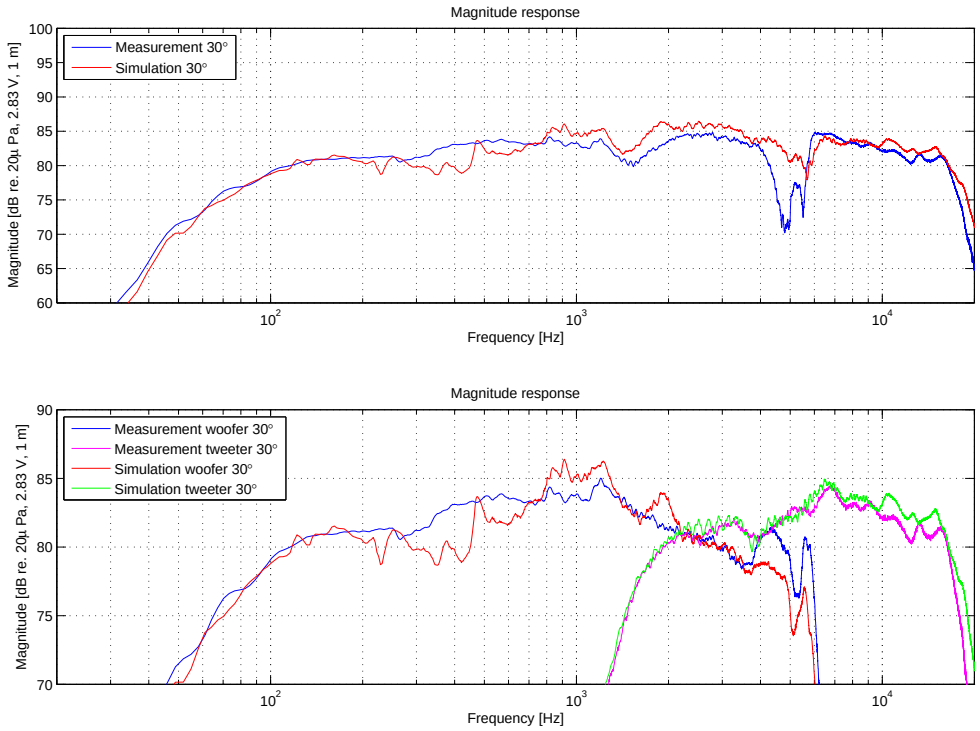

Figure 7.4: *Simulation and measurement of reference loudspeaker 30° off-axis.*

CHAPTER 8

AUTOMATIC CROSSOVER NETWORK OPTIMIZATION

This chapter describes how the crossover network can be optimized by using the loudspeaker model designed in chapter 7. The optimization method is steepest descent, which is presented in chapter 4.

8.1 Optimization Conditions

The optimization is chosen to work on the crossover network components. The optimization is further chosen to optimize on two different listening angles, namely 0° and 30° off-axis in the horizontal direction. These two angles are chosen in order to optimize the loudspeaker response in a typical listening angle range. For example in a stereo setup, the listening angle is typically 30° [2, page 571].

The optimization is made with an adjustable weighting of the 0° and 30° off-axis positions. The weighting can easily be changed. This feature makes it possible to optimize the loudspeaker response to a desired listening position.

The evaluated frequencies, are the frequencies chosen as described in section 5.3 on page 58. The filter components, which are the optimization parameters, are scaled to have the same order of magnitude. This is described in section 5.3 on page 58.

Optimization provides a lot of possibilities. In practise, series filters are hard to design, since the driver impedances influence all transfer functions in the complete crossover network. With the optimization algorithm made in this project, it is possible to optimize any kinds of filters. It is furthermore easy to try out first order and higher order filters.

8.2 Choice of Optimization Parameters

The optimization parameters are the crossover filter components. These are presented together with the chosen start values in table 8.1 on the next page.

Filter Component	Start Value	Scaling factor and unit
C_w	3.98	10^{-6} F
C_t	3.98	10^{-6} F
L_w	1	10^{-3} H
L_t	1	10^{-3} H
R1	2.2	$1 \cdot \Omega$
R2	22	$1 \cdot \Omega$

Table 8.1: *Filter components used in the optimization.*

The start values are the component values calculated for the reference loudspeaker, described in section 5.4.1 on page 60. When running the optimization it is made possible to change the polarization of the tweeter. This should be tried out in order to see what result is best.

Since no ideal inductors excist, a function is made to calculate the series resistance as function of the inductance. The values are based on inductors with wires having a diameter of 1 mm. [4].

8.3 Construction of Performance Function

The performance function is described as the difference between the optimization result, OPTR, and a target response, as described in section 4.1 on page 49. The result of the optimization, in each iteration, is the output from the loudspeaker model with the current set of filter component values. The target response can be chosen in several ways, and this project focuses on a target response having a flat magnitude response.

Since a loudspeaker works in a limited frequency range, a specific frequency range is chosen before optimization. The maximum frequency f_{max} is chosen to 15 kHz, which is assessed to be a good approximation of how high in frequency most tweeters have a linear magnitude response on-axis and 30° off-axis. The minimum frequency f_{min} is calculated from the simulated woofer closed box magnitude response. The frequency is chosen according to where the magnitude is -3 dB.

The target response level is, in each iteration, calculated as the mean value of the current magnitude response, OPTR. This way, the optimization focuses on the deviations from the mean sensitivity level. The current target response reference level can be described as:

$$\text{ref} = \text{mean}\big(\ \text{abs}(\text{OPTR}(f_{min} : f_{max}))\ \big) \tag{8.1}$$

Including the adjustable weightings X and Y, which are the weightings for 0° and 30° respectively, the performance function can be calculated as:

$$P \quad = \quad X \cdot \sum_{f_{min}}^{f_{max}} (\text{OPTR}_{0^\circ} - \text{ref})^2 \ + \ Y \cdot \sum_{f_{min}}^{f_{max}} (\text{OPTR}_{30^\circ} - \text{ref})^2 \tag{8.2}$$

8.4 Reorganization of Model Structure

In order to increase the performance of the optimization algorithm, the structure of the loudspeaker model is reorganized. The flowchart on figure 8.1 shows the reorganized structure.

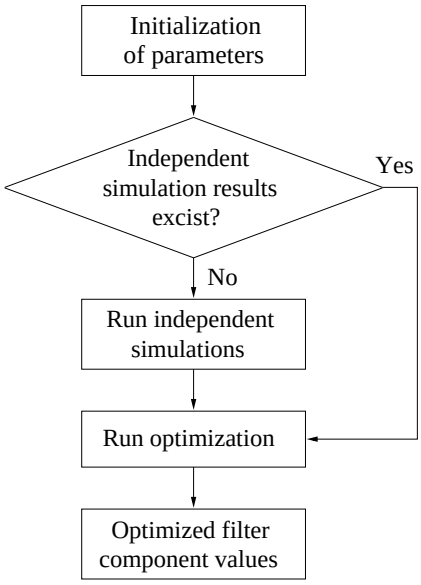

Figure 8.1: *Reorganized model structure used in optimization algorithm.*

First the different parameters are initialized, which are presented in the following list.

- Stepsize
- Filter component start values
- Tweeter polarity
- Loudspeaker driver parameters
- Constants as ρ and c etc.
- Outer box dimensions and plate thickness
- Woofer and tweeter positions on the front baffle
- Weighting between on-axis response and 30° off-axis response
- Magnitudes based on dB or pascal values

The next box in the flowchart tests if the independent simulation results exist. This is because they only have to be executed once, so a repeated execution of the optimization will be faster. The independent simulations are presented in the following list.

- Edge diffraction simulations at both 0° and 30° for both the woofer and tweeter.
- Beam simulations at 0° and 30° are calculated for both drivers.

- Box simulation for low frequency roll off.
- Measurements of infinite baffle acoustical frequency responses of the woofer and tweeter.
- Simulations of electrical impedances of the woofer and tweeter.

After the initialization is done, the optimization is performed. After 1000 iterations the optimization software returns a set of optimized filter component values.

The initialization part and the independent parts, that have been moved out from the iteration loop, takes approximately 1 minute and 30 seconds to run. The reduced optimization part takes approximately 20 ms per iteration. From this perspective, the reorganization of the model structure saves a lot of time in the optimization execution time.

8.5 Result of Optimization

This section presents the results of the optimization. The optimization runs on the box designed in section 5.4.2 on page 62. By trials, the polarity of the tweeter is chosen not to be reversed, and the weighting of the 0° and 30° responses are chosen to 5:1 respectively. Finally the magnitude is evaluated in dB.

Table 8.2 shows the optimization start values together with the optimized filter component values.

Filter Component	Start Value	Optimized Value
C_w	3.98 μF	18.89 μF
C_t	3.98 μF	3.80 μF
L_w	1 mH	3.34 mH
L_t	1 mH	0.96 mH
R1	2.2 Ω	9.77 Ω
R2	22 Ω	21.41 Ω

Table 8.2: *Filter component start values and optimized values.*

When constructing the optimized crossover network, standard component values are chosen. The list below shows how the components are realized.

- 3.80 μF capacitor: Parallel connection of 3.3 μF and 0.47 μF
- 18.89 μF capacitor: Parallel connection of 15 μF, 0.68 μF and 3.3 μF
- 0.96 mH inductor: 1 mH inductor with resistance of 0.5 Ω
- 3.34 mH inductor: 3.3 mH inductor with resistance of 1 Ω
- 9.77 Ω resistor: 10 Ω resistor
- 21.41 Ω resistor: 22 Ω resistor

Results of the optimized crossover network are presented in figure 8.2 and figure 8.3.

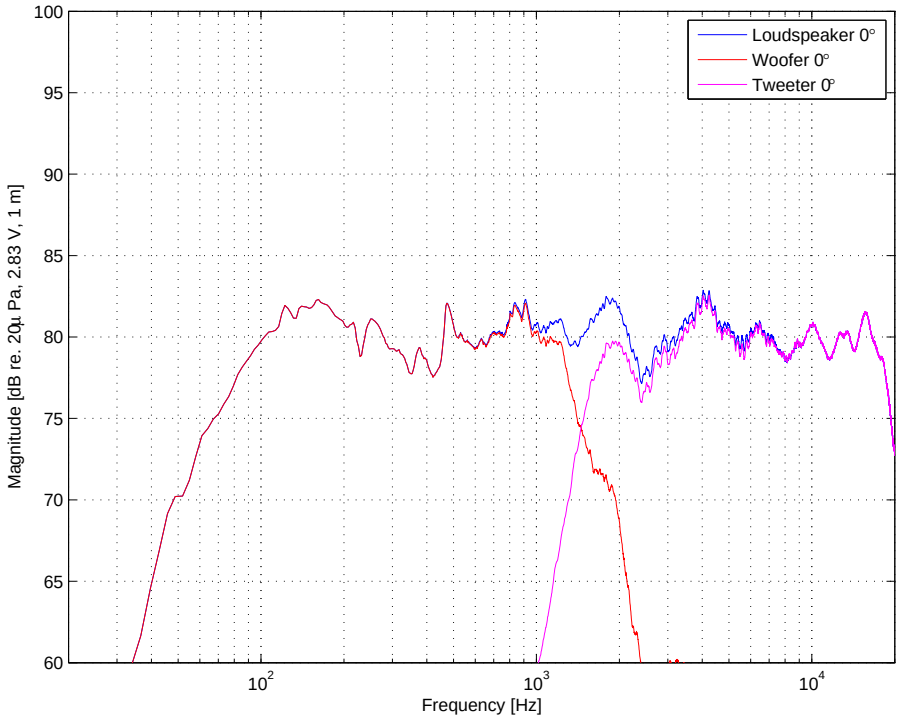

Figure 8.2: *Simulated on-axis response with optimized crossover network.*

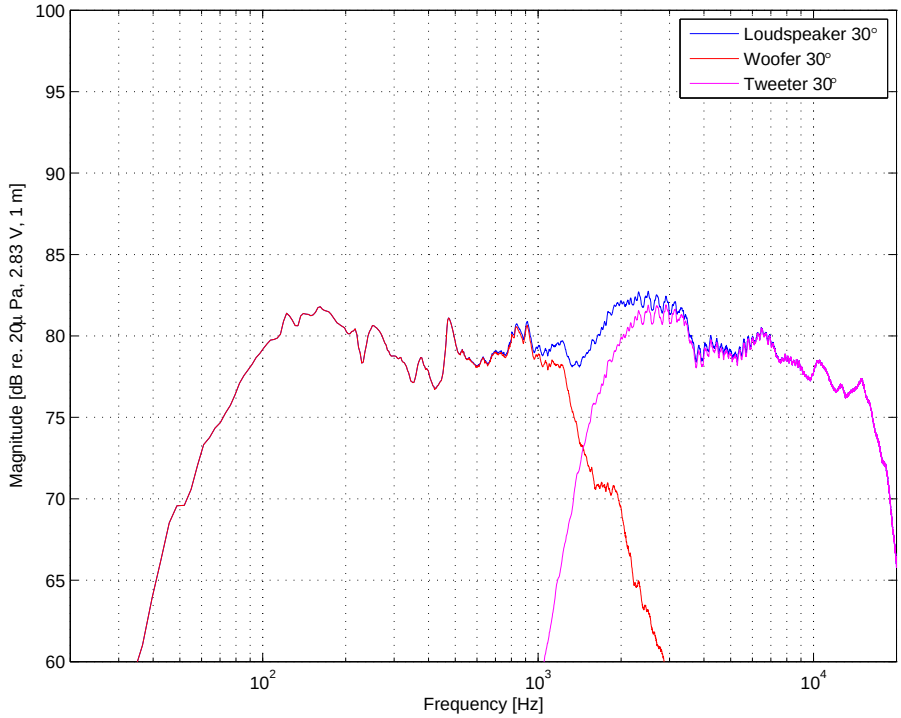

Figure 8.3: *Simulated 30° off-axis response with optimized crossover network.*

It can be seen, that the crossover frequency is positioned at approximately 1500 Hz and the slopes are smooth. The weighting between 0° and 30° puts most effort on the on-axis response, which can be seen on figure 8.2. This response is most flat with an overall level at approximately 80 dB SPL.

The optimization program can be found on the enclosed CD-ROM. A readme.1st file describes the use of the program.

The next chapter presents results and evaluation of the optimization, and comparison to the reference speaker.

CHAPTER 9

EVALUATION OF REFERENCE AND OPTIMIZED LOUDSPEAKER

This chapter presents the measurements of the reference loudspeaker, the optimized loudspeaker and comparisons between these.

On-axis Measurements

The measured on-axis magnitude response of the reference loudspeaker is shown in figure 9.1 on the next page. It can be seen, that the cut-off frequencies for both drivers are far from the desired 2.5 kHz. This is due to the change of the electrical transfer function of the crossover, introduced by the true impedances of the drivers in stead of 8 Ω resistors, and membrane break up contributions for the woofer. The effective cut-off frequency for the woofer is approximately 6 kHz and for the tweeter it is 1.8 kHz. The result of this is interference between the drivers in a wider range. This can be seen from 2 kHz to 4 kHz where the drivers sum in phase and gives a raise to the magnitude response. From 4 kHz to 6 kHz a cancellation is seen between the drivers. Furthermore it can be seen, that the level decreases from 500 Hz and downwards. This is caused by edge diffractions.
When the roll off at low frequencies is disregarded, the difference from the lowest level at 5.5 kHz to the highest level at 17 kHz is found to be approximately 22 dB and the sensitivity is approximately 84 dB SPL/1W/1m.

In figure 9.2 on the facing page the on-axis measurement of the optimized loudspeaker can be seen. The cut-off frequencies between the drivers change, so they are positioned at the same frequencies. The crossover frequency is now 1.5 kHz. The effect of this is less overlap between the drivers, hence less interference. Furthermore the acoustical slopes for both drivers at the crossover frequency are smooth and the membrane break up contributions for the woofer have been damped. The bafflestep has also been removed, which lowers the sensitivity of the loudspeaker.
When the measurement of the reference speaker is compared with the corresponding simulations shown in figure 8.2 on page 93 it can be seen, that the model has predicted the response of the optimized loudspeaker very well.
When the roll off at low frequencies is disregarded, the difference from the lowest level at 700 Hz to the highest level at 4 kHz is found to be 5 dB and the sensitivity is approximately 80 dB SPL/1W/1m.

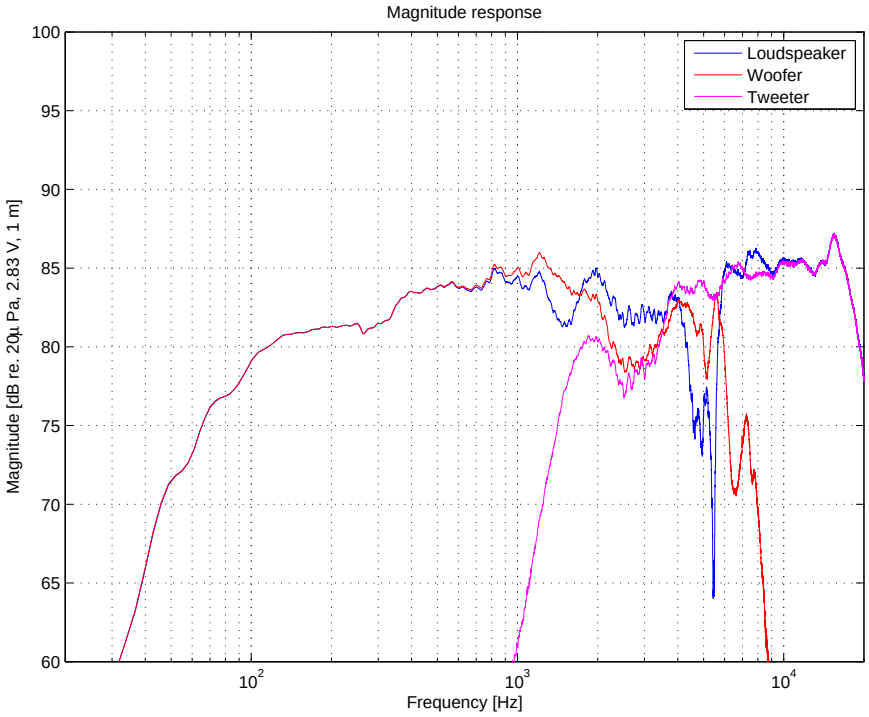

Figure 9.1: *Measured reference loudspeaker on-axis.*

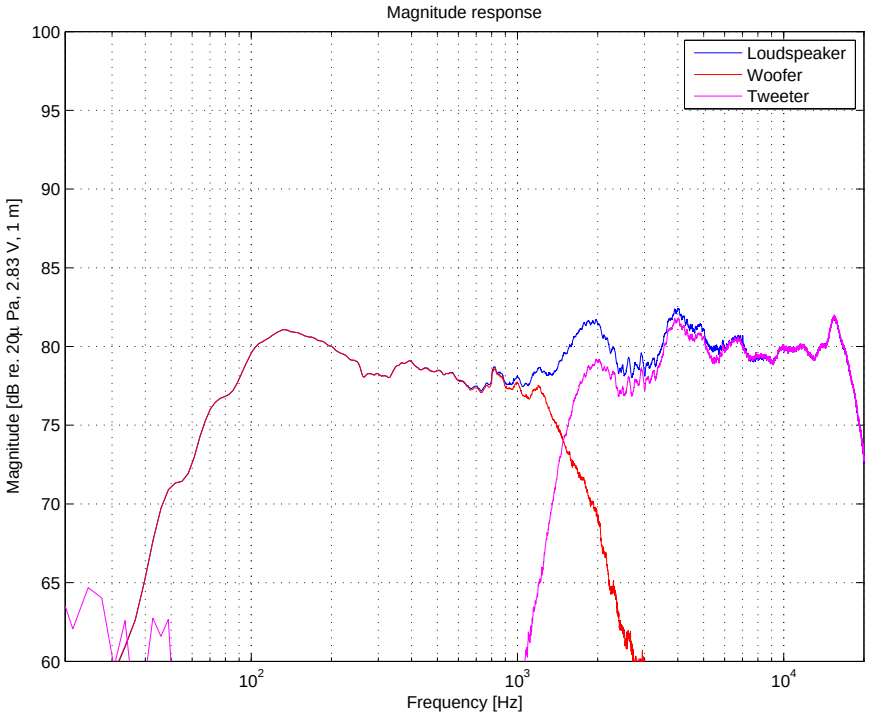

Figure 9.2: *Measured optimized loudspeaker on-axis.*

30° Horizontally Off-axis Measurements

The measurement of the reference loudspeaker 30° horizontally off-axis is shown in figure 9.3 on the facing page. From the plot can be seen, that the two drivers still overlap in frequency, and there is a cancellation at 5 kHz. It can also be seen, that the tweeter beams from 5 kHz and upwards.
When the roll of at low frequencies is disregarded, the difference from the lowest level at 5 kHz to the highest level at 6 kHz is approximately 15 dB.

Figure 9.4 on the next page shows the measurement of the optimized loudspeaker 30° horizontally off-axis. It can be seen, that there is less overlap between the drivers, hence less cancellations. It can be seen that the drivers beam, as it was also seen in the reference speaker measurement. At this plot it is also noticeable at the woofer. The beaming of the woofer results is in the area from 200 Hz to 2 kHz where the level is lower.
When the measurement of the reference speaker is compared with the corresponding simulation shown in figure 8.3 on page 94 it can be seen, that the model also has predicted the response 30° off-axis of the optimized loudspeaker very well.
When the roll off at low frequencies is disregarded, the difference from the lowest level at 1 kHz to the highest level at 3 kHz is found to be approximately 6 dB.

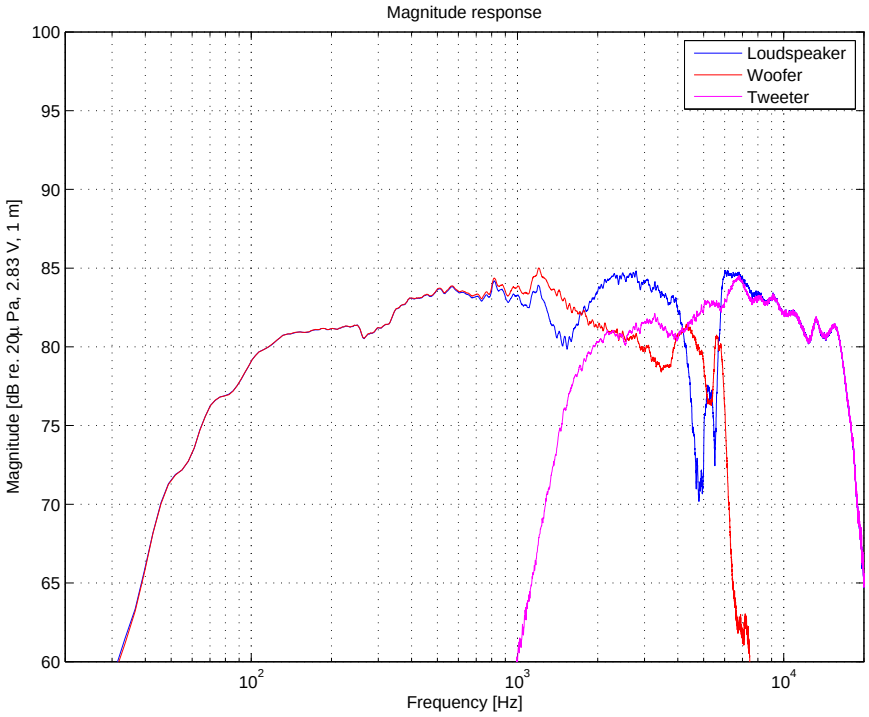

Figure 9.3: *Measured reference loudspeaker 30° horizontally off-axis.*

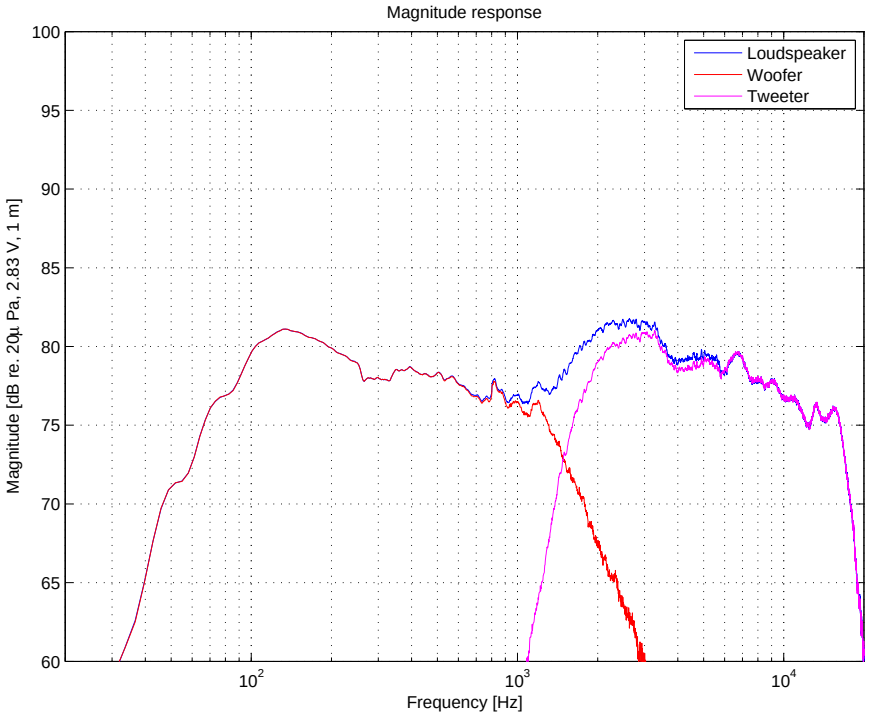

Figure 9.4: *Measured optimized loudspeaker 30° horizontally off-axis.*

30° Vertically Upwards Measurements

Figure 9.6 on the next page shows the measurement of the reference loudspeaker 30° vertically upwards. At this microphone position the drivers still overlap in frequency, hence the cancellation at 5 kHz is still present.

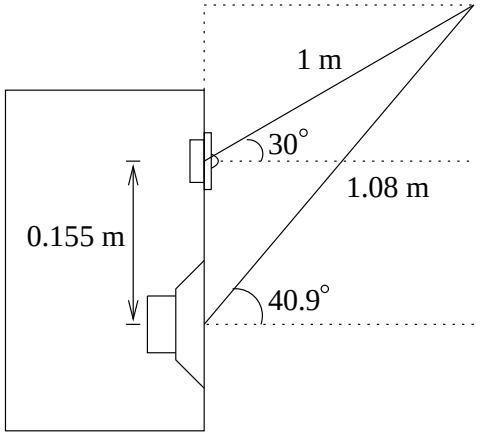

Figure 9.5: *Measurement angles and distances 30° upwards.*

As it can be seen in figure 9.5 there are different measurement angles to the drivers. The angle to the tweeter is at 30° since the tweeter is the reference point. The angle to the woofer changes to 40.9° by moving the measurement position 30° up. The result of this, is that the woofer starts beaming at a lower frequency compared to the 30° horizonally off-axis measurement. Furthermore it can be seen that the level of the woofer is approximately 1 dB lower than the 30° horizontally off-axis measurement. This is caused by the increased distance from the microphone to the woofer. From this distance change, the expected level decrease is calculated to 0.67 dB.
When the roll off at low frequencies is disregarded, the difference from the lowest level at 5 kHz to the highest level at 6 kHz is found to be approximately 8 dB.

Figure 9.7 on the next page shows the measurement of the optimized loudspeaker 30° vertically upwards. A cancellation at 1.5 kHz is seen. This is introduced by the change in distance to the woofer, which causes the sound from the drivers to be out of phase at the microphone position. Furthermore, the beaming and level change, as dicussed for the reference speaker above, occurs.
When the roll off at low frequencies is disregarded, the difference from the lowest level at 1.5 kHz to the highest level at 4.5 kHz is found to be approximately 22 dB.

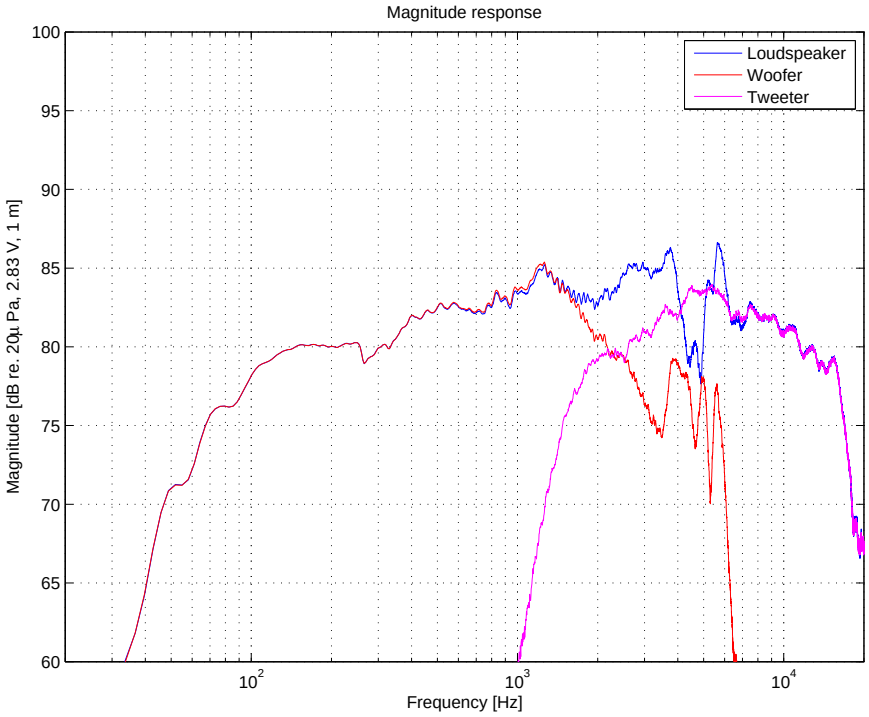

Figure 9.6: *Measured reference loudspeaker 30° vertically upwards.*

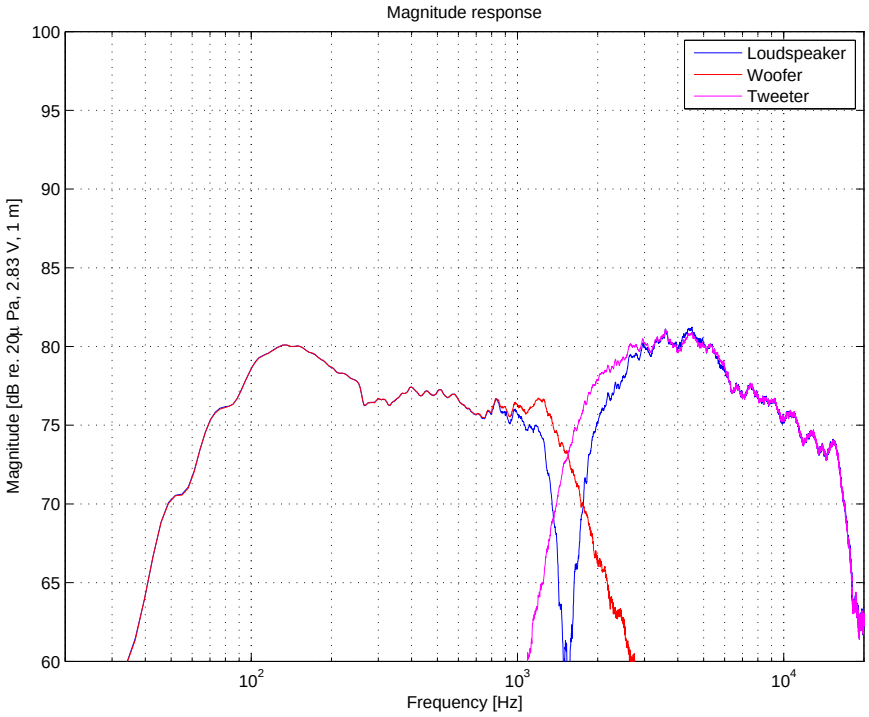

Figure 9.7: *Measured optimized loudspeaker 30° vertically upwards.*

30° Vertically Downwards Measurements

Figure 9.9 on the facing page shows the measurement of the reference loudspeaker 30° vertically downwards.

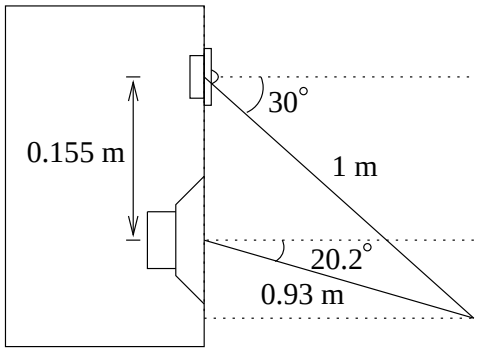

Figure 9.8: *Measurement angles and distances 30° downwards.*

It can be seen from figure 9.8, that the change off the woofer measurement angle and distance is opposite of moving 30° upwards. The result is less beaming of the woofer, and the level of the signal is increased. This together with interference causes the peaks and dips from 1 kHz to 5 kHz. From the distance change, the expected level decrease is calculated to 0.66 dB for the woofer.
When the roll off at low frequencies is disregarded, the difference from the lowest level at 2 kHz to the highest level at 4.7 kHz is found to be approximately 15 dB.

Figure 9.10 on the facing page shows the measurement of the optimized loudspeaker 30° vertically downwards. This response is similar to the response 30° upwards. The only change is that the level of the woofer is increased and the cancellation at 1.5 kHz is less pronounced.
When the roll off at low frequencies is disregarded, the difference from the lowest level at 1.5 kHz to the highest level at 4.5 kHz is found to be approximately 14 dB.

Summary

From the measurements presented in this chapter it is shown that the optimized loudspeaker has a more flat magnitude response and there are less pronounced changes when moving off-axis. Furthermore the drivers have less overlap in frequency.
By informal listening tests the impression of the improvements is more and deeper bass in the optimized loudspeaker. The loudspeaker sounds bigger than it is, and has a more consistent sound image, when compared to the reference speaker.

The changes introduced by the optimization are considered to be an improvement to the loudspeaker, and the optimization is regarded succesfull.

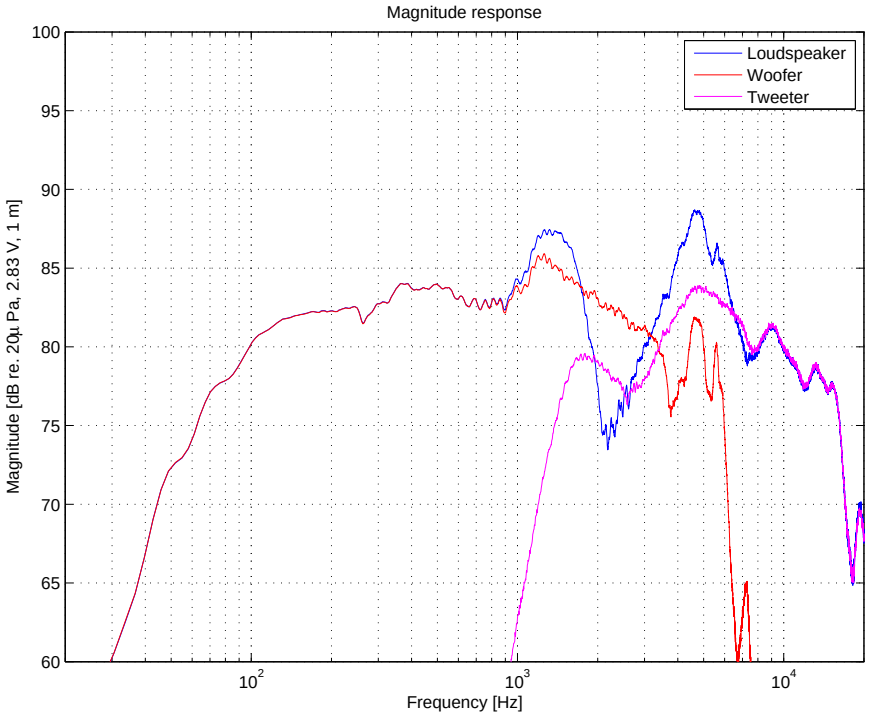

Figure 9.9: *Measured reference loudspeaker 30° vertically downwards.*

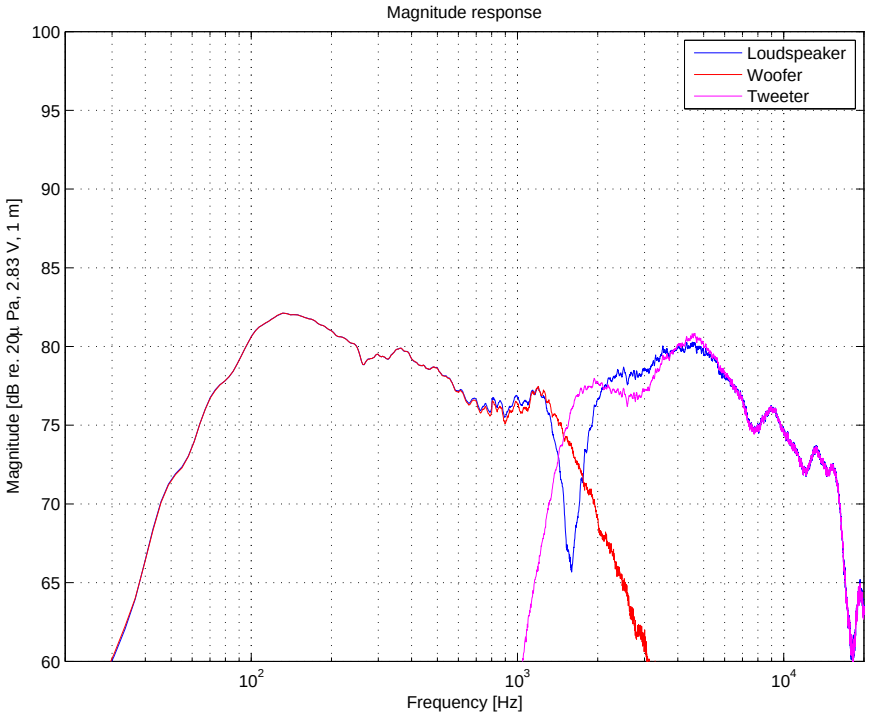

Figure 9.10: *Measured optimized loudspeaker 30° vertically downwards.*

CHAPTER 10

CONCLUSION

This master thesis investigates loudspeaker modelling and optimization in order to improve the performance of current loudspeakers. According to the stated initiating problem, the question is whether it is possible to improve a loudspeakers magnitude response and dispersion by optimizing the crossover network. The conclusions, together with a description of the work done in order to answer the initiating problem, are presented in the following.

Several theories related to loudspeaker design are investigated to specify which factors influence the response of a loudspeaker. This includes how a closed box changes the low frequency output, and how the cabinet edges contribute with sound. Furthermore, driver beaming, driver interference and crossover networks are investigated to fulfill the factors that influence the total response. All theories are verified by measurements to ensure they are valid, and that the implementations are made correctly. The verifications show that the theories are valid.

The different theories are used to make a model of a complete loudspeaker. The model takes infinite baffle measurements of the drivers as inputs, together with the associated impedance measurements. This way, the model can be used to calculate a loudspeakers magnitude response at different listening positions. The calculations are based on the chosen cabinet and crossover network. The impedance measurements are basis for estimating loudspeaker driver parameters. The model is as well as the theories verified by measurements, and the model verification concludes that the model is valid with only minor errors.

Finally, an optimization program is made to be able to optimize a loudspeakers response to a flat magnitude response. The optimization is made with the loudspeaker model as basis, and optimizes by adjusting the component values in a 2. order parallel crossover network. The algorithm makes use of the steepest descent method. The optimization works on two different listening positions; one in front of the tweeter and one 30° off-axis in the horizontal direction. By selecting a weighting between these two positions, it is possible to optimize the loudspeaker differently, and according to several different applications. Both the loudspeaker model and optimization algorithm are implemented in Matlab.

By simulations and measurements it is concluded, that the optimization works as intended, and it is possible to improve a loudspeakers magnitude response and dispersion. The optimized crossover network results in a loudspeaker having a more flat magnitude response both on-axis and 30° horizontally off-axis, which is an improvement when comparing it to a constructed reference loudspeaker based on a standard crossover network.

Further Investigations

This section presents possible further investigations for this project.

- Extension for vented box systems, since these types of systems often provide a lower cut-off frequency.
- Model extension for loudspeakers with more than two drivers.
- It could be interesting to model how a listening room influences the response of a loudspeaker setup, since room contributions can alter the loudspeaker response significantly.
- The optimization could be extented with constraints to ensure that the crossover frequency is placed in a specified frequency range. Furthermore the optimization could also be made capable of optimizing the driver positions in order to minimize edge diffractions.
- A user interface could be developed for the model and the optimization in order to ease the use of the programs.

BIBLIOGRAPHY

[1] Leo L. Beranek. *Acoustics*. Acoustical Society of Amerika, 1993.

[2] John Borwick. *Loudspeaker and Headphone Handbook*. Focal Press, third edition, 2003.

[3] Vance Dickason. *The Loudspeaker Design Cookbook*. Audio Amateur Press, sixth edition, 2000.

[4] Frequence. Frequence homepage. http://www.frequence.dk.

[5] Johnson, Johnson, Hilburn, and Scott. *Electric Circuit Analysis*. John Wiley & Sons, INC., third edition, 1999.

[6] Lawrence E. Kinsler, Austin R. Frey, Alan B. Coppens, and James V. Sanders. *Fundamentals of Acoustics*. John Wiley & Sons, Inc., fourth edition, 2000.

[7] Morten Knudsen and Henrik Rasmussen. *Systemidentifikation*. Institut for Elektroniske Systemer, Aalborg Universitetscenter, 1987.

[8] Henrik Møller. Den elektrodynamiske højttalers princip. Technical report, Institut for Elektroniske Systemer, Aalborg Universitet, 1987.

[9] John Vanderkooy. A simple theory of cabinet edge diffraction. *Journal of the Audio Engineering Society*, Vol. 39(No. 12):page 923–933, 1991.

[10] Visaton. Visaton homepage. http://www.visaton.de.

[11] Jr. W. Marshall Leach. *Introduction to Electroacoustics & Audio Amplifier Design*. Kendall/Hunt, third edition, 2003.

APPENDIX A

MAGNITUDE RESPONSE OF SECOND ORDER CROSSOVER NETWORK

This appendix describes the magnitude response of a second order crossover network, which consists of a lowpass and highpass filter. The polarity of the highpass filter is reversed, which makes the two filters in phase at the crossover frequency.

Derivation

s = jω

$$\left|\frac{\omega_n^2}{s^2+s\frac{\omega_n}{Q}+\omega_n^2}+\frac{-s^2}{s^2+s\frac{\omega_n}{Q}+\omega_n^2}\right| =$$

$$\left|\frac{\omega_n^2+\omega^2}{-\omega^2+j\omega\frac{\omega_n}{Q}+\omega_n^2}\right| =$$

$$\frac{\omega_n^2+\omega^2}{\sqrt{(-\omega^2+\omega_n^2)^2+(\omega\frac{\omega_n}{Q})^2}} =$$

$$\frac{\omega_n^2+\omega^2}{\sqrt{\omega^4+\omega_n^4-2\cdot\omega^2\cdot\omega_n^2+\omega^2\frac{\omega_n^2}{Q^2}}} =$$

Q is now set to $1/2$

$$\frac{\omega_n^2+\omega^2}{\sqrt{\omega^4+\omega_n^4+2\cdot\omega^2\cdot\omega_n^2}} = \frac{\omega_n^2+\omega^2}{\sqrt{(\omega^2+\omega_n^2)^2}} = 1$$

The derivation shows, that a second order crossover network with $Q = 1/2$ has a flat magnitude response. It can also be shown that the response will have a +3dB bump at the crossover frequency if the Q is set to $1/\sqrt{2}$, which is the Butterworth filter.

APPENDIX B

MEASUREMENT REPORTS

This appendix describes the measurements conducted in this project. They are used and presented in the verification chapter and the impedance measurements are basis for the parameter estimations.

B.1 General Acoustical Measurement Setup

This appendix presents a general measurement setup, since all acoustical measurements are conducted using the same equipment in the same setup.

Equipment

All acoustical measurements are conducted in the large anechoic room at Aalborg University. It is chosen to use a maximum length sequence (MLS) system as measuring system. The used equipment is presented in table B.1.

Equipment	Manufactor	Type	AAU number
Microphone	B&K	4133	06548
Microphone preamplifier	B&K	2639	08640
Measuring amplifier	B&K	2636	08022
MLS system	–	–	37493
Power amplifier	Pioneer	A-616	08249
Sound level calibrator	B&K	4230	08373

Table B.1: *Measurement equipment.*

To gain a high measurement accuracy, the measurements are split into two parts, one for low frequencies and one for high frequencies. In this way, it is possible to use a high sample rate to retain a large bandwidth and use a low sample rate combined with a long MLS-signal for creating accurate results at low frequencies. The setup file for the MLS-system contains the settings shown in table B.2 on the following page.

Measurement Setup

The measurement setup can be seen in figure B.1 on the next page.

A low frequency measurement and a high frequency measurement is conducted when measuring the woofer. This is to get the mentioned accuracy at low frequencies and large bandwidth for high fre-

	Low Frequency	**High Frequency**
Acquisition length	65536	65536
Antialiasing filter	Butterworth	Butterworth
Bandwidth	1 kHz	25 kHz
Sampling frequency	4 kHz	100 kHz
Average cycles	8	8
Amplitude	$\pm 2.83\ V_{RMS}$	$\pm 2.83\ V_{RMS}$
MLS order	2^{16}	2^{16}

Table B.2: *MLS-system setup for acoustical measurements.*

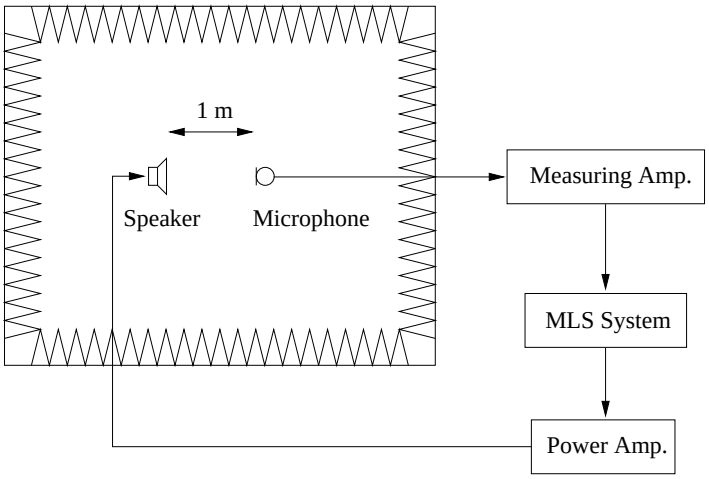

Figure B.1: *Measurement setup.*

quencies. These two measurements are afterwards put together with an intersection at 1 kHz. The tweeter is only measured with the high sample rate.

To be shure that the measurement system does not influence the measured responses, a short circuit measurement of the MLS-system is made and used as reference. This way the influence of the antialiasing filter etc. cancels out. The measuring system is calibrated with the sound level calibrator.

B.2 General Impedance Measurement Setup

This appendix presents a general measurement setup, since all impedance measurements are conducted using the same equipment in the same setup.

Equipment

All impedance measurements are conducted in the large anechoic room at Aalborg University. It is chosen to use a maximum length sequence (MLS) system as measuring system. The MLS-system is the only equipment used for measuring driver electrical impedance. The setup file for the MLS-system contains the settings shown in table B.3 on the facing page.

Acquisition length	65536
Antialiasing filter	Butterworth
Bandwidth	25 kHz
Sampling frequency	100 kHz
Average cycles	8
Amplitude	$\pm 0.4922\ V_{RMS}$
MLS order	2^{16}

Table B.3: *MLS-system setup for electrical impedance measurements.*

Measurement Setup

The measurement setup can be seen in figure B.2.

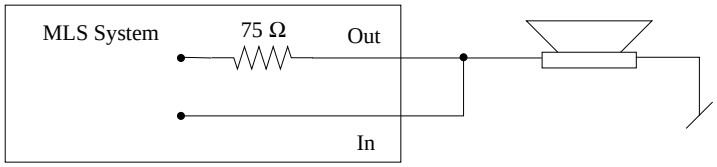

Figure B.2: *Setup for impedance measurement.*

To be shure that the measurement system does not influence the measured responses, a short circuit measurement of the MLS-system is made and used as reference. This way the influence of the antialiasing filter etc. cancels out.

B.3 Infinite Baffle Measurements

Aim

This appendix describes the infinite baffle measurements conducted with the woofer and tweeter. This is both acoustical impulse response and electrical impedance measurements.

Equipment

The used equipment and software setup for these measurements can be seen in appendix B.2 on the preceding page.

Measurement Setup

The measurement setup can be seen in figure B.3.

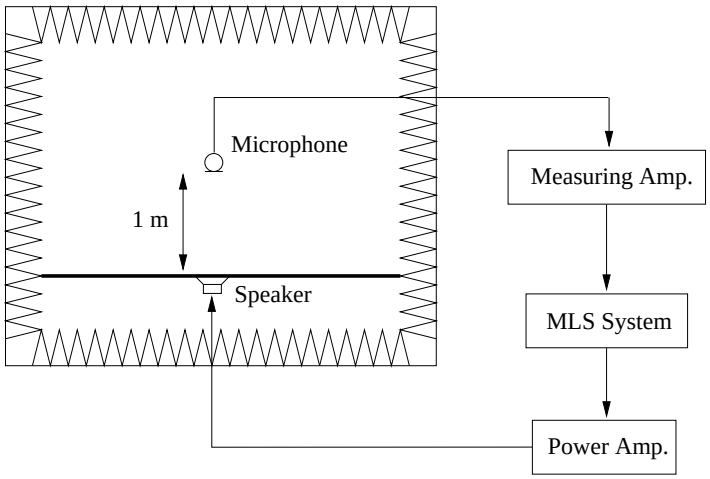

Figure B.3: Measurement setup for infinite baffle measurements.

Measurement Description

An infinite baffle is set up in the anechoic room in order to do the measurements. The measurements are carried out in 1 m distance for 0°, 30°, 60° and 80°. The last three angles show the beam patterns of the drivers. The drivers are flush mounted in the baffle.

Results

The measurement results are illustrated in the following figures.

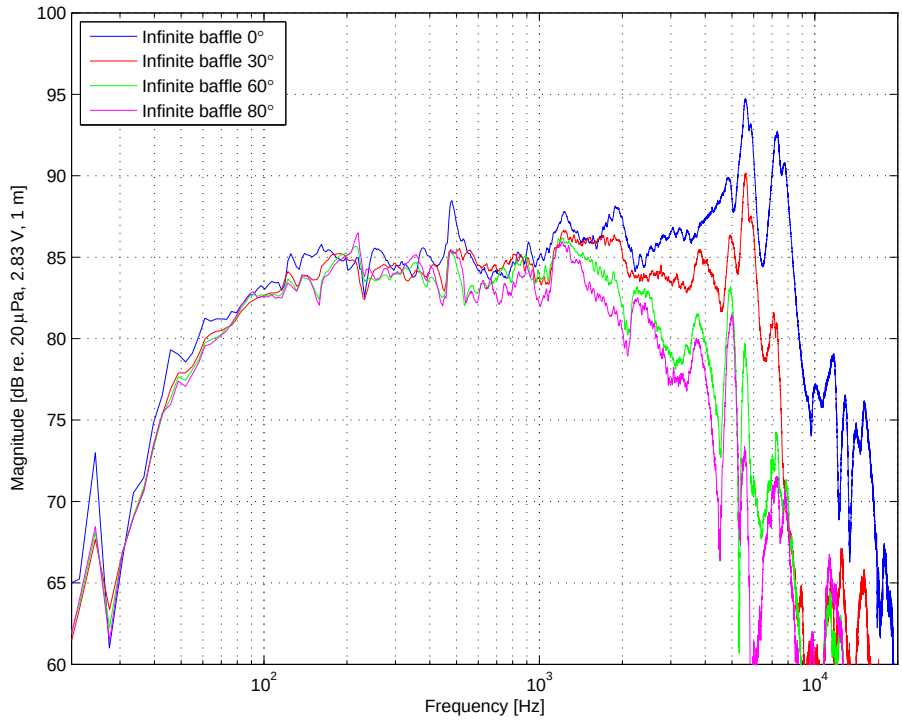

Figure B.4: *Infinite baffle measurements of woofer at 1 m distance for 0°, 30°, 60° and 80°.*

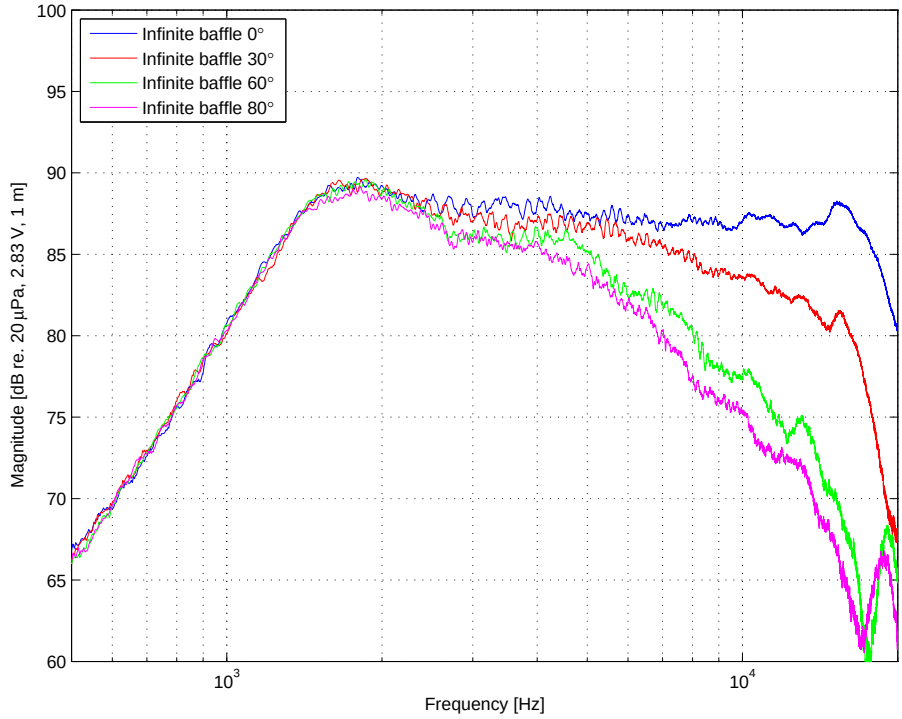

Figure B.5: *Infinite baffle measurements of tweeter at 1 m distance for 0°, 30°, 60° and 80°.*

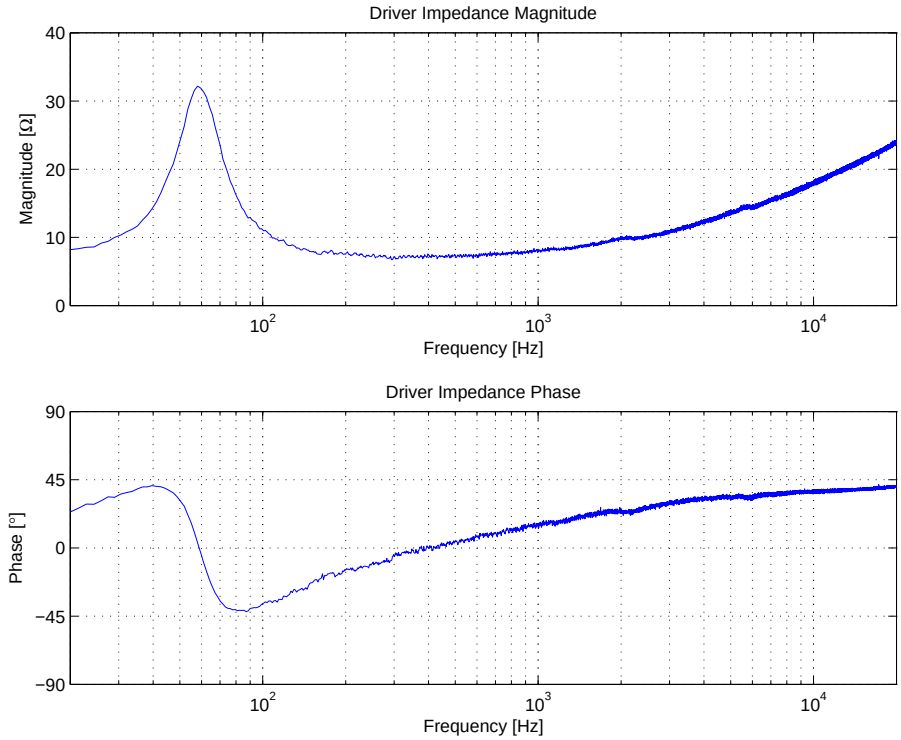

Figure B.6: *Infinite baffle impedance measurement of woofer.*

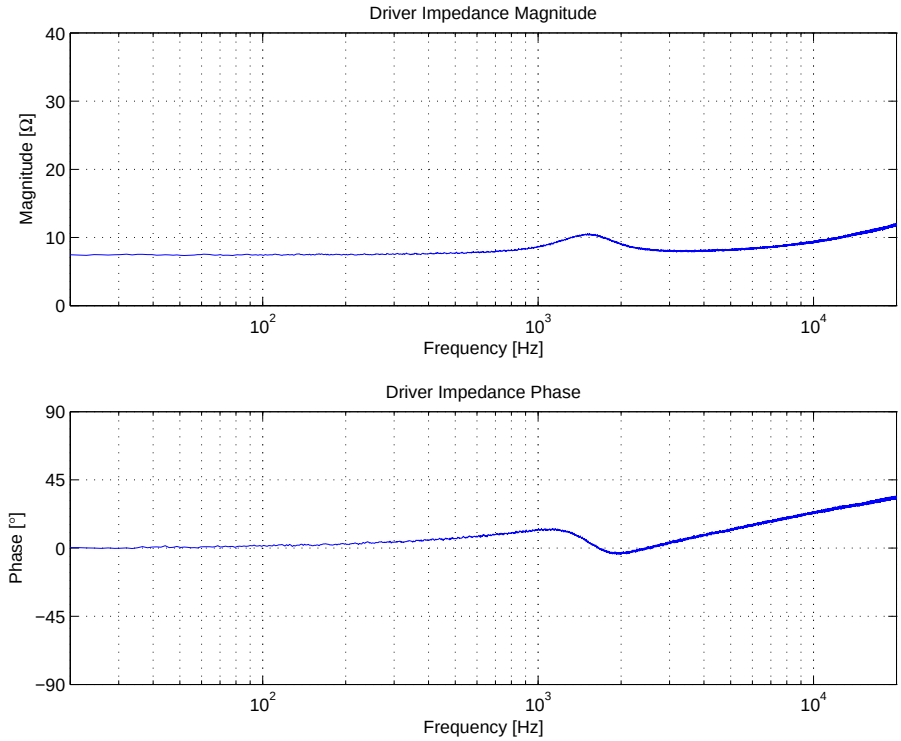

Figure B.7: *Infinite baffle impedance measurement of tweeter.*

B.4 Closed Box Measurements

Aim

This appendix describes the closed box measurements conducted with the woofer. The front baffle is the infinite baffle. It is both acoustical impulse response and electrical impedance measurements.

Equipment

The used equipment and software setup for these measurements can be seen in appendix B.2 on page 113.

Measurement Setup

The measurement setup can be seen in figure B.8.

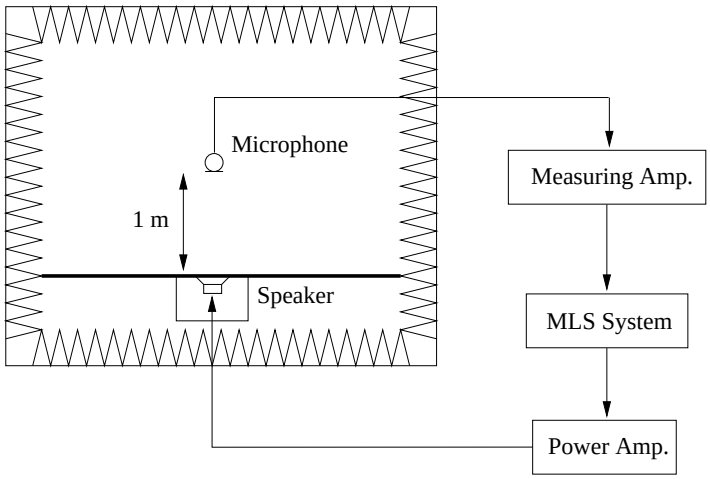

Figure B.8: *Measurement setup for closed box measurements.*

Measurement Description

The measurements are carried out in 1 m distance for 0°, 30°, 60° and 80°. The last three angles show the beam patterns of the drivers. The closed box is mounted on the backside of the infinite baffle. The box is loosely stuffed with damping material.

Results

The measurement results are illustrated in the following figures.

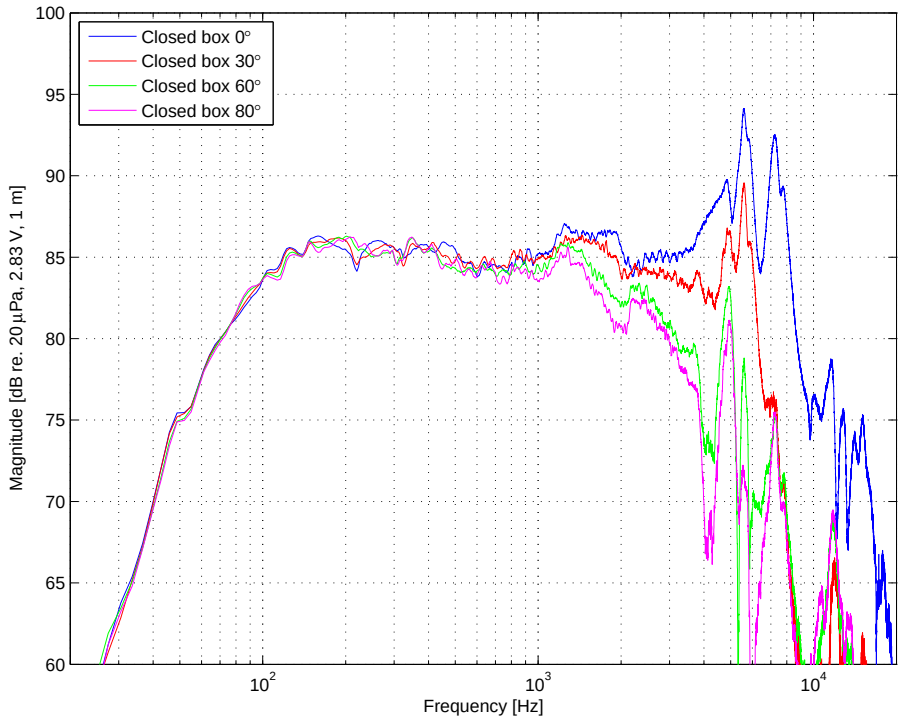

Figure B.9: *Closed box measurement of the woofer with infinite front baffle.*

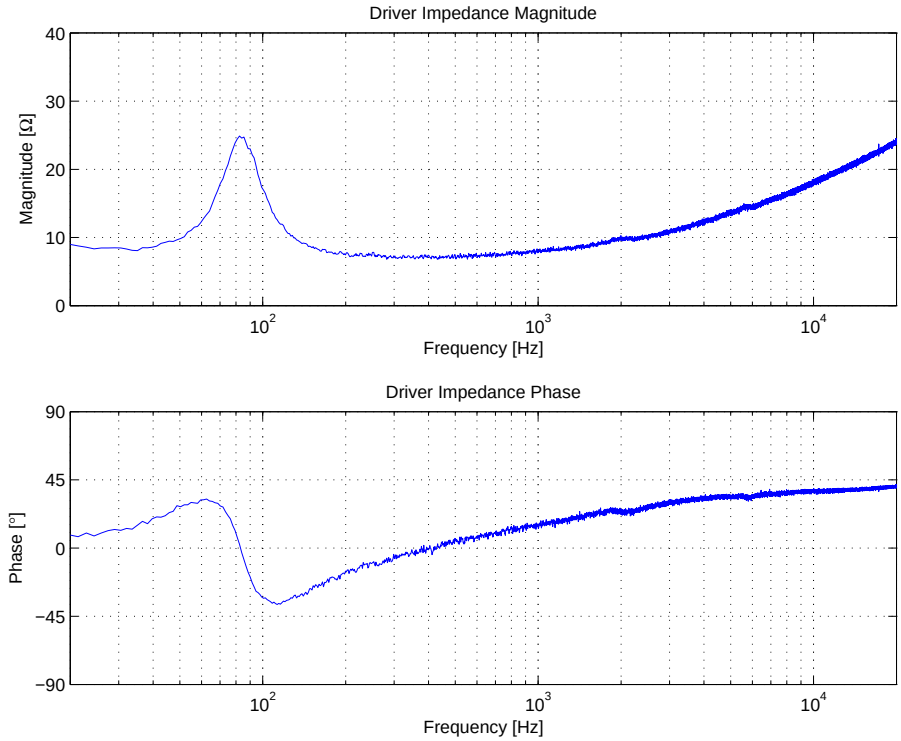

Figure B.10: *Closed box impedance of the woofer with infinite front baffle.*

B.5 Crossover Acoustical Measurements

Aim

This appendix describes the crossover measurements conducted with the woofer and tweeter placed in the infinite baffle. Acoustical impulse responses are measured.

Equipment

The used equipment and software setup for these measurements can be seen in appendix B.2 on page 113.

Measurement Setup

The measurement setup can be seen in figure B.11.

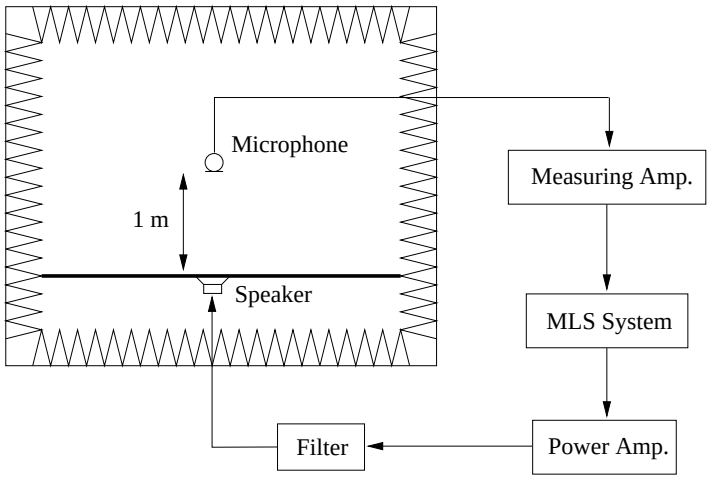

Figure B.11: *Measurement setup for acoustical crossover measurements.*

Measurement Description

The measurements are carried out in 1 m distance for 0°, 30°, 60° and 80°. The last three angles show the beam patterns of the drivers. The crossover filters designed in section 5.4.1 on page 60 are connected after the power amplifier.

Results

The measurement results are illustrated in the following figures.

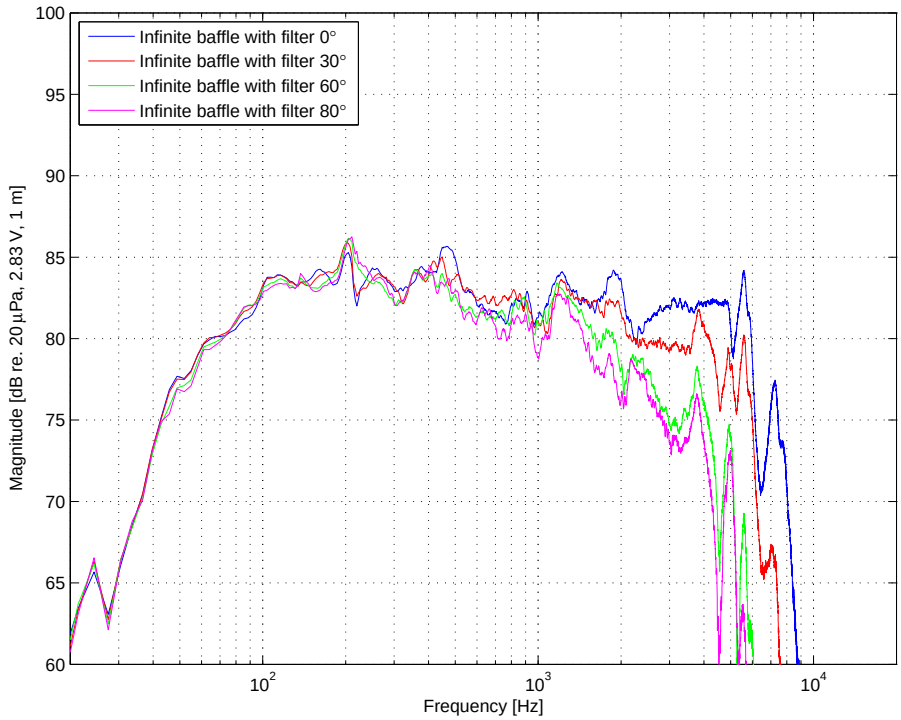

Figure B.12: *Infinite baffle measurement of the woofer with lowpass filter.*

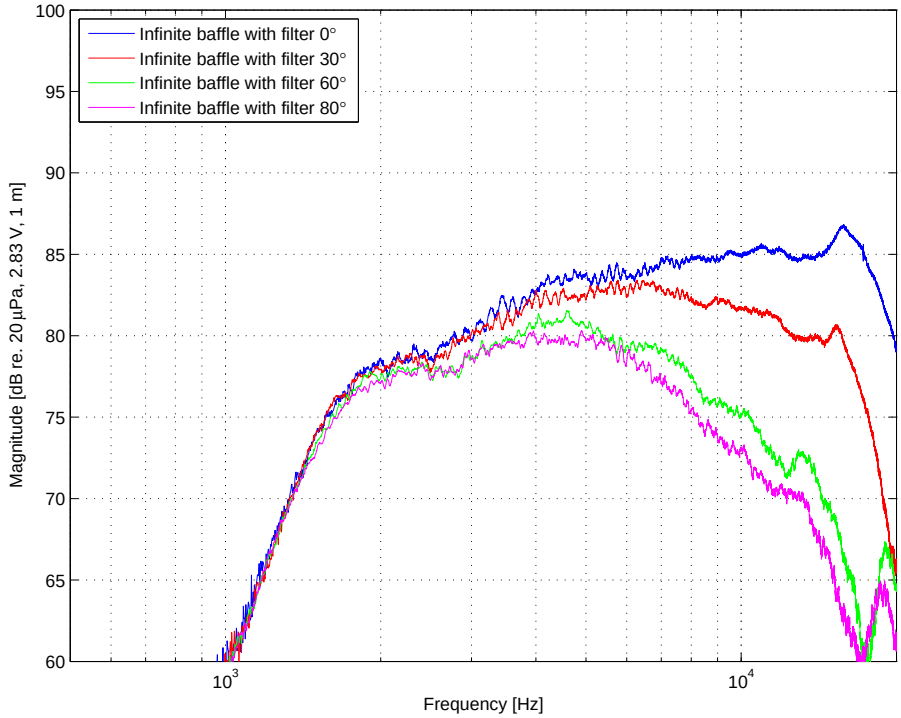

Figure B.13: *Infinite baffle measurement of the tweeter with highpass filter.*

B.6 Interference Measurements

Aim

This appendix describes the interference pattern measurements conducted with two woofers. It is measurements of acoustical impulse responses.

Equipment

The used equipment and software setup for these measurements can be seen in appendix B.2 on page 113.

Measurement Setup

The measurement setup can be seen in figure B.14.

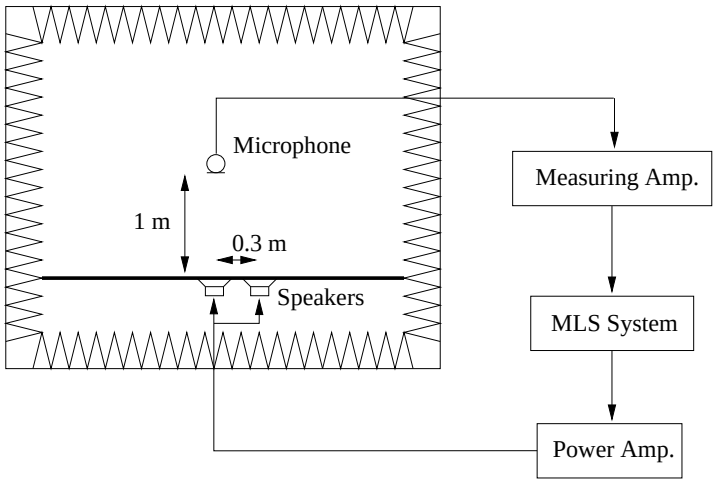

Figure B.14: *Measurement setup for interference measurements.*

Measurement Description

The measurements are carried out in 1 m distance for -80° to 80° with a resolution of 10°. The reference point is in front of one of the woofers. The drivers are flush mounted in the baffle with a distance of 0.3 m.

Results

Some of the measurement results are illustrated in the following figures.

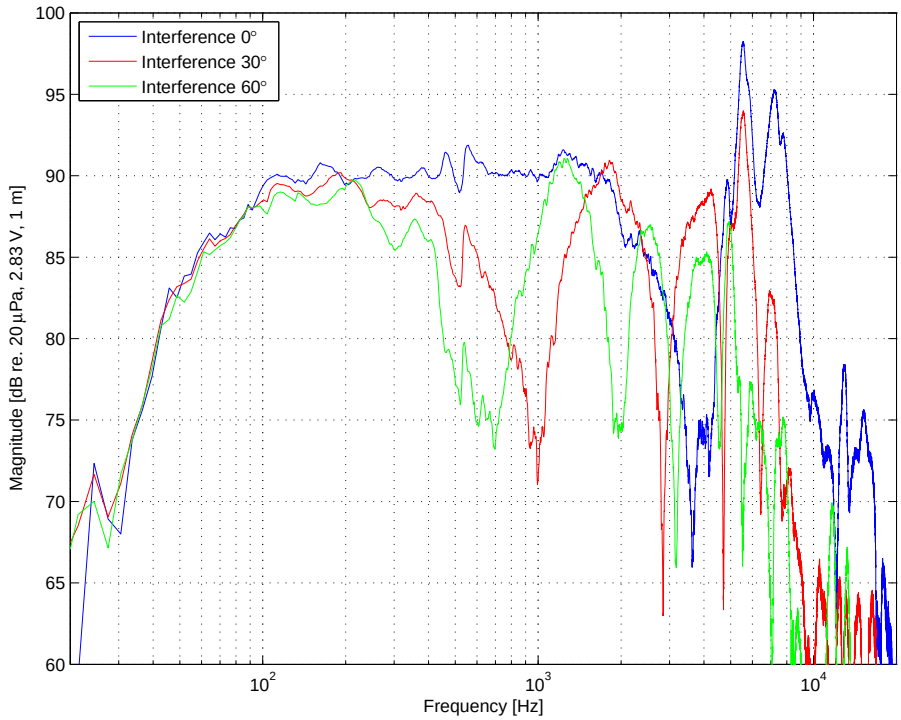

Figure B.15: *Interference measurements of two woofers at 1 m distance for 0°, 30° and 60°.*

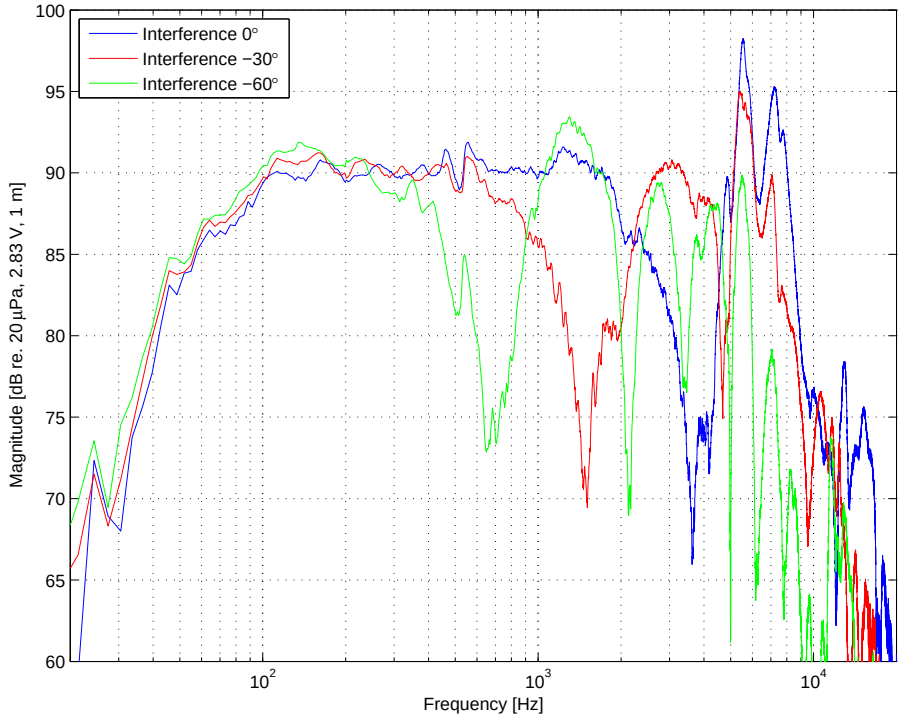

Figure B.16: *Interference measurements of two woofers at 1 m distance for 0°, -30° and -60°.*

B.7 Edge Diffraction Measurements

Aim

This appendix describes the edge diffraction measurements conducted with the woofer and the tweeter. It is measurements of acoustical impulse responses.

Equipment

The used equipment and software setup for these measurements can be seen in appendix B.2 on page 113.

Measurement Setup

The measurement setup can be seen in figure B.17.

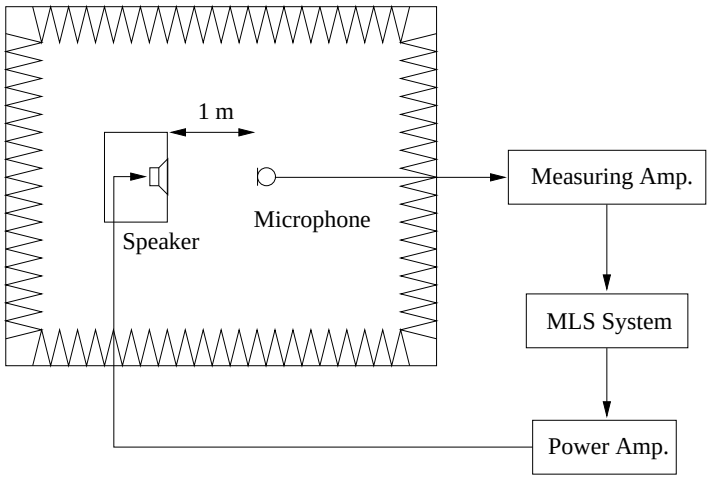

Figure B.17: *Measurement setup for diffraction measurements.*

Measurement Description

The measurements are carried out in 1 m distance at 0°, 30°, 60° and 80° with respect to the driver. The drivers are mounted in the box which is positioned on a loudspeaker stand.

Results

The measurement results are illustrated in the following figures.

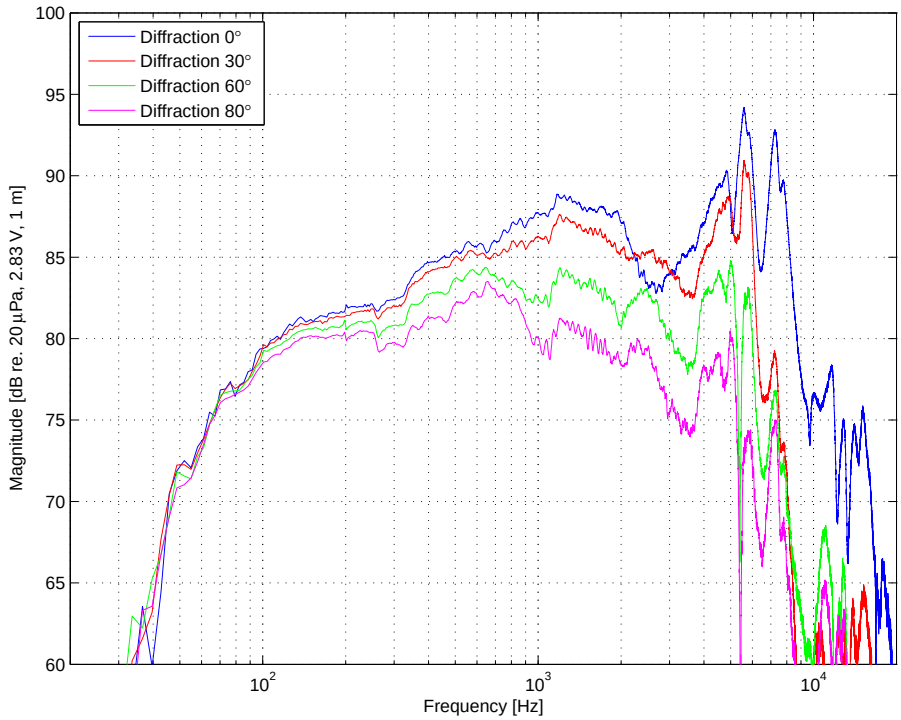

Figure B.18: *Edge diffraction measurements of the woofer at 1 m distance for 0°, 30°, 60° and 80°.*

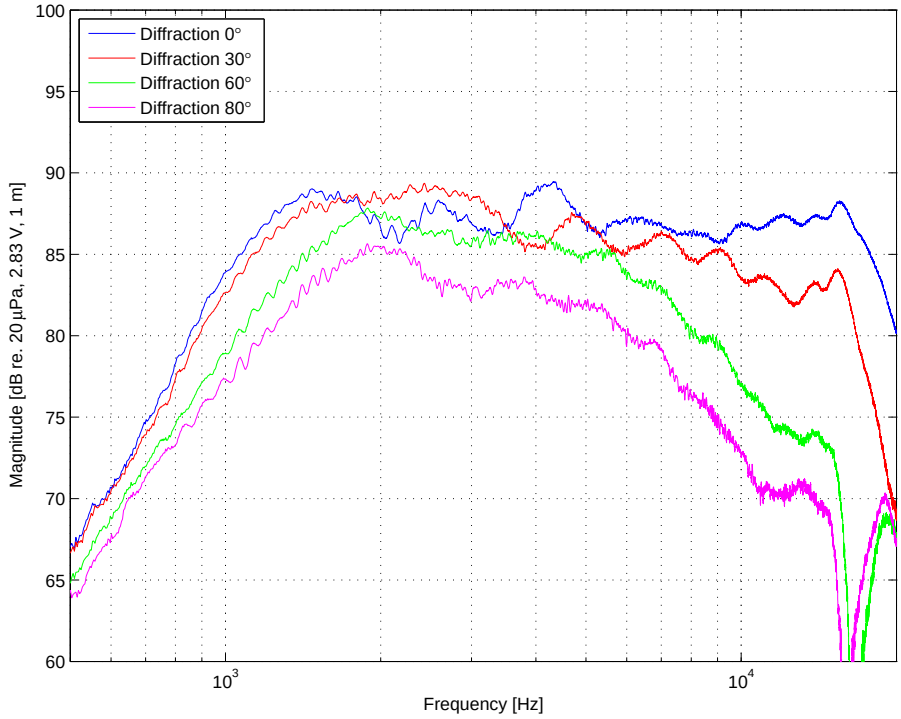

Figure B.19: *Edge diffraction measurements of the tweeter at 1 m distance for 0°, 30°, 60° and 80°.*

B.8 Damping Material Measurements

Aim

This appendix describes the measurements of damping material influence, conducted with the woofer. It is measurements of acoustical impulse responses and electrical impedance.

Equipment

The used equipment and software setup for these measurements can be seen in appendix B.2 on page 113.

Measurement Setup

The measurement setup can be seen in figure B.20.

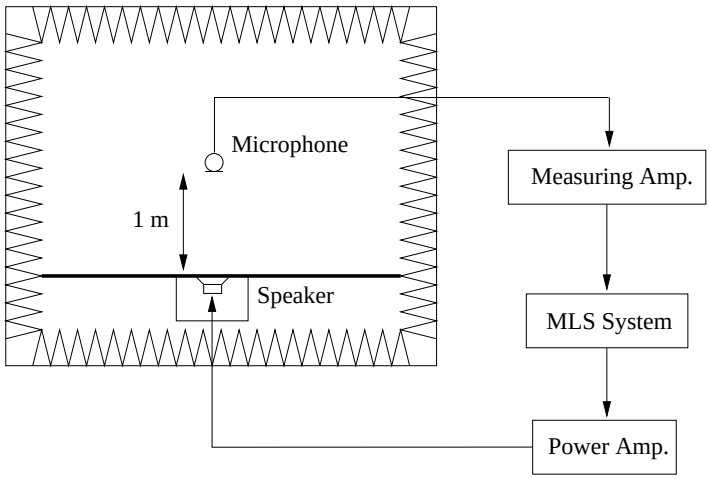

Figure B.20: *Measurement setup for measurements of damping material influence.*

Measurement Description

The measurements are carried out in 1 m distance at 0°, The woofer is mounted in the infinite baffle, and the box is mounted behind the woofer. Measurements are conducted with an empty box and with a box loosely stuffed with Acoustilux.

Results

The measurement results are illustrated in the following figures.

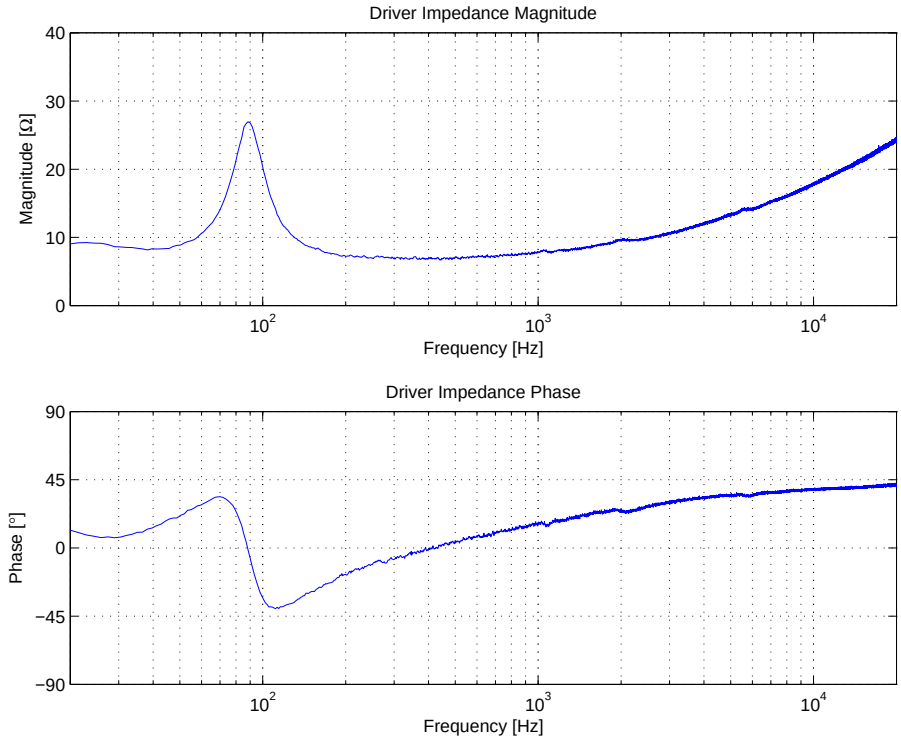

Figure B.21: *Measurements of the impedance of the woofer without damping material.*

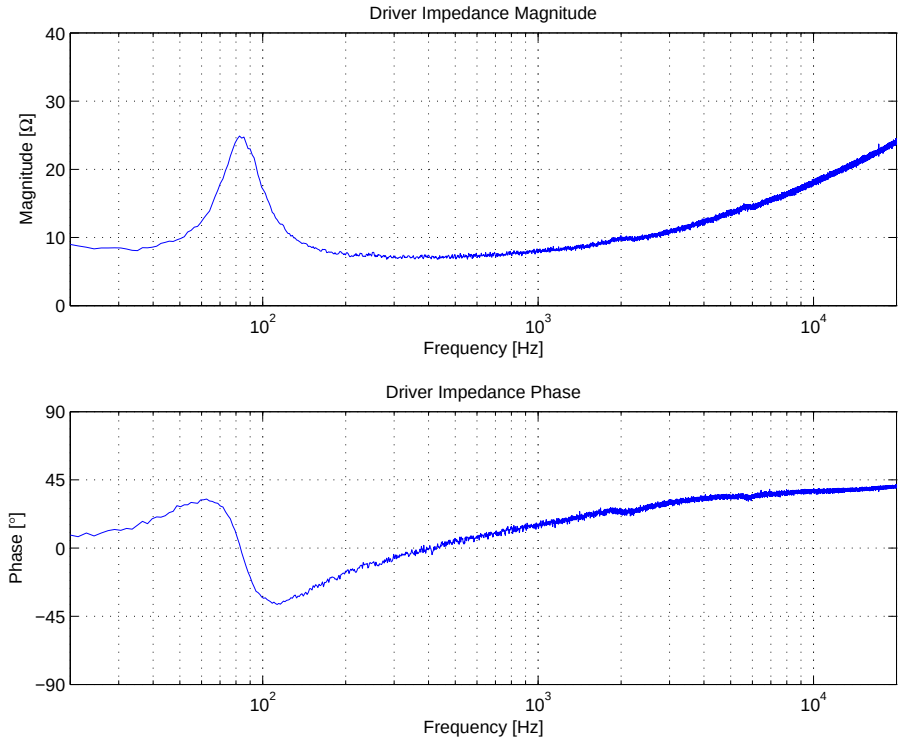

Figure B.22: *Measurements of the impedance of the woofer with damping material.*

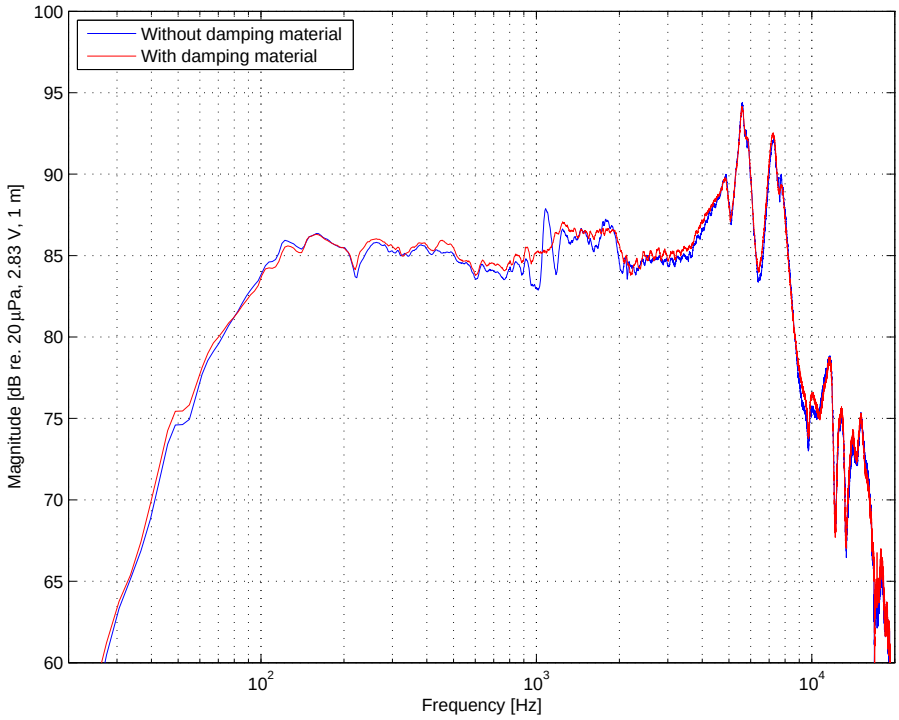

Figure B.23: *Measurements of the woofer at 1 m distance with and without damping material.*

B.9 Measurements of the Reference Speaker

Aim

This appendix describes the measurements of the reference speaker. It is measurements of acoustical impulse responses.

Equipment

The used equipment and software setup for these measurements can be seen in appendix B.2 on page 113.

Measurement Setup

The measurement setup can be seen in figure B.24.

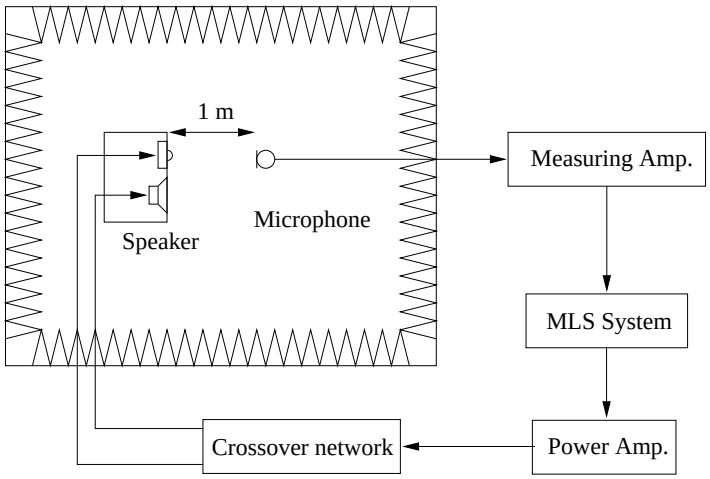

Figure B.24: *Measurement setup for the reference speaker.*

Measurement Description

The measurements are carried out in 1 m distance at 0°, 30°, 30° upwards and 30° downwards. The woofer and the tweeter is mounted in the box. The filter for the reference speaker is used, and measurements are conducted with the woofer, the tweeter and both drivers connected. The box is loosely stuffed with Acoustilux.

Results

The measurement results are illustrated in the following figures.

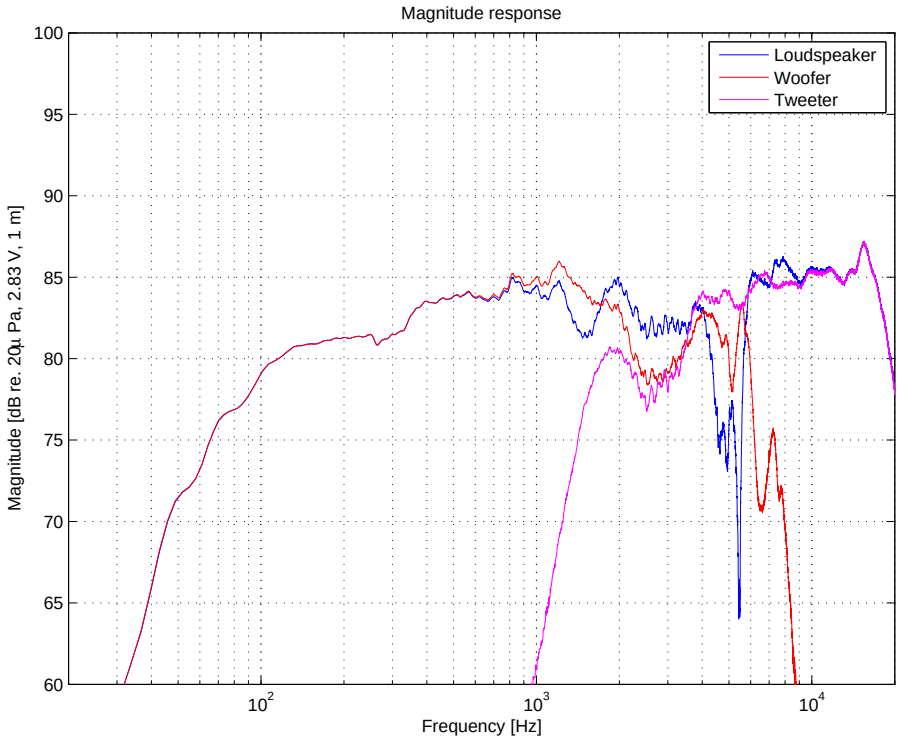

Figure B.25: *Measurements of the reference speaker on-axis.*

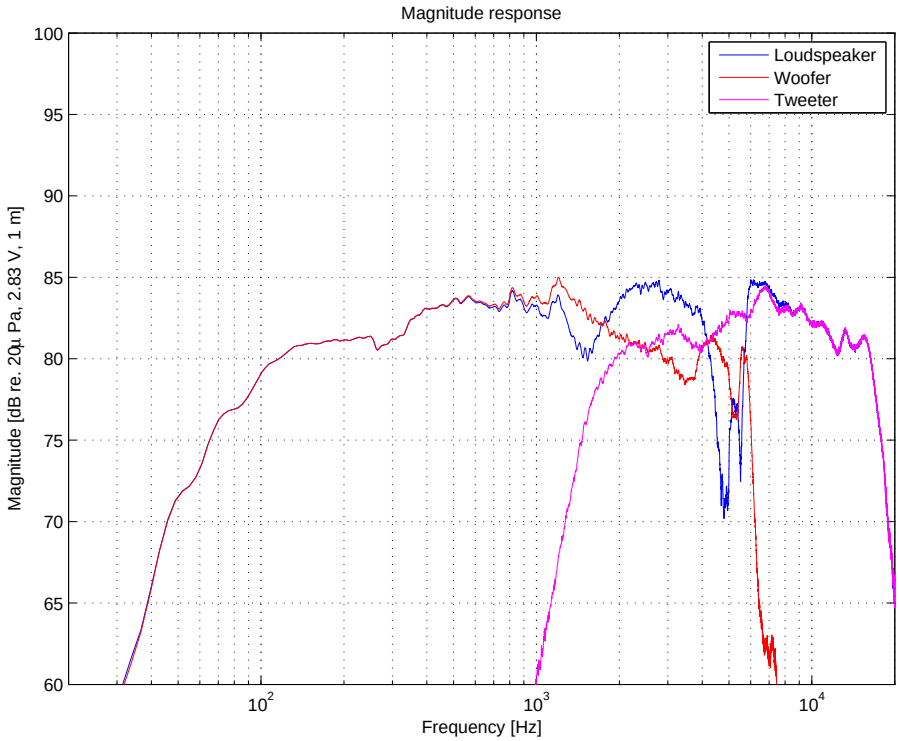

Figure B.26: *Measurements of the reference speaker 30° off-axis.*

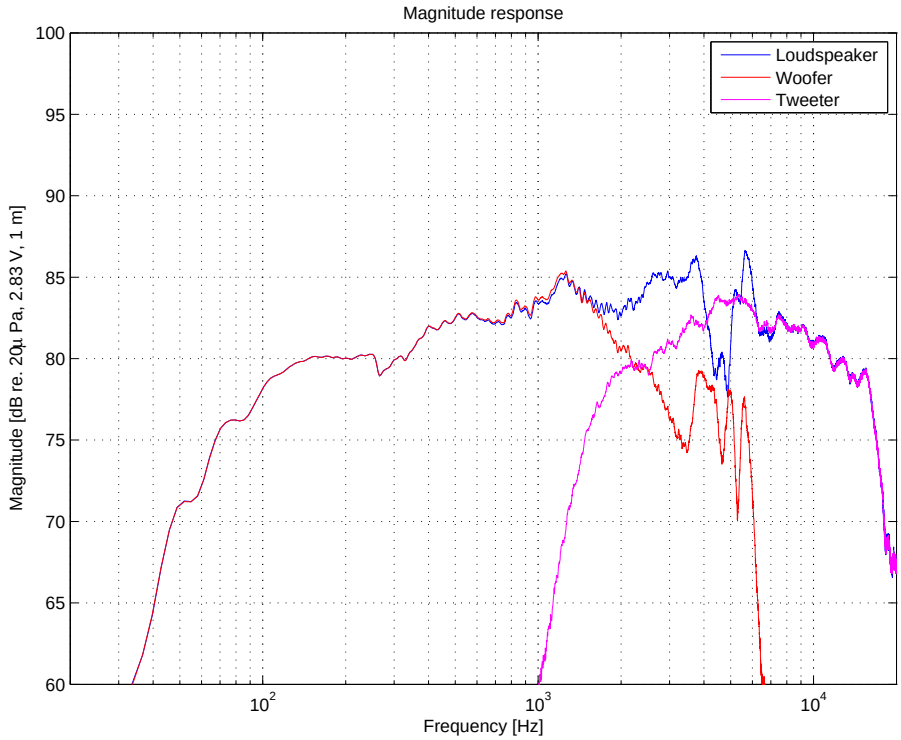

Figure B.27: *Measurements of the reference speaker 30° upwards.*

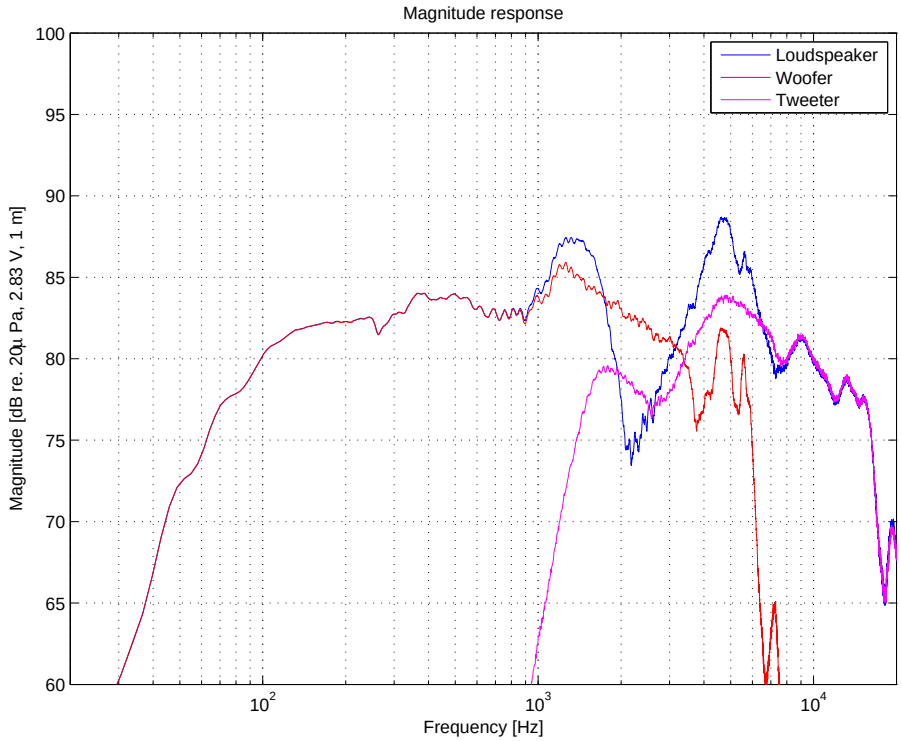

Figure B.28: *Measurements of the reference speaker 30° downwards.*

B.10 Measurements of the Optimized Speaker

Aim

This appendix describes the measurements of the optimized speaker. It is measurements of acoustical impulse responses.

Equipment

The used equipment and software setup for these measurements can be seen in appendix B.2 on page 113.

Measurement Setup

The measurement setup can be seen in figure B.29.

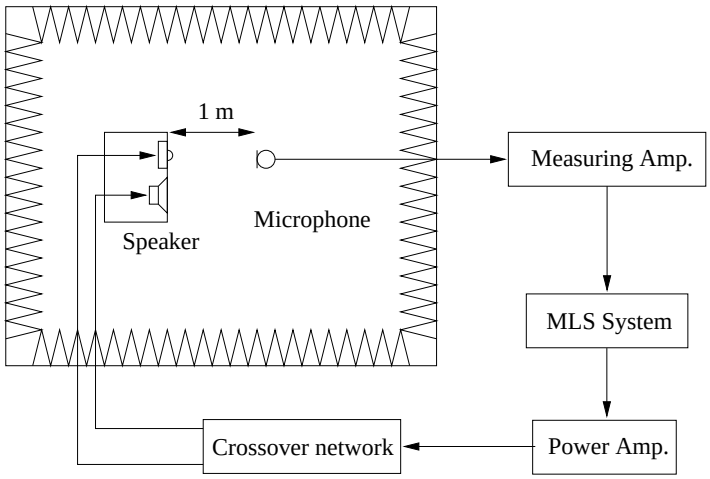

Figure B.29: *Measurement setup for the optimized speaker.*

Measurement Description

The measurements are carried out in 1 m distance at 0°, 30°, 30° upwards and 30° downwards. The woofer and the tweeter is mounted in the box. The filter for the optimized speaker is used, and measurements are conducted with the woofer, the tweeter and both drivers connected. The box is loosely stuffed with Acoustilux.

Results

The measurement results are illustrated in the following figures.

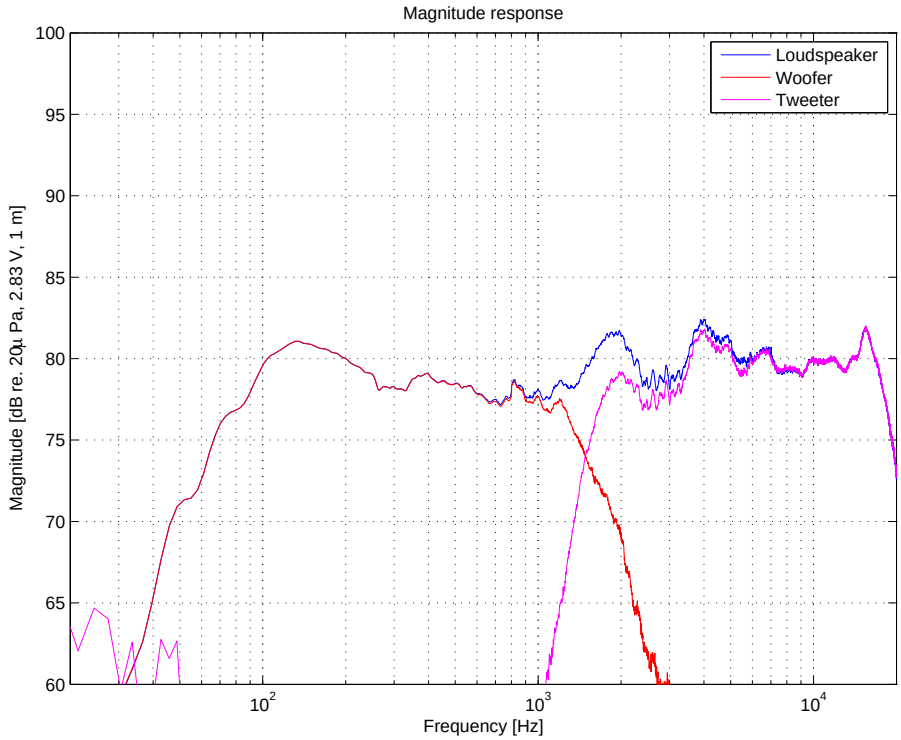

Figure B.30: *Measurements of the optimized speaker on-axis.*

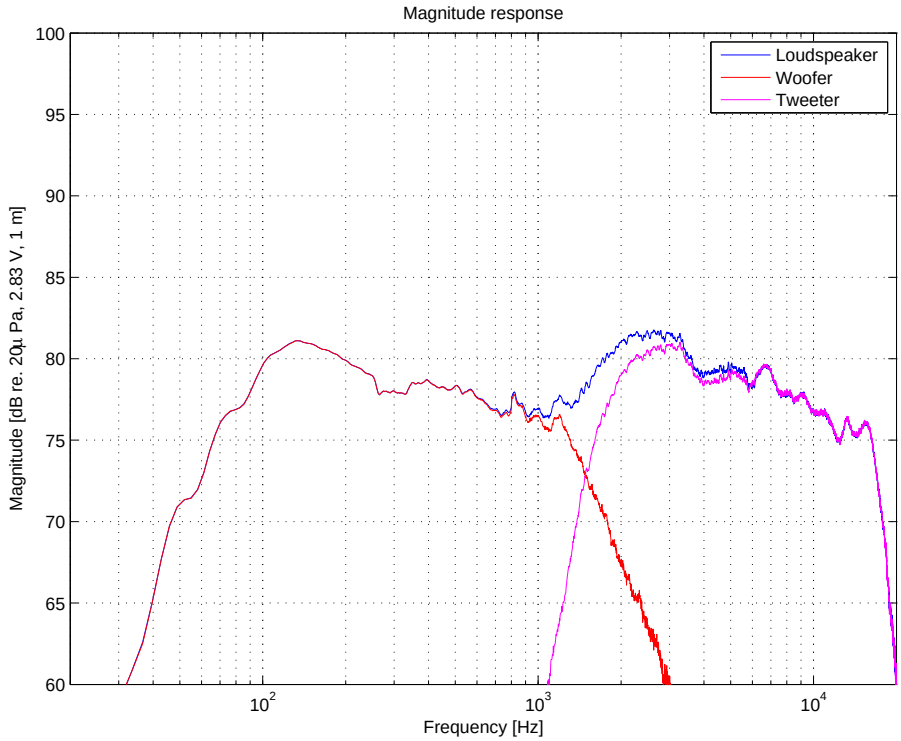

Figure B.31: *Measurements of the optimized speaker 30° off-axis.*

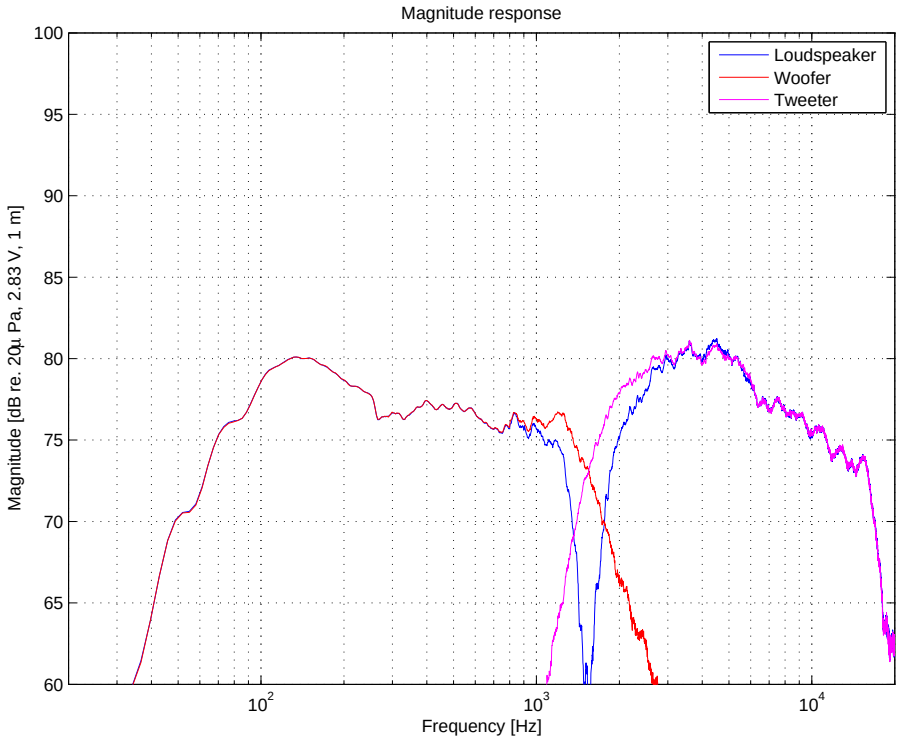

Figure B.32: *Measurements of the optimized speaker 30° upwards.*

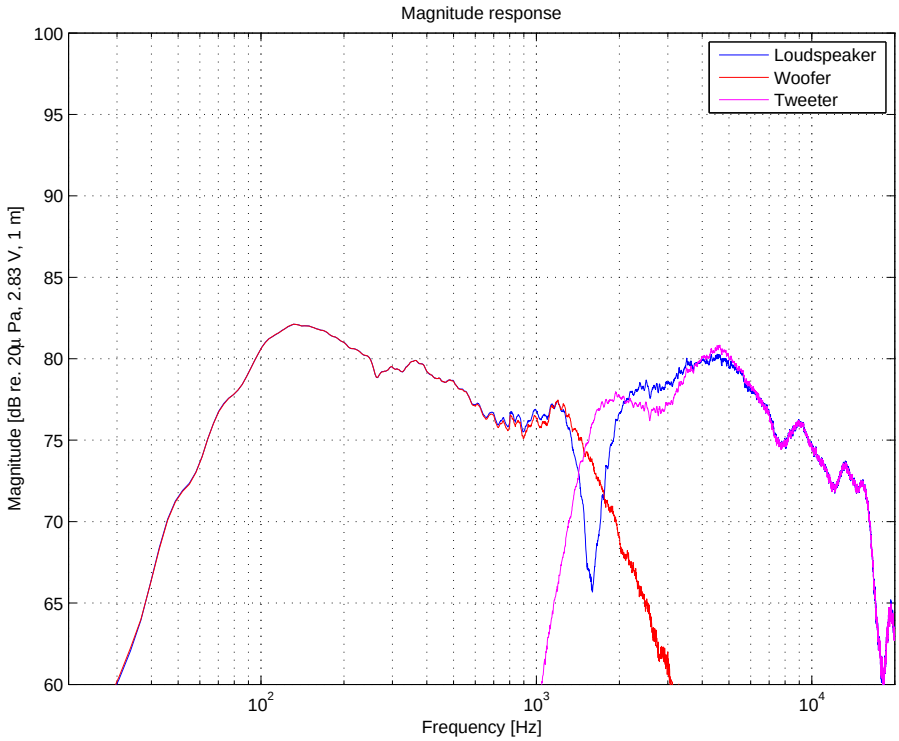

Figure B.33: *Measurements of the optimized speaker 30° downwards.*